Reconsidering the glaciogenic origin of Gondwana diamictites, Dwyka Group, South Africa

Mats O. Molén[1,1] and J. Johan Smit[2,2]

[1]Umeå FoU AB
[2]Tsunami Resources

November 30, 2022

Abstract

The Gondwana Late Paleozoic Ice Age is probably best represented by the Dwyka Group in South Africa. Striated and grooved surfaces or pavements are commonly considered to be subglacially formed, as are diamictites which have been interpreted as in situ or reworked tillites. These interpretations were tested by investigation of outcrops in formerly well studied areas, throughout South Africa. Detailed analyses focused on striated surfaces/pavements and surface microtextures on quartz sand grains in diamictites. The sedimentological context of four pavements, interpreted to be glaciogenic, display features commonly associated with sediment gravity flows, rather than glaciation. A total of 4271 quartz sand grains were subsampled from outcrops that are mainly considered to be tillites formed by continental glaciation. These grains, analyzed by SEM, do not demonstrate the characteristic surface microtextures combinations of fracturing and irregular abrasion associated with Quaternary glacial deposits, but mainly a mix of surface microtextures associated with multicyclical grains. The Dwyka Group diamictites warrant reinterpretation as non-glacial sediment gravity flow deposits.

Reconsidering the glaciogenic origin of Gondwana diamictites, Dwyka Group, South Africa

Mats O. Molén,[1]* and J. Johan Smit[2]

1. Umeå FoU AB, Vallmov 61, S-903 52 Umeå, Sweden

2. 9 Gradwell Street, Parys, 9585, South Africa

* corresponding author, email: mats.extra@gmail.com.

Abstract

The Gondwana Late Paleozoic Ice Age is probably best represented by the Dwyka Group in South Africa. Striated and grooved surfaces or pavements are commonly considered to be subglacially formed, as are diamictites which have been interpreted as in situ or reworked tillites. These interpretations were tested by investigation of outcrops in formerly well studied areas, throughout South Africa. Detailed analyses focused on striated surfaces/pavements and surface microtextures on quartz sand grains in diamictites. The sedimentological context of four pavements, interpreted to be glaciogenic, display features commonly associated with sediment gravity flows, rather than glaciation. A total of 4271 quartz sand grains were subsampled from outcrops that are mainly considered to be tillites formed by continental glaciation. These grains, analyzed by SEM, do not demonstrate the characteristic surface microtextures combinations of fracturing and irregular abrasion associated with Quaternary glacial deposits, but mainly a mix of surface microtextures associated with multicyclical

grains. The Dwyka Group diamictites warrant reinterpretation as non-glacial sediment gravity flow deposits.

Keywords: Surface microtexture, sediment gravity flow, Late Paleozoic Ice Age, pavement, Nooitgedacht

1. Introduction

1.1. Process-related geology

The research question in this study is weather the geological features in the Dwyka Group of South Africa indicate glacial conditions or not.

Schermerhorn published a comprehensive review which documented evidence for a sediment gravity flow origin of ancient tillites, shown in his classic work on Late Precambrian diamictites (Schermerhorn, 1974,1976a, 1976b, 1977), even though an older paper by Crowell (1957) is considered to be the first covering this research area. Since then there has been a growing understanding that many pre-Pleistocene glaciogenic deposits could have been formed by different kinds of sediment gravity flows like turbidity currents, slumps, slides and especially cohesive debris flows (e.g. Eyles, 1993; Eyles & Januszczak, 2007; Vesely et al., 2018; Fedorchuk et al., 2019; Kennedy & Eyles, 2021).

In this context the origin of the Permo-Carboniferous Dwyka Group diamictites of South Africa, was studied. As most documentation of the general geology of the Dwyka Group formerly published does not need discussion, only geologci features which are especially important for the origin of the deposits were examined in detail. Independent of the process - glaciation or sediment gravity flow - the source and age of the sediments will be similar, e.g. data published by Griffis et al. (2021) and interpreted in a glaciogenic context still hold, even if the process may be different.

Commonly researchers start with the interpretation that the Dwyka Group is to a large part glaciogenic, as this is the current understanding of the geologic features. In the present work the starting assumption is the evidence from geological processes of Pleistocene and recent glaciations, i.e. a process-related issue (Shanmugam, 2021; Molén, 2022a, 2022b), and not former interpretations. The most distinctive geological feature from the Dwyka Group interpreted as glaciogenic is striated and grooved surfaces, i.e. “glacial pavements”. Therefore a sample of well known striated surfaces were studied in detail, and were compared to striated surfaces produced by Quaternary glaciers and by sediment gravity flows (e.g. Peakall et al., 2020). Furthermore, surface microtextures on quartz grains will display evidence of any glaciogenic transport history of diamictites, even if sediments had been reworked by e.g. slides or sediment gravity flows (Mahaney, 2002; Molén, 2014). Therefore, to uncover the transport history of the Dwyka Group diamictites, quartz sand grains were studied by SEM.

1.2. Origin of geologic features – glaciogenic or from sediment gravity flows

Differences between glaciogenic and mass flow features often can be revealed by comparing data from different geologic disciplines (e.g. compare Shanmugam et al., 1994; Major et al., 2005; Talling et al., 2007, 2012; Dakin et al., 2013; Shanmugam, 2016; Molén, 2017, 2021, 2022a, 2022b; Dietrich & Hofmann, 2019; Peakall et al., 2020; Cardona et al., 2020). Geologic features which are commonly interpreted as glaciogenic, for example, striated, grooved and polished bedrock, including all kinds of chevron structures/crescentic gouges/chattermarks, grooves and nailhead striations, can form as a result of different kinds of mass movements, such as avalanches, slides and different kinds of sediment gravity flows (Draganits et al., 2008; Dakin et al., 2013; Molén 2017, 2021, 2022a, 2022b; Kennedy & Eyles, 2021). A lahar generated by the Mount St. Helens eruption truncated volcanic boulders and produced, in places "... a surface similar to a glacial pavement cut in conglomerate" (Scott, 1988, p. A43). A process somewhat similar to glacial plucking may be caused by sediment gravity flows, and sometimes by fluvial action, even on the face of hard granite (Whipple et al., 2000; Dakin et al., 2013; Kennedy & Eyles, 2021; Molén, 2022a).

1.3. Geology of the Dwyka Group

1.3.1. History of research, tectonic context, evidence of sediment gravity flows

The Dwyka Group is mainly present in large basins, the Karoo Basin of South Africa and the Aranos/Kalahari Basin, the main part in Botswana and Namibia. The unit is conformably overlain by the Ecca Group shales to a great depth (e.g. Baiyegunhi & Gwavava, 2016; Götz et al., 2018; Bell et al., 2020).

The Dwyka Group has to a large part been studied with the commonly accepted interpretation, or paradigm, that this sedimentary unit was the geologic consequence of a major glaciation. In 1856 the diamictites were interpreted to be of volcanic origin (Sandberg, 1928; Norman, 2013), and later as mudflows or from meteorite impacts, including striated surfaces (Geophysical Discussion, 1960; Master, 2012; Rampino, 2017). The glaciogenic interpretation was first published in 1870 (Hancox & Götz, 2014), generally accepted in 1898 (Sandberg, 1928), and basically has withstood critical comments and alternative geological interpretations. During the early investigations of the Dwyka Group, most sections were considered as deposited subglacially, but as more data have accumulated, the interpretations have become more complicated, including many and varied glacial advances and retreats, and recognizing the presence of sediment gravity flows and rain-out deposits (Visser, 1986, 1990, 1994, 1996, 1997; Visser et al., 1997a, 1997b; Isbell et al., 2008; Dunlevey & Smith, 2011).

The current work is mainly concerned with the Karoo Basin, an area which was primarily controlled by tectonism (Von Brunn, 1994; Visser, 1997; Bangert & Von Brunn, 2001; Isbell et al., 2008). Partly overlapping, and extending outside of the time period of the deposition of the Dwyka Group, large compressional events are associated with the Cape orogeny (Scheiber-Enslin et al., 2015). In the southern part of South Africa, the Dwyka Group has been tectonically deformed during uplift and partially metamorphosed (Fagereng, 2014). In conclusion, the Karoo Basin show evidence of downwarping as a lithospheric deflection (Dietrich & Hofmann, 2019). The basin may be seen as a retroarc foreland basin, and the Dwyka Group forms the basal part of this basin (Johnson et al., 1997; Catuneanu et al., 2005; Barbolini et al., 2018; Hansen et al., 2019; Dietrich & Hofmann, 2019).

In areas with Dwyka Group sediments in Namibia, interpreted to be subglacial, the basal unconformity below diamictites may be highly irregular and heterogenous, with areas of sediment injections into the underlying basement, and “elongated boulders” of sediment displaying fractures (Le Heron et al., 2021) i.e. an appearance partly similar to jigsaw-puzzle textures which are common in sediment gravity flow deposits (Dufresne et al., 2021; Molén 2021). Furthermore, in Namibia, Martin (1981) described "pre-glacial valleys" that were glaciated and also crossed obliquely by glaciers. As the valleys are interpreted to be mainly pre-glacial, perhaps originating by tectonism and glaciated during the Neoproterozoic (Bechstädt et al., 2018), it may be difficult to know if there is any impact from more recent glaciers, as the pre-glacial appearance is still present. The descriptions of these valleys are general glaciogenic interpretations of different geologic features (Dietrich et al., 2021), but details which have not been documented may often reveal alternative interpretations of, for example, striations and roche moutonnées (Molén, 2022a, 2022b). Namibian ("pre-glacial") valleys do not display typical characteristics of fjords (i.e. no ridge at the outlet, not narrow) despite it may be the current interpretation (Dietrich et al., 2021). Valleys in northern South Africa have uneven floors (Visser, 1987). The Virgina Valley (Orange Free State), which has been described as a fjord, does not display the typical narrowness, overdeepening and a prominent "sill" or ridge at the outlet typical of fjords (Magnerud et al., 2019), but is a rather wide and shallow valley (Visser & Kingsley, 1982). Hanging valleys, including in magmatic/metamorphic bedrock, are often present in subaqueous and other non-glacial canyons (Dill, 1964; Shepard & Dill, 1966; Mitchell, 2006; Lamb, 2008; Amblas et al., 2011; Normandeau et al., 2015), and are not exclusive to glaciation. Hanging valleys that have been reported from the Dwyka Group may therefore be interpreted to be non-glacial (Visser, 1982; Hancox & Götz, 2014). U-shaped valleys commonly form by non-glacial processes, so the shape by itself is not evidence of glaciation (Lamb, 2008; Amblas et al., 2011; Coles, 2014; Puga Bernabéu et al., 2020).

The Dwyka Group sediments consist of very complex layered successions with many diamictites, sandstones and shales superimposed or interfingering with and/or eroded into each other (Visser et al., 1987; Visser & Loock 1982, 1988; Visser, 1988, 1989a, 1989b; Dietrich & Hofmann, 2019), similar to and often interpreted to be sediment gravity flow deposits. The glaciogenic outcrops both in South Africa and in South America, have lately been reinterpreted to have originated from many smaller glaciers and not one large glacier that was continuous and covering large parts of Gondwana (Dietrich et al., 2019; Fedorchuk et al., 2019), even though there is still an ongoing discussion (Craddock et al., 2019; Griffis et al., 2021). Therefore, reinterpretation of the Dwyka Group diamcitites may not affect the interpretation of any other Gondwana diamictites, as the glaciation at any rate is considered to be patchy or discontinuous during its long duration. Massive diamictites have been discovered to be often stratified and to be aprons, fans or debris flows and not deposited subglacially (Visser, 1994, 1997; Visser et al., 1997a; Huber et al., 2001; Haldorsen et al., 2001; Isbell et al., 2008; Dietrich & Hofmann, 2019; pers. comm., Johan Visser, 2020), and some authors believe that there are only very few places where there is subglacial basal/lodgement tillite (Visser, 1997; Isbell et al., 2008) while others are more likely to interpret diamictites as subglacially formed (e.g. Blignault & Theron, 2015). Horan (2015) reinterpreted much of the Dwyka Group as having been deposited in a large lake. All these new interpretations and data make it difficult to know what is considered to be primarily glaciogenic.

Where massive diamictite rests on igneous (or metamorphic) bedrock, there are often large areas displaying a thin layer (maximum 1 m in thickness) superimposed on the bedrock of brecciated and reworked but not (heavily) abraded bedrock material, similar to what may also be present discontinuously at the base of cohesive sediment gravity flows (Festa et al., 2016).

In addition there is evidence of soft sediment deformation or thinly bedded sedimentary deposits superposed on the breccia (Visser, 1981, 1997; Isbell et al., 2008), indicating a less powerful environment than underneath a glacier and similar to facies produced by sediment gravity flows. Such a sequence may be interpreted as tectonic shattering of the bedrock followed by sediment gravity flows (Molén, 2021). However, brecciation may also be formed in the basal shear zone below mass flows (Cardona et al., 2020), while bedrock in the subglacial environment is plucked and heavily abraded.

1.3.2. Dropstones and paleotransport

Outsized clasts which are generally interpreted as dropstones are present in the Dwyka Group and are commonly small (Tavener-Smith & Mason, 1983). Solitary clasts, well rounded or angular, which are enclosed by sediments with a similar appearance as around dropstones, commonly are also transported by floating vegetation and in sediment gravity flows. There are boulders up to 70 kg in Carboniferous coal seams (Price, 1932; Liu & Gastaldo, 1992), and boulders transported by modern floating (commonly larger) tree roots are up to 3 m (Bennett et al., 1996). In Cretaceous and Carboniferous sediments, boulders were transported up to 100 km by floating vegetation (Hawkes, 1943; Liu & Gastaldo, 1992). But more importantly, there is commonly an abundance of clasts, occasionally in sizes up to meters in diameter, within sediment gravity flow deposits and embedded in a clayey and in instances rhythmic matrix (e.g. Bouma, 1964; Embley, 1982; Molén, 2017, 2021, 2022a; Peakall et al., 2020). If the “dropstones” only display evidence of sediment draping and compaction, it may indicate a sediment gravity flow. If there is penetration of clasts, these may have been dropped by an agent but may also have been transported by sediment gravity flows (Kennedy & Eyles, 2021; Molén, 2021, 2022a, 2022b). Tavener-Smith & Mason (1983) and Haldorsen et al. (2001), document “dropstones” from South Africa which are mainly draped by or within single strata of rhythmites or other sedimentary strata, and Visser (1983b) describe outsized clasts in debris flow deposits, none that is different from occurrences of outsized clasts in non-glaciogenic deposits (e.g. Molén 2017, 2021; Kennedy & Eyles, 2021).

Rhythmites in the Dwyka Group have been interpreted to be deposited from turbidity currents or tidal activity (Isbell et al., 2008).

Within the diamictites, in what is described as the northern valley facies association of the Dwyka Group, most clasts are local. In what is described as the southern platform facies association (downstream from the northern valley facies) there is more far-transported material (Visser & Loock, 1982; Visser, 1986).

Paleoslopes in the area are commonly referred to, but seldom measured (e.g. Visser et al., 1997a), but there is no evidence of large areas with lower slopes than below that documented for sediment gravity flows or slides of 0.05-1°, in instances for up to distances of 1000 km (Yincan et al., 2017; Shanmugam, 2021; Molén, 2022a).

1.3.3. Pavements/striated surfaces

Usually striations and grooves on bedrock are curved and irregular below glaciers (Flint, 1961; Iverson, 1991). By contrast they are often straight if caused by tectonism or slides, and they may be both straight and curved due to sediment gravity flows but commonly are parallel or sub-parallel (e.g. Lindsay, 1970; Schermerhorn, 1970, 1971; Savage, 1972; Deynoux & Trompette, 1976; Glicken, 1996; Peakall et al., 2020).

Soft sediment striations and pavements are commonly produced below sediment gravity flows, including crossed striations up to 90°, and in rare cases below flow tills (which is a kind of sediment gravity flow) (Evenson et al., 1977; Kneller et al., 1991; Pickering et al., 1992; Dakin et al., 2013; Molén, 2022a), covering areas of up to c. 300 km^2 and for distances in excess of 40 km (Peakall et al., 2020). Soft sediment pavements have not been documented to commonly (or not at all) form by direct glacial action.

Striated surfaces are numerous within and underneath the Dwyka Group sediments, and are considered as probably the prime geologic evidence of glaciation. Many of the Dwyka striated surfaces were formed in unconsolidated material (Dietrich & Hofmann, 2019; Le Heron et al., 2019), and striations and grooves are often parallel (e.g. Savage 1972). In soft sediments, striated surfaces which are interpreted to be glaciogenic are often superimposed, or stacked, in many layers above each other. Similar stacked surfaces with parallel striations are not known from Pleistocene deposits where it is known that glaciers were the final depositional agent. They are similar to so-called tectonic hydroplastic slickensides or internal grooves and striations that form in soft sand and mud (Enos, 1969; Petit & Laville, 1987; Simms, 2007; Cesta, 2015; Le Heron et al., 2014), but they are sometimes interpreted as internal movements in sand caused by overriding ice (Deynoux & Ghienne, 2004; Le Heron et al., 2005, 2019).

Commonly the Dwyka Group striated surfaces/pavements display features which are strikingly different from Quaternary glacially striated surfaces. Six examples of such differences are:

a) Striations continue unbroken from on top of a "tillite" into the striations on the pavement below (Flint, 1961).

b) Striations are present in triple superposed/stacked soft sediment surfaces on top of a striated surface/pavement in Ventersdorp lava (Visser, 1988).

c) Thin soft sediment beds are present between striated pavement and diamictite (Slater et al., 1932; Visser, 1988; Visser & Loock, 1988).

d) A soft sediment striated surface is cut into ripple laminated siltstone (Visser, 1983a).

e) Fossil plants are present on top of a striated pavement and compressed below "tillite" (du Toit, 1926; Sandberg, 1928).

f) A soft sediment striated surface is draped with mudrock with crustacean track ways, which passes up to diamictite (Von Brunn, 1996).

1.3.4. Interpreting climate data

The model calculations of pCO_2 during the Phanerozoic are inconclusive (Montañez et al., 2016; Myers, 2016; Dahl & Arens, 2020), and recent reviews of paleotemperatures had to dismiss about half of the data to make it fit in with current interpretations of paleoclimate (Scotese et al., 2021). The $\delta^{13}C_{org}$ does not change in the post-glacial Ecca Formation which conformably overlies the Dwyka Group (Scheffler et al., 2003). The $\delta^{13}C_{org}$ in the Dwyka Group is displaying evidence of primarily an algal origin (Scheffler et al., 2003). Therefore ^{13}C-discrimination cannot be used as a final answer for past CO_2-levels.

The fossil vegetation of the Late Carboniferous and Early Permian South Africa deposits does not include plants described as displaying physiological adaptations typical of cold or subpolar climate species (Anderson & McLachlan, 1976; McLoughlin, 2011; Hancox &

Götz, 2014). Fossils of the Glossopteris flora are closely associated with the Dwyka Group diamictites, and have even been discovered between "tillite" and the underlying "ice-polished bedrock" (du Toit, 1926; Sandberg, 1928). Coalified plant fragments also occur within massive "tillites", and coal seams are often situated superimposed on, or between, "tillites" (Anderson & McLachlan, 1976; Stavrakis, 1986; Stavrakis & Smyth, 1991; Visser, 1989a; Hancox & Götz, 2014). Coal seams that may be interbedded with "glaciogenic" diamictites have in many instances coalesced with other coal seams to form one thick coal seam (Stavrakis & Smyth, 1991). The mixing of diamictites and coal beds of the Dwyka Group may be considered to be a result of reworking (Hancox & Götz, 2014), but coal seams that are interbedded between stacked Dwyka diamictite deposits are often thin, and complete sequences appear to be a kind of debris flow deposits (Hancox & Götz, 2014). Some deposits may be considered to be hyperpycnite beds sorted into dense and diluted parts with or without plant material, and these deposits may later transform into a full spectrum of sediment gravity flows (Zavala & Arcuri, 2016; Shanmugam, 2019; Zavala, 2019, 2020). The absence of fossils in most parts of the Dwyka Group deposits may be an indication of water depth or transport distance, i.e. deeper water or sorting during longer transport. Fossils are seldom reported from within debris flow deposits, but in Holocene glaciogenic deposits there may be trees and other plants if these were growing nearby (Fleisher et al., 2006; Ryder & Thomson, 2011).

As most of the Dwyka Group has now been reinterpreted as "glacial marine" deposits from a middle paleolatitude far from the South Pole (Craddock et al., 2019; around 30-60°S as depicted by Kent & Muttoni, 2020), it makes it difficult to distinguish these deposits from non-glacially derived sediment gravity flow deposits. Some parts of the wide-spread Permo-

Carboniferous “tillites” have previously been interpreted to have been deposited close to 30°S (John, 1979; Chumakov & Zharkov, 2002; Catuneanu et al., 2005; Kent & Muttoni, 2020), while at about the same time there were apparently no (or very limited in area) glaciers at the Permo-Carboniferous South Pole in Antarctica (Isbell et al., 2012, 2013; Montañes & Poulsen, 2013; Craddock et al., 2019). Likewise, there was no glaciation in South Africa when it was at or close to the South Pole during the Devonian and Early Carboniferous even though glaciation has been interpreted in South America at the same time (Ruban et al., 2007; Kent & Muttoni, 2020; Caputo & Santos, 2020). So a polar position by itself does not indicate glaciation per se.

2. Research area

The general geology and stratigraphy of the Dwyka Group has been thoroughly documented by many researchers. The current work is based on these former descriptions of the research areas and will not be repeated here. The question is whether or not the current climatological interpretation is correct. Several documented diamictite and striated surface/pavement outcrops of the Dwyka Group were chosen for field work, to investigate features that might shed light on their origin. Samples for SEM-research were collected from Dwyka diamictite deposits from geographically distant parts of South Africa, to cover both the northern and southern area. Whenever possible, samples were collected at different levels and outcrops. Striated surfaces were studied at Nooitgedacht, Douglas, Oorlogsklof and Durban.

All research areas are marked in Fig. 1 and listed in Table 1. (Detailed descriptions are in Supplemental material.)

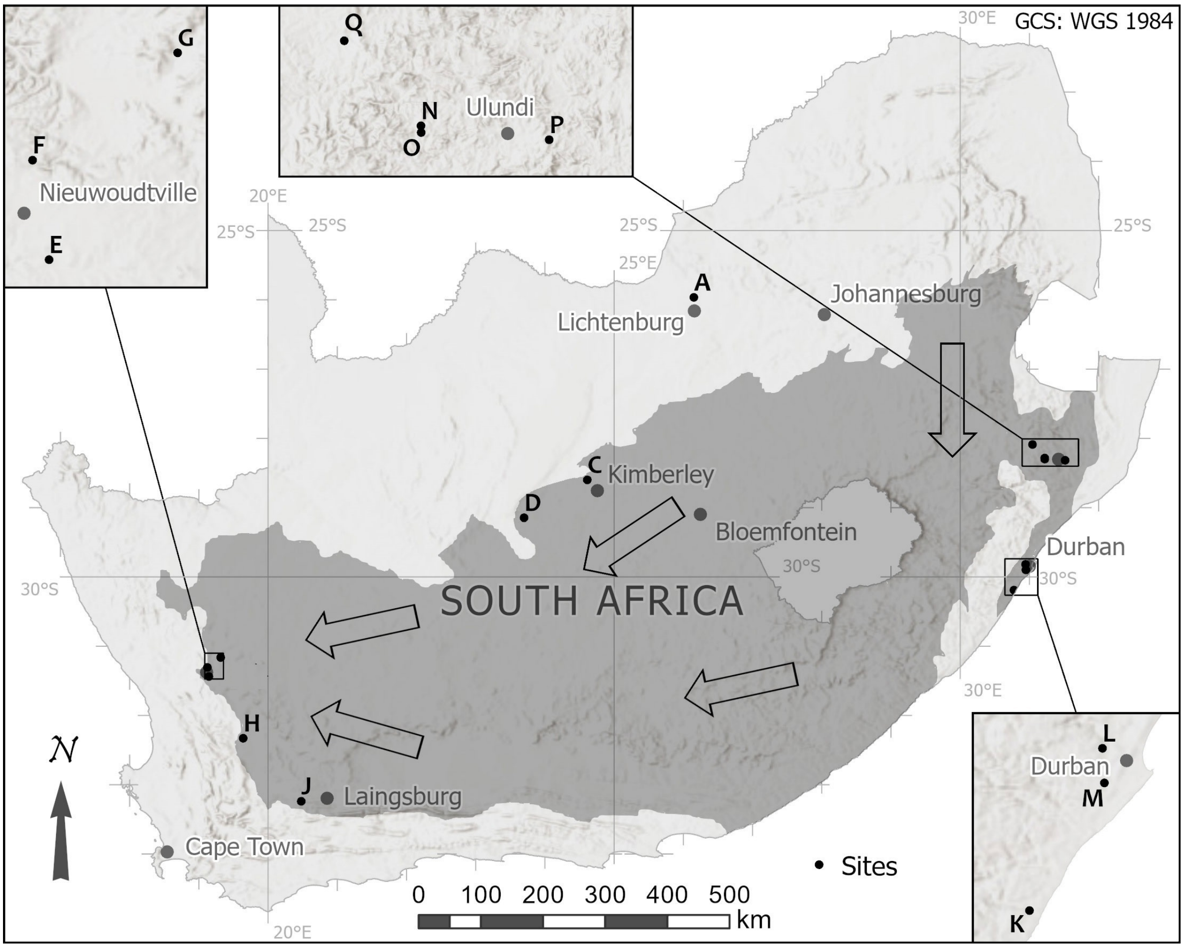

Fig. 1. Research area and field locations. C is Nooitgedacht, diamictite and striated surface. D is Douglas pavement. E is Oorlogsklof, soft sediment pavement. F is Nieuwoudtville. G is Kransgat River, Koringhuis. H is Elandsvlei. J is Matjiesfontein. K is Umkomaas River

Valley. L is Durban University of KwaZulu-Natal Westville Campus. M is Durban, Coedmore Quarry. N is West of Denny Dalton. O is Southwest of Denny Dalton. P is east of Ulundi. Q is Surreyvale. The Karoo Basin is marked with darker color, approximately, after Catuneanu et al. (2005). General major ice-flow directions, large arrows, after Visser (1997) Cape Geosites (2014) and Dietrich & Hofmann (2019).

3. Methods

Pavements were recorded and documented in the field, as reported in Results. SEM methods are described below.

3.1. SEM studies of surface microtextures on quartz sand grains.

The generation of surface microtextures during glaciation is well documented (Mahaney, 2002; Molén, 2014, 2017). Even if the final deposition of sediments may be non-glaciogenic, e.g. sediment gravity flows or rainout till that do not reshape the complete grain surfaces and leave little or no imprint on the grain surfaces, the surface microtextures will display evidence of a former glaciogenic history (Molén, 2014). Only if grains have been dumped onto the top of a glacier (supraglacial), or transported inside the ice (englacial) and never reaching the basal part of the glacier, or in periglacial sediments, typical glaciogenic surface microtextures will not be generated (Molén, 2014, 2017; Woronko, 2016). Surface microtextures will originate quickly and in large numbers, only if it is an all penetrating and continuous energetic environment like below a glacier, and these surface microtextures will probably almost immediately display evidence of subglacial stress (Molén, 2014). In a less all penetrating energetic environment there has to be an extended time period to create numerous surface microtextures. In sediment gravity flows the energy dissipation is momentous and more "sporadic", which may create fractures on single grains but commonly not simultaneous irregular abrasion on the same fractured surfaces.

The methods used in the current study were especially detailed and designed a) to discover any evidence of mechanical and chemical artificial generation of surface microtextures during sampling and laboratory work, and also b) to remove any post-depositional grain coatings (Supplemental material). The more general methods are documented in detail by Molén (2014), and SEM-methods are shortly described in Tables 2-3.

In total 71 samples were processed for SEM (Table 1). Surface microtextures on quartz grains are best displayed on the size fraction 0.25-2 mm (Molén, 2014), and therefore this size fraction is analyzed in the current research. Commonly 30-50 grains were studied from each sample, and hundreds of grains from each research area, in order to detect and then avoid any possible anomalies in the subsamples. Detailed descriptions are in Supplemental material.

C. Nooitgedacht, diamictite on Ventersdorp lava pavement.

C-1-1	Thin black hard diamictite crust on top of pavement.
C1b, C2a C2b, C2bb, C2c, C3a, C3b, C3c, C4	Diamictite. C1b, C2b, C2c, C3b and C3c are stratified.
C3bm	String 1-10 mm of sediment between pavement and diamictite.

C4m	Black string 2-3 mm of sediment between pavement and diamictite.
F. Nieuwoudtville.	
F1a, F1aa, F1b, F2, F2b, F3a, F3b. F3c, F5	Diamictite. F5 is stratified.
F4, F4b	Conglomerate.
F4c	Weathered sandstone pebble in sample F4, i.e. source rock.
G. Kransgat River, Koringhuis homestead/farm.	
G1a, G1b, G1c, G2a, G2b, G2c	Diamictite.
H. Elandsvlei farm area	
H1, H1a, H2b, H2c	Diamcitite
J. South of Matjiesfontein	
J1a, J1b, J1c, J1d	Diamcitite
K. Umkomaas River Valley	
K1a, K1b, K1bb, K1c, K2, K2b, K3b, K3c	Diamictite.
L. Durban, University of Kwazulu-Natal Westville Campus.	
L1, L1b, L1br, L1c	Mainly sand and silt. Pavement.
M. Durban, Coedmore Quarry.	
M1, M2, M3, M4, M6	Extra hard, much clay. Black.
N, O. Denny Dalton.	
N1a, N2a, N2b, O1a, O2	Diamictite.
P. R66 at Ulundi.	
P1, P1a, P3a, P3b, P5b, P5c, P5e, P5 norm., P5s.	Diamictite. P5s is thin sandy string.

Q. Surreyvale.	
Q1, Q3	Diamictite.

Table 1. General descriptions of all Dwyka Group samples. All samples consist of > 90% clay, silt and fine sand, except if otherwise mentioned. Details are in Supplemental material.

3.1.1. Methodology for SEM studies and surface microtextures classification

The method used to study surface microtextures is based on geological processes and not only the general appearance of grain surfaces (Molén, 2014; Table 2). The surface microtextures are ordered in a 2-History Diagram, depending on the freshness of the grain surfaces (Table 3, Figs. 2-7), for interpretation and visual documentation of the geological history. This diagram, with enhancing connecting lines, also displays an easily distinguishable "geological signature" of the appearance of each sample, which will not show up in a histogram or any other diagram (Molén, 2014). Definitions and labels are in accordance with Tables 2-3.

History-1 surface microtextures are defined as recent, i.e. they are defined as having been generated by the last geological process which shaped the grain surfaces, and except for weathering surface microtextures, appear to be fresh. History-2 includes all surfaces which display weathering that shaped the grain preceding the origin of the History-1 surface microtextures, and are labelled as F2, f2, A2, SP2, EN2 or C2.

The geological history of quartz grains starts with crystallization from a magma or in a metamorphic rock (EN/C), then release from bedrock (F/f), transport (F/f/A) and weathering

(SP), in different combinations. For example, weathered grains, released from bedrock and then abraded by ice will document large fresh fractures and (irregular) abrasion as the most recent geological history (History-1) and weathered surfaces and crystal surfaces from a previous history (History-2) of the host bedrock, i.e., F1, A1, SP2 and EN2 or C2. Small scale fractures (f) often are of lesser genetic importance, as they easily originate from small forces/collisions and may almost always be hypothesized for History-2.

Some researchers may only record a few minute surface microtextures, which may originate in different environments, on a small sample of grains, as evidence to deduce an interpretation of the origin of a sedimentary deposit, while the overall appearance of all surface microtextures on a large number of grains in the deposit may indicate a different origin.

MECHANISM	**MICROTEXTURE**	**ENVIRONMENT**
Crushing	large scale fractures (**F**)	glacial, tectonic, crystallisation, rock slide/fall, high energy environments
	small scale fractures (**f**)	water, glacial, wind, gravity flow
Abrasion	rounded edges, rounded microtextures, grooves (**A**)	water, glacial, wind, gravity flow
Chemical	solution, precipitation (**SP**)	weathering, contact reactions, lithification

Crystal growth	embayments, nodes (**EN**) crystal surfaces (**C**)	metamorphism, crystallization precipitation, lithification, crystallization

Table 2. The predominant processes that influence the surface of a quartz grain, and symbols/abbreviations for the different surface microtextures (details in Molén, 2014, but this table is partly modified to include more variations of surface microtextures).

SM	**AREA COVERAGE**	**EXCLUDES**
F1	≥20-25%; or sum of many 5-20% **f1** covering ≥50-55%	**f1** (except if many ≤4% covering ≥10-15%); and **SP1** (except if sequence of origin is unknown)
f1	5-20%; or sum of many ≤4% covering ≥10-15%	
A1	≥15-20%	
SP1	≥10-15%	**SP2** (except if sequence of origin is evident)
EN1	≥10-15%	
C1	≥5-10%	
F2	See definition of **F1**	**f2**

Table 3. Definition of surface microtextures (SM). Percentages are approximate and calculated from comparison of how large an area of the grain surface which is covered by a surface microtexture. If, for example, many very small f1, about 4% or less coverage each, in total cover more than 10-15%, then both F1 and f1 are recorded as surface microtextures. There are many special small-scale fractures in this size, which are recorded in tills and other environments (Mahaney, 2002; Molén, 2014). The percentages of the History-2 surface microtextures are similar to the History-1 definitions, except that they are weathered.

The quartz grains that were recorded in the current research were divided into two main groups, those with and without fresh F1-fractures, but only if F1 was the single surface microtexture in the most recent history and there were no other fresh surface microtextures like EN1 or A1. The reason for this was twofold: 1) It is unknown how many fractures are from a) depositional processes or from b) post-depositional processes like compression or recent anthropogenic road construction/mining work or sampling/laboratory processes, and if 2) there is a mix of grains displaying only F1-fractures as the most recent history and grains displaying A1/SP1, this mixture of grains will skew the result in a 2-History Diagram (Molén, 2017).

The A1/SP1 group was used in most analyses and interpretations of the geological history of the diamictites, as these had not acquired any single recent/final fracturing.

The SEM analysis of the Dwyka Group samples was conducted with a "table top" Hitachi TM

3000 equipped with a backscattered electron detector for imaging and an energy dispersive X-ray spectrometer (Bruker, Quantax 70 system) for element analysis. Imaging was done at both 5 and 15 kV and element analysis at 15 kV with a high probe current.

.

4. Results

4.1. SEM studies of surface microtextures.

4.1.1 Documentation of surface microtextures.

The details of the laboratory processes and field data from all South African samples are documented in Supplemental material.

The 71 Dwyka samples analyzed included 4271 quartz grains of size 0.25-2 mm. Of these 664 grains displayed F1 as the single most recent surface microtexture (and no other History-1 surface microtextures). In this study 3110 grains from diamictites which have been interpreted as tillites or reworked tillites, which had not been simply fractured (i.e. no single F1), displayed A1/SP1 for between 96-100% of the grains (Fig. 7). These grains also displayed f1 (9-24%) and/or only SP1 with no abrasion. Other sediments, i.e. sediments in between the striated surface and diamictite (samples C3bm and C4m), a small conglomerate (samples F4-F4c), and sandstone (samples L1-L1c), displayed 83-100% A1/SP1.

4.1.2. Comparison of surface microtextures of South African diamictites to Quaternary glacial deposits

In order to reveal any similarities to till, quartz grains from the South African diamictites were compared to quartz grains deposited from Quaternary glaciers (Figs. 2-7). The result is displayed in a 2-History Diagram (Fig. 7). In order to compare to different glaciers, a till deposited from the thinnest, recent glacier studied was chosen as an example of a very low degree of processed till, i.e. Tärna Glacier in Västerbotten County, Sweden (Molén, 2014). This glacier was probably no more than c. 10-30 m thick at the place where this till was deposited, and such a small glacier will not impose large forces on the grains (Figs. 2G-H). With this comparison, evidence of even a very thin Dwyka glacier could be detected. Comparison was also made to Pleistocene tills which were deposited by large continental glaciers with different substrata (Figs. 2E-F), Precambrian magmatic/metamorphic shield in Västerbotten, Sweden, and mainly a sedimentary Paleozoic substratum in Southern Ontario, Canada (Fig. 3B; Molén, 2014).

In Fig. 7 the result of the documentation of surface microtextures from the Dwyka Group diamictites for the group A1/SP1 are in one group, as all samples are almost identical. If the diagrams displayed a mix of quartz grains from different geological histories, this scatter would blur the diagram, and information would be lost (Molén, 2017). Therefore, all grains with unaltered large fractures (F1) as the single most recent geological incident, and no other recent (History-1) surface microtextures like chemically unweathered abrasion (A1) or weathering (SP1), are not included in the diagram that shows all diamictites. (More detailed discussions, including examples of photomicrographs, are in Supplemental material.)

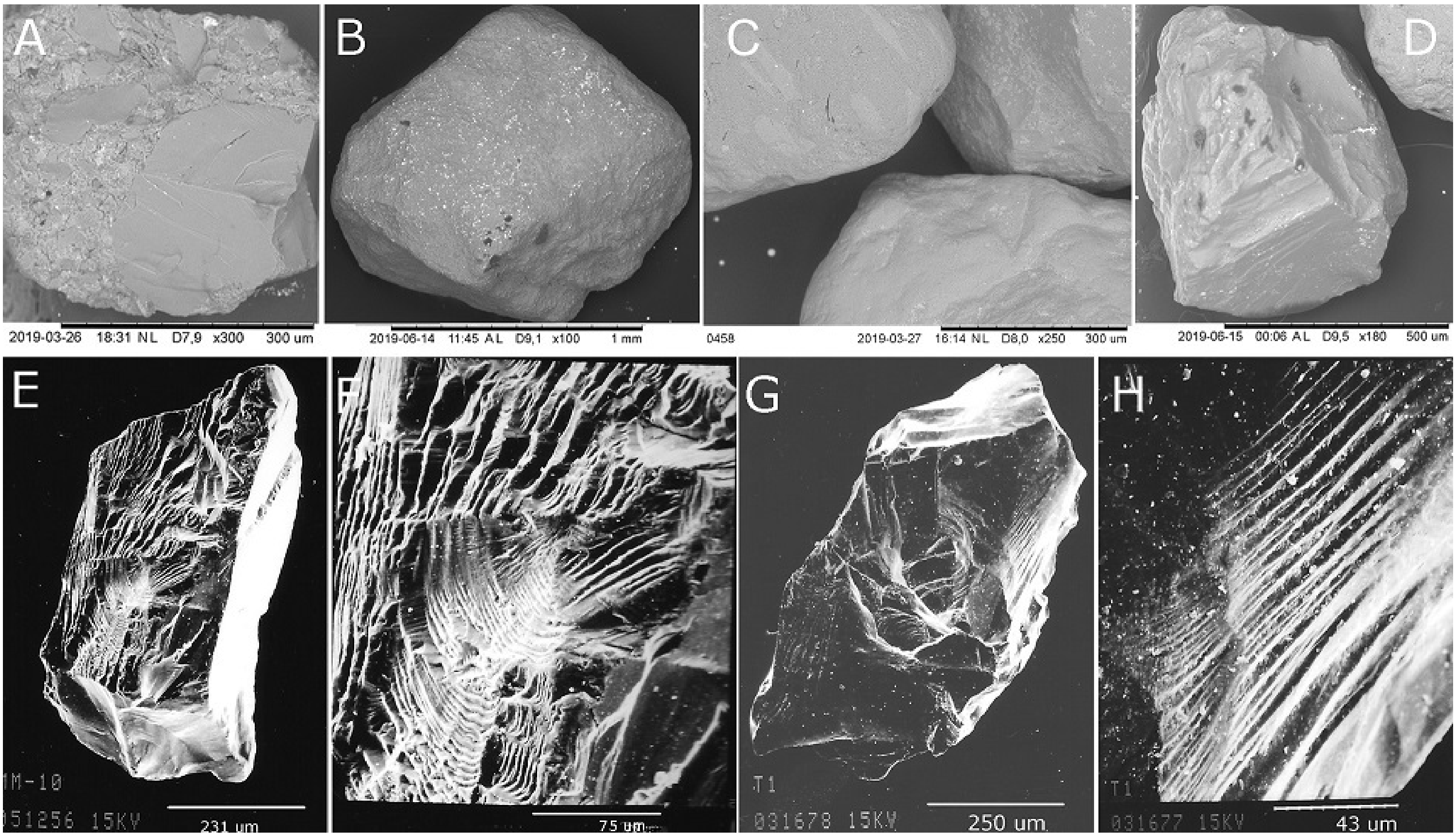

Fig. 2. A-D, Dwyka Group. E-H, Quaternary tills, Sweden (Molén, 2014). A – Three quartz grains embedded in silt and clay, similar to all samples from the Dwyka Group (sample F4, a conglomerate). The grains are already fractured inside compact and lithified clay, which makes it likely that the fractures originated during transport and deposition in the conglomerate. B – A typical grain from the Dwyka diamictite samples. These grains are commonly regularly abraded and weathered (A1/SP1), and many have been fractured before abrasion/weathering, i.e. the grains may display F2 or f2. Grain is classified as A1, SP1, f2 (sample C3a, Nooitgedacht). C – Closeup of three typical Dwyka Group grains (sample O2, Denny Dalton). All grains display A1/SP1. The upper two grains also display F2. D – Sample G2b, from the site that was interpreted by Visser (1996), as having been deposited in front of a grounded marine ice sheet. This quartz grain displays the most general overall similarities to a glaciogenic grain, of all quartz grains in this study. The original appearance of this grain

was probably multicyclical. The grain was later heavily fractured. The fractures have been subsequently weathered and regularly abraded, i.e. the fractures have not been abraded much in one place and little or not at all in other places (i.e., they are not irregularly abraded), but there is evidence of regular/“soft” abrasion and weathering all over the grain. Grain is classified as A1, SP1, F2. E – Example of a quartz grain from Pleistocene waterlain till, from an area of magmatic/metamorphic bedrock substratum, Sweden. The appearance of the grains from this site is very different compared to that of all South African grains, including the grains from sample G which have been interpreted to be rainout till in front of a grounded marine ice sheet (Visser, 1996) (e.g. Figs. 2D and 5). The grain in the picture is heavily fractured and irregularly abraded. Irregular abrasion is more evident at bottom right (fracture is rounded only at the corner and at lowermost right bottom), and bottom left (only the left part of the fracture is abraded). F – Closeup of the grain in picture E which shows that the white areas of the fractures, in the middle and lower left, are more abraded than the other fractures. G – A grain from Tärna glacier, Sweden, a thin Neoglacial glacier. This grain is heavily fractured and irregularly abraded unlike all Dwyka grains. H – Closeup of grain in picture G which shows that fractures have been irregularly abraded, as is typical of glaciogenic grains. But, as this glacier is very thin, there is not much abrasion on the grains from this area.

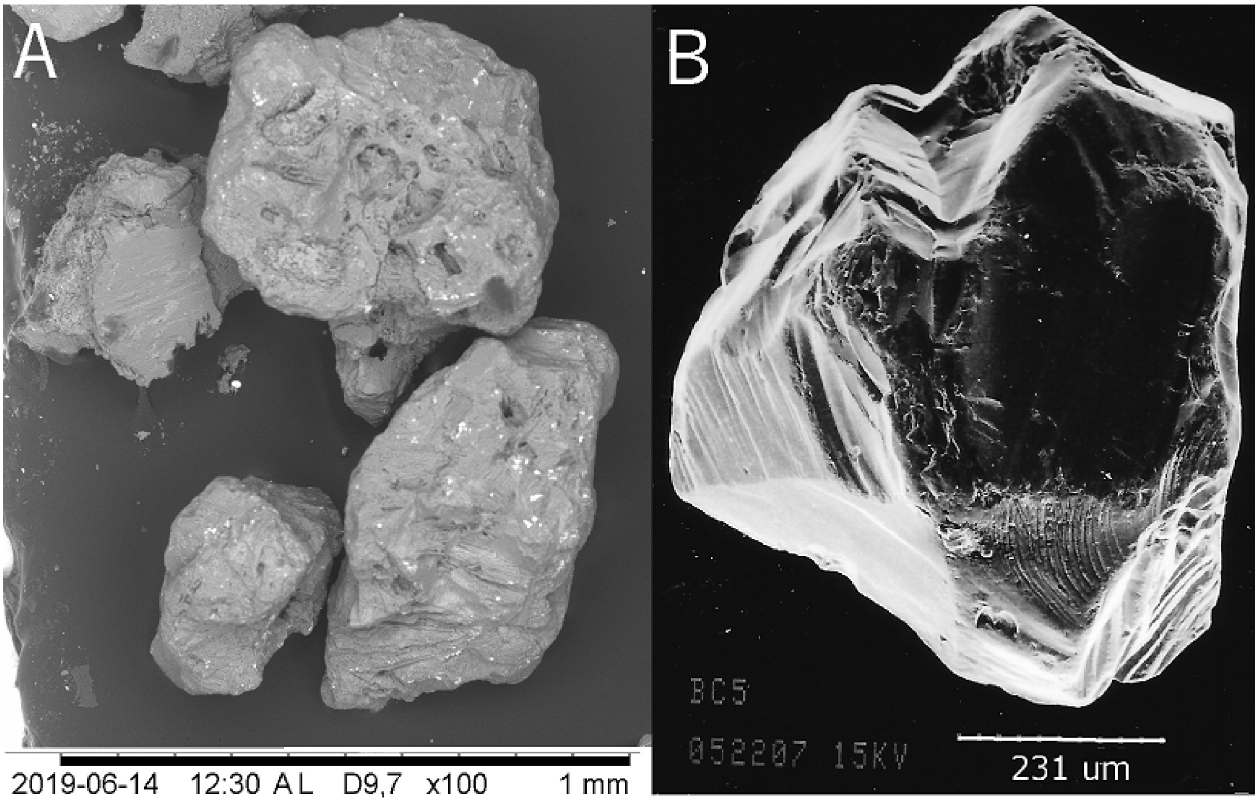

Fig. 3. A – Sample C4m, the thin dark sedimentary layer between the diamictite and the striated pavement. All four quartz grains are heavily weathered. One grain displays a large fracture which is classified as F1 (upper left grain). B – Grain from Pleistocene till in Southern Ontario (Molén, 2014). The source area for this till is similar to much of the source material of the Dwyka diamictites, i.e. a substratum of multicyclical sedimentary rocks or sediment. This grain is heavily fractured, over and over again (the fractures have acquired subsequent fractures on top of or through them without any weathering in between), but the general outline of a multicyclical grain is still evident. The abrasion is strong and irregular, i.e. not the same on all surfaces, as is typical of glaciogenic grains. Classification is F1/A1.

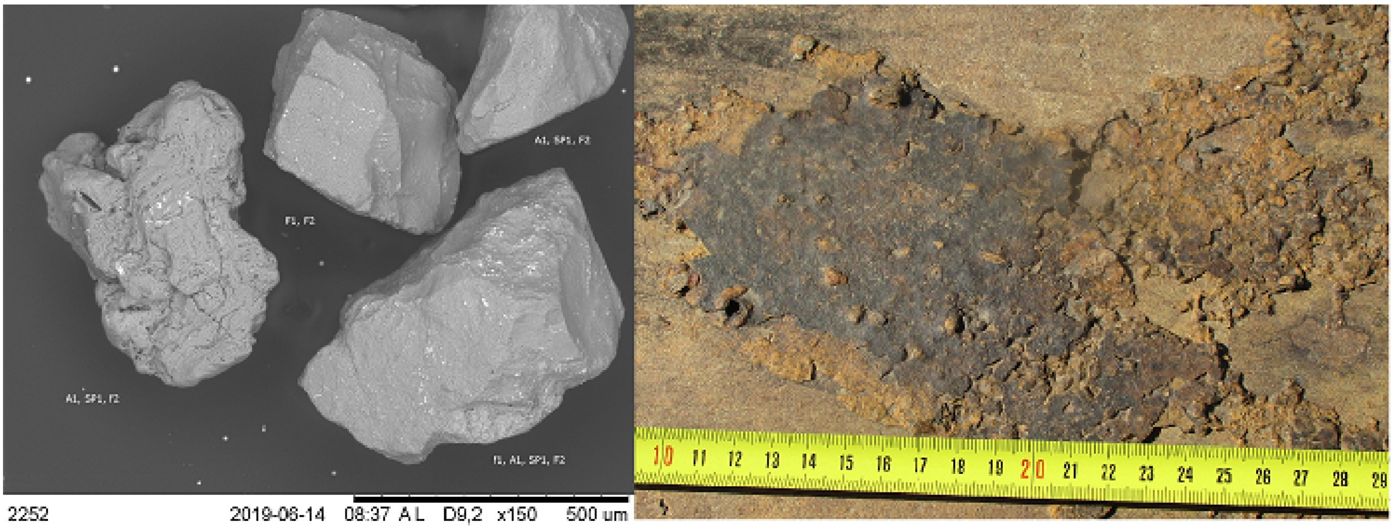

Fig. 4. Quartz grains from sample C-1-1 from the thin, blackened by weathering, diamictite crust directly on top of the Ventersdorp lava, Nooitgedacht pavement (right photo). The quartz grains are labelled with the identified surface microtextures. The grain on the left is similar to many of the quartz grains from the thin dark sediment between the diamictite and the pavement (sample C4m, Fig. 3A). The two grains to the right are more or less fractured and rounded and display the most common surface microtextures A1/SP1, combined with other surface microtextures. The middle upper grain only displays fractures, which in larger magnification could be sorted into older and more recent fractures. No grain show irregularly abraded fractures typical of glaciogenic grains. There are only fractures which have been regularly abraded, or not abraded at all, and weathered grains (i.e. multicyclical grains, most recent history is A1/SP1).

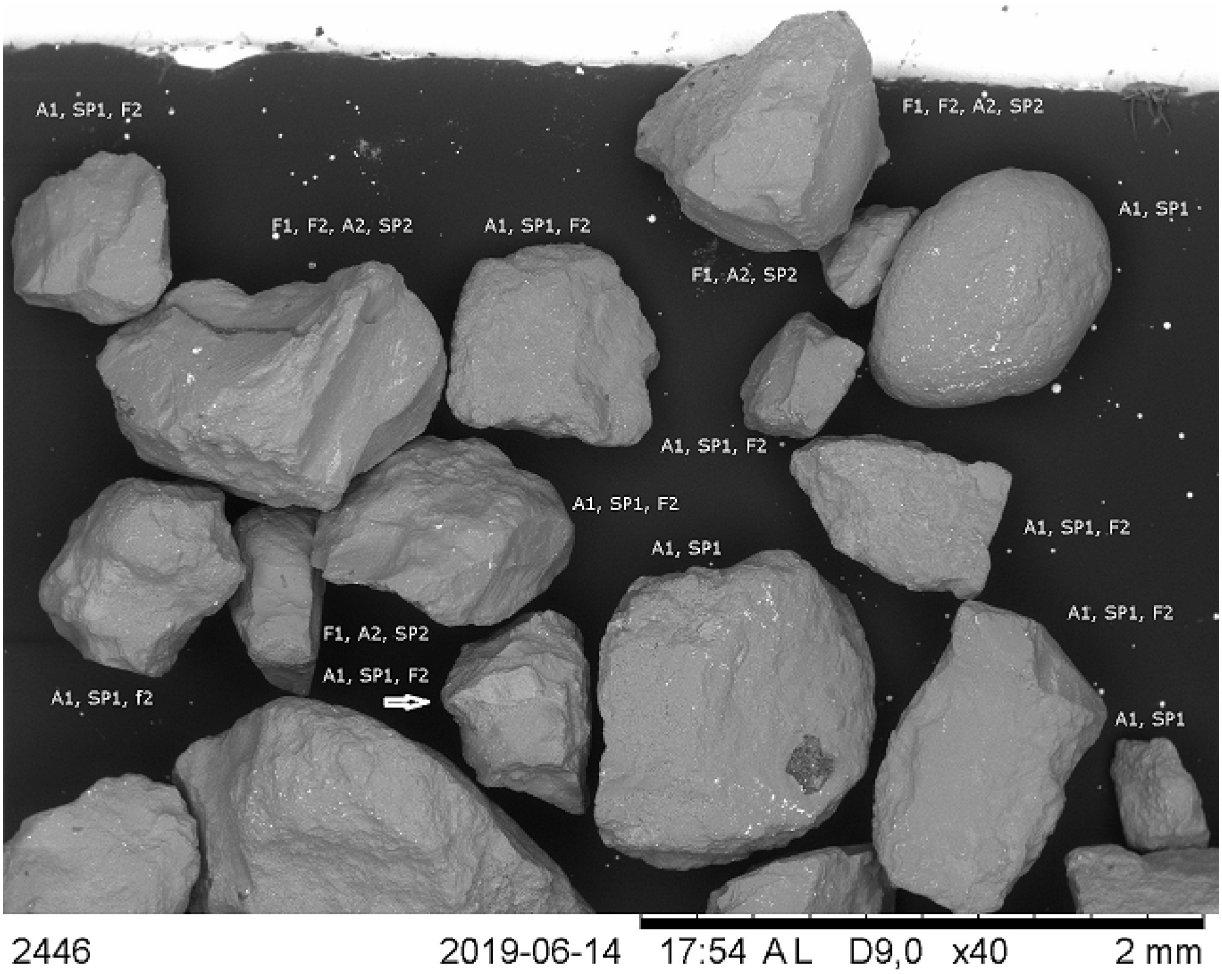

Fig. 5. Sample G1a, “deposited in front of a grounded marine ice sheet” (Visser, 1996). These grains are very different from e.g. Pleistocene waterlain till from Scandinavia (Figs. 2, E-F; Molén, 2014). Some grains are almost spherical, and none display the typical glaciogenic appearance of fractures that have been irregularly abraded. If the grains are fractured, the fractures are either solely sharp or otherwise more or less regularly rounded all over their edges, i.e. display regular abrasion which is common in for example aqueous environments but not formed by glaciers.

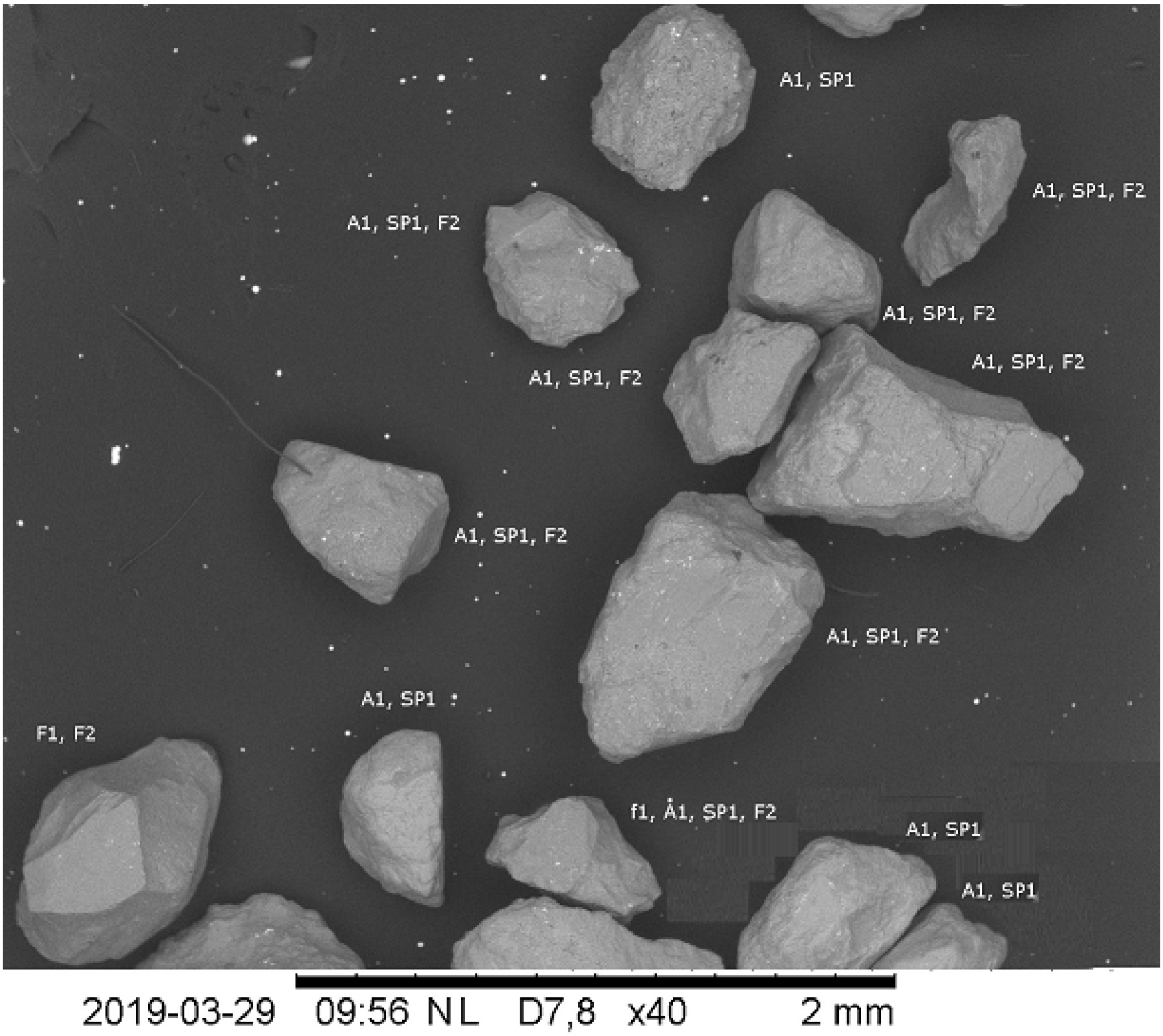

Fig. 6. Grains from sample M2, from Coedmore Quarry, Durban. There are no glaciogenic surface microtextures on any grain.

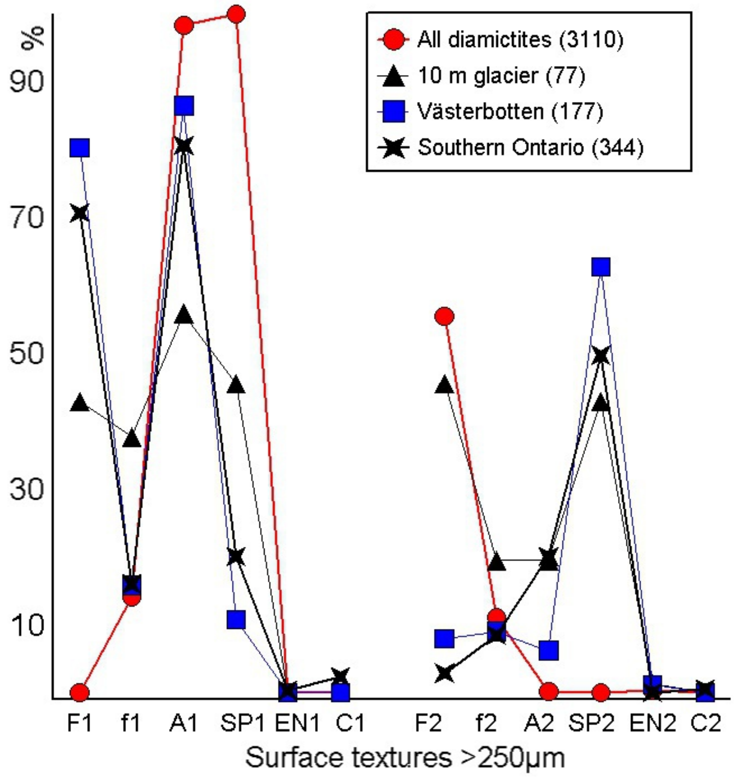

Fig. 7. A 2-History Diagram displaying all Dwyka Group diamictite grains that do not show unaltered F1. (Samples C3bm, C4m, conglomerate (F4:s) and striated surface (L1:s) are not included.) Dwyka diamictites (**circles**) are compared to relevant examples from Pleistocene and recent glaciers. Curve marked by **triangles** is from the smallest glacier studied by the present author, probably not much more than 10-30 m thick (Tärna Glacier, Neoglacial; Molén, 2014). Curve marked by **squares** is from tills deposited by thick Pleistocene glaciers with magmatic/metamorphic bedrock as source rocks, Västerbotten County, Sweden. **Star** marked curve is from Southern Ontario, Canada, Pleistocene glaciation, from tills originating to a large part from sedimentary bedrock. The connecting lines in the diagram are drawn to enhance visibility, as described in Molén (2014). These lines are important, as they indicate the general trend of the different surface microtextures, and therefore easily visualize a distinguishable “geological signature” of the appearance of each sample. The latter will not

show up in a histogram. Typical geological signatures in this diagram are multicyclical (A1/SP1, all diamictites), large glaciers (much F1/A1) and small glacier (less F1/A1). Number of studied quartz sand grains within parentheses, inside box.

4.2. Pavements

The four striated surfaces/pavements that were studied in the current work display clusters of mainly parallel striations. The only pavement that was covered by a confirmed diamictite was at Nooitgedacht. Iverson (1991) described the appearance of glacial striations as generally short and deflected, due to internal clast movement inside the glaciers. The striations documented in the current research displayed many different appearances.

4.2.1. Nooitgedacht

The pavement area at Nooitgedacht is probably the best known of all pre-Pleistocene pavements in the world. Many small outcrops displaying striated surfaces are exposed in an area of a few thousand square meters (Slater et al., 1932). The striated surfaces are formed on top of Neoarchean Ventersdorp Supergroup andesite lava and are subjacent to diamictites.

The pavements display striations with different appearances in distinct areas. Master (2012) identified three main sets of bearings: 1) 225°-232°, 2) 240°-256° and 3) 203°-216°. But, there is a large variation of bearings, which is partly controlled by small local highs or steep surfaces (Fig. 8A). A more detailed investigation of striations and grooves show that they are commonly ordered in distinct “groups” displaying different appearances and bearings. Each group commonly displays internally parallel straight striations (Fig. 8B).

- Some areas display striations in so many directions that they appear to be fan shaped. Upon closer inspection, however, they appear to be clusters of parallel striations displaying different bearings, meeting and crossing each other at different points (Fig. 8B).
- The striations are often up to about a meter in length for the thinner ones, and longer for thicker/grooves. Deeper striations or grooves are often many meters long (Fig. 8C). Usually these are straight, parallel if two or more are next to each other, but not curvilinear (even if some may show diversions, as is also possible by gravity flow induced striations).
- On steeper surfaces striations are deflected but may still remain more or less parallel (Fig. 9).
- In some areas (Fig. 9A) striations are very short, more than 80% may be less than 10 cm long, and only 2% may be longer than 50 cm (100 striations measured, Supplemental material).
- In some places there is a thin veneer-like layer of diamictite material on top of the striated surface which has been molded into soft sediment grooves and ridges (Fig. 10).
- After removing the diamictite a very thin brown colored sediment was evident, which was plastered onto the volcanic striated surface (Fig. 10C). Sedimentary relationships similar to this were also observed at other striated surfaces (e.g. Fig. 11A). This sediment in between the diamictite and the striated volcanic surface was almost totally molded into small and large ridges and grooves displaying an appearance of striations (Fig. 10C). In the area just outside of the diamictite cover, the brown sediment had turned black by weathering and had been partly removed by weathering/erosion, and there is only a very thin dark/black sediment left with few of the striations from the brown sediment preserved. Furthermore, where the black sediment had weathered away, the volcanic

basement surface displayed even fewer and less deep striations than on the black sediment surface (Fig. 10C). In conclusion, most of the striations and grooves were only present as soft molded sediment, and only a few of these passed through the sediments and down onto the volcanic basement pavement.

- At one site striations on Ventersdorp lava continued as soft sediment striations on a diamictite surface on the same plane (Fig. 11A).
- In a few areas no striations were recorded, or they were very thin. Some of these areas appeared to be small bypass zones as observed in sediment gravity flows (Fig. 11B) (Peakall et al., 2020; Cardona et al., 2020).

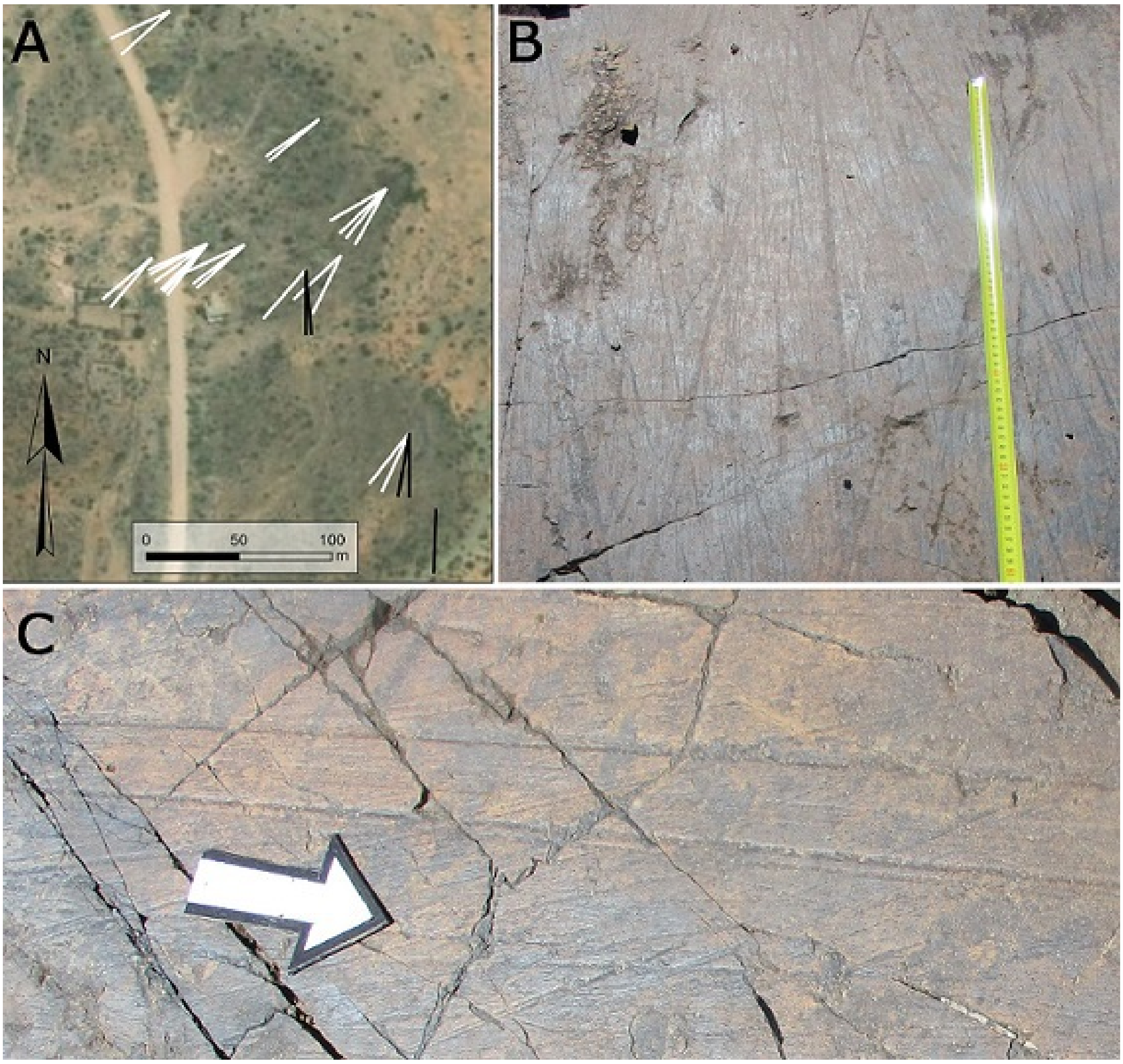

Fig. 8. Nooitgedacht. A – Google Earth image (-28.601, 24.612) displaying the main directions of the striations at different pavement outcrops at Nooitgedacht. The striations which are almost straight south (black lines) were deflected by local highs on steep surfaces. The pavement marked with one black line, in the far south, is photographed in Figs. 9B-C, and the one just above, displaying different bearings, is in Fig. 9A. B – Example from an area displaying thin striations which are commonly less than 1 m long, straight and in parallel groups, which make them appear as regular fans. Note that the striations are criss-crossing, forming almost a conjugate pattern. Ruler is 60 cm long. C – Two almost parallel grooves many meters long that were probably generated by one single clast. Thinner striations are crossing the grooves. Arrow is 25 cm.

The thin veneer of sediment between the striated surface and the diamictite was mentioned by Slater et al. (1932; see also Visser & Loock (1988) and Visser (1988), who described similar sediments in the near vicinity). The thickness varies between 1 and 10 mm (Figs. 10, 11A). The sediment display stratification on a mm scale, similar to the superimposed diamictite (Table 1). The thinner dark lower layers (e.g. sample C4m, Fig. 3A, but also partly sample C-1-1, Fig. 4) contain quartz grains which apparently came from a highly weathered area, possible a former saprolite.

The volcanic bedrock at Nooitgedacht often displays stoss sides that are steep and lee sides that are gentle, as opposed to roche moutonnées, but are labeled drumlinoid complexes by Visser (1988) and Visser & Loock (1988). At the lee sides there is often a short and steep flat regular scarp surface sloping down to a lower level of the volcanic bedrock displaying approximately the same angle (Figs. 9A, 11). At a few places more than one small scarp is present, with a flat surface between (Fig. 11B). The flat scarp surfaces are in some places striated. These regular structures display an appearence that is similar to cut sheeting joints. At one place striations in the bedrock continued to a diamictite surface that displays soft sediment striations (Fig. 11A).

The volcanic basement bedrock frequently display recent exfoliation in cm-thick layers, both on horizontal surfaces and inclined surfaces, following the surface of the outcrops (Figs. 9B, 11B). There is no evidence of strong unbound glacial abrasion.

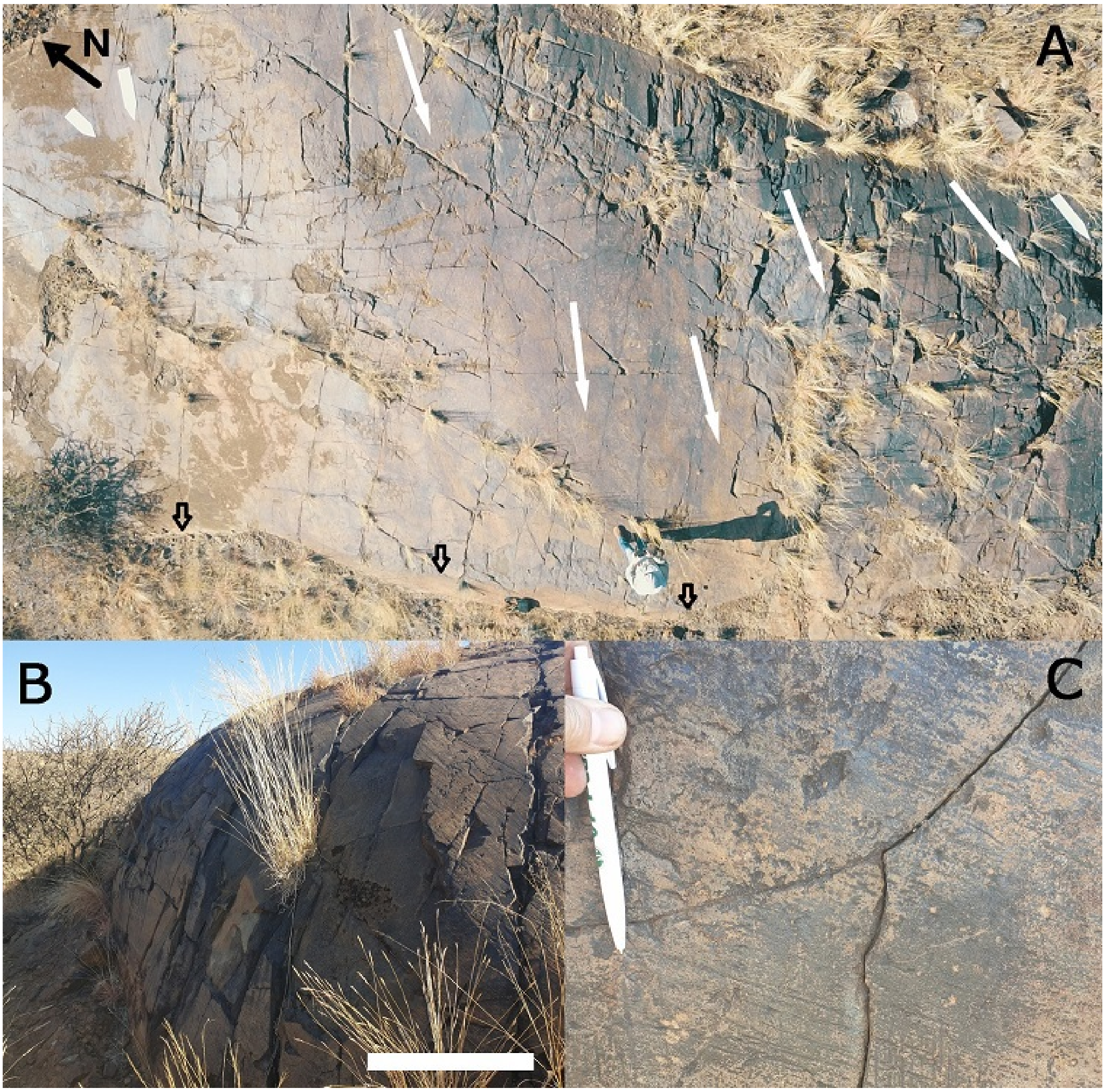

Fig. 9. Nooitgedacht. A – Vertical overview of one of many small striated surfaces (see location in Fig. 8A). All white arrows point in the directions of the striations. In the lower part of the photograph, at the lee side edge of the striated surface, there is a small scarp displaying a uniform and steep flat 10-40 cm long slope (marked with small black arrows), down to the next flat level of the outcrop (grass-covered). The appearance of this lee side structure may be interpreted as a cut sheeting joint surface, as there are no large irregularities

at this surface. Next to the north arrow and the two small white arrows there is a confined area where the striations are short (approximately four square meters in size; 80% of the striations are <10 cm) and in more varied directions (Supplemental material). Striations at the upper right of the pavement are on a steeper surface and are slightly deflected to be more parallel to the slope of this surface. Those on the near flat surface, higher up on the outcrop, are mainly passing straight over and are following the outline of that surface. B – This outcrop has an almost vertical wall that is striated horizontally (location marked in Fig. 8A). A large part of the surface is recently exfoliated to a depth of a few cm, following the outline of the volcanic bedrock, with a rugged surface below. Scale is approximately 25 cm. C – Closeup of part of Fig. 9B. There are 10-20 cm long vertical striations which are crossing the horizontal striations almost perpendicularly, which shows there was been an intermittent short change in the direction of movement.

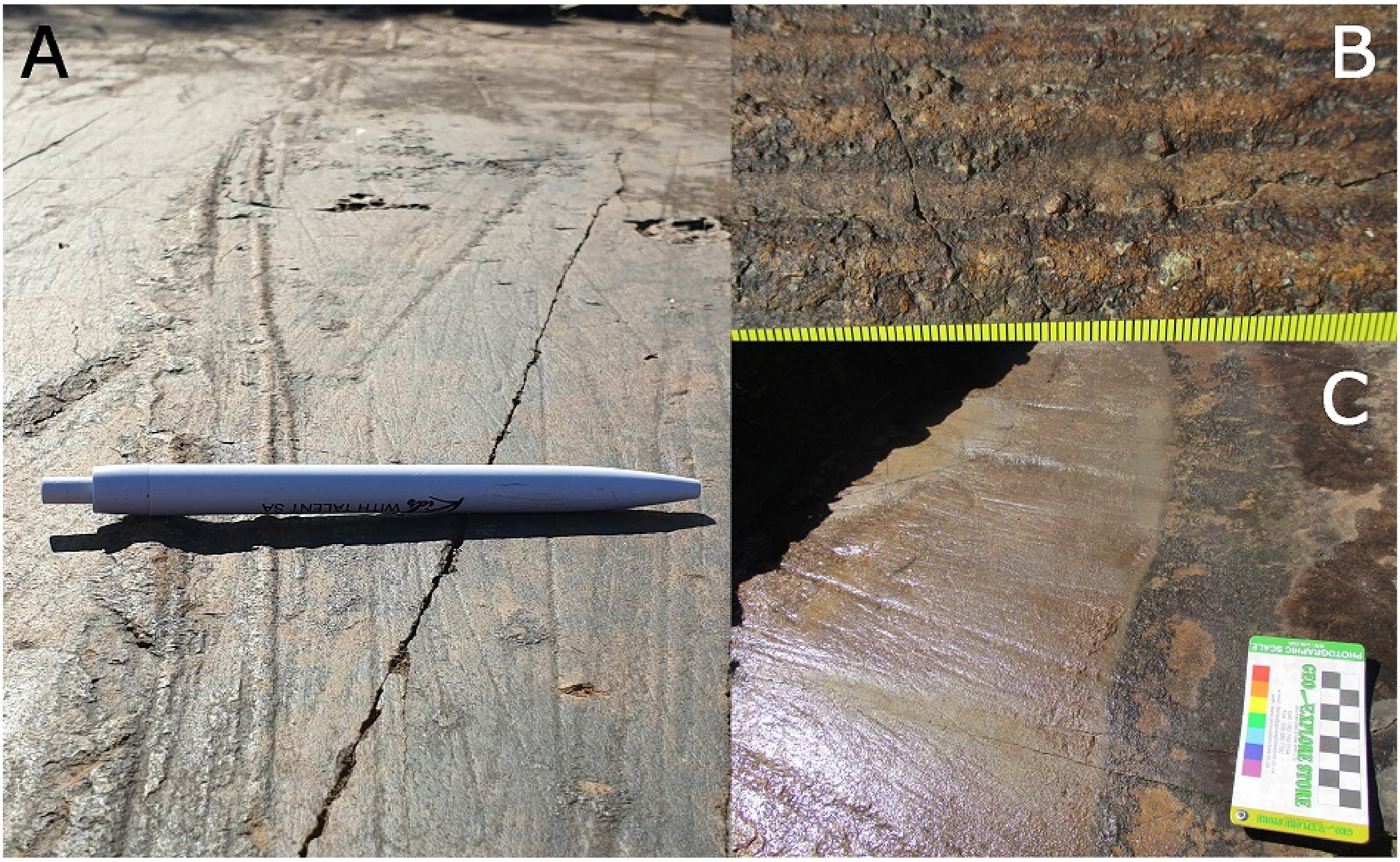

Fig. 10. Nooitgedacht. A – Small molded sediment ridge which show “bouncing” (upper part of picture), then makes a bend and splits into two and later three ridges (compare to similar ridges in Baas et al., 2021, their Fig. 16). B – Grooves and ridges molded in diamictite on top of Nooitgedacht striated surface. These are not striations on the bedrock but grooves smeared internally inside the diamictite, on top of the bedrock. Similar features were recorded from a few striated surfaces. Scale lines are mm. C – After removing a part of the diamictite it was apparent that there is a thin sediment plastered onto the lava. This brown sediment (left) is made of internal small and large striations/grooves or moldings covering the complete surface in the sediment, and are not striations on bedrock. This sediment had disappeared quickly by weathering, so just outside of the diamictite there was only a very thin blackened sediment surface with few striations/grooves/moldings left (middle). Where the black sediment cover

had weathered away, the Ventersdorp lava was at the surface and displayed only a few shallow striations (right).

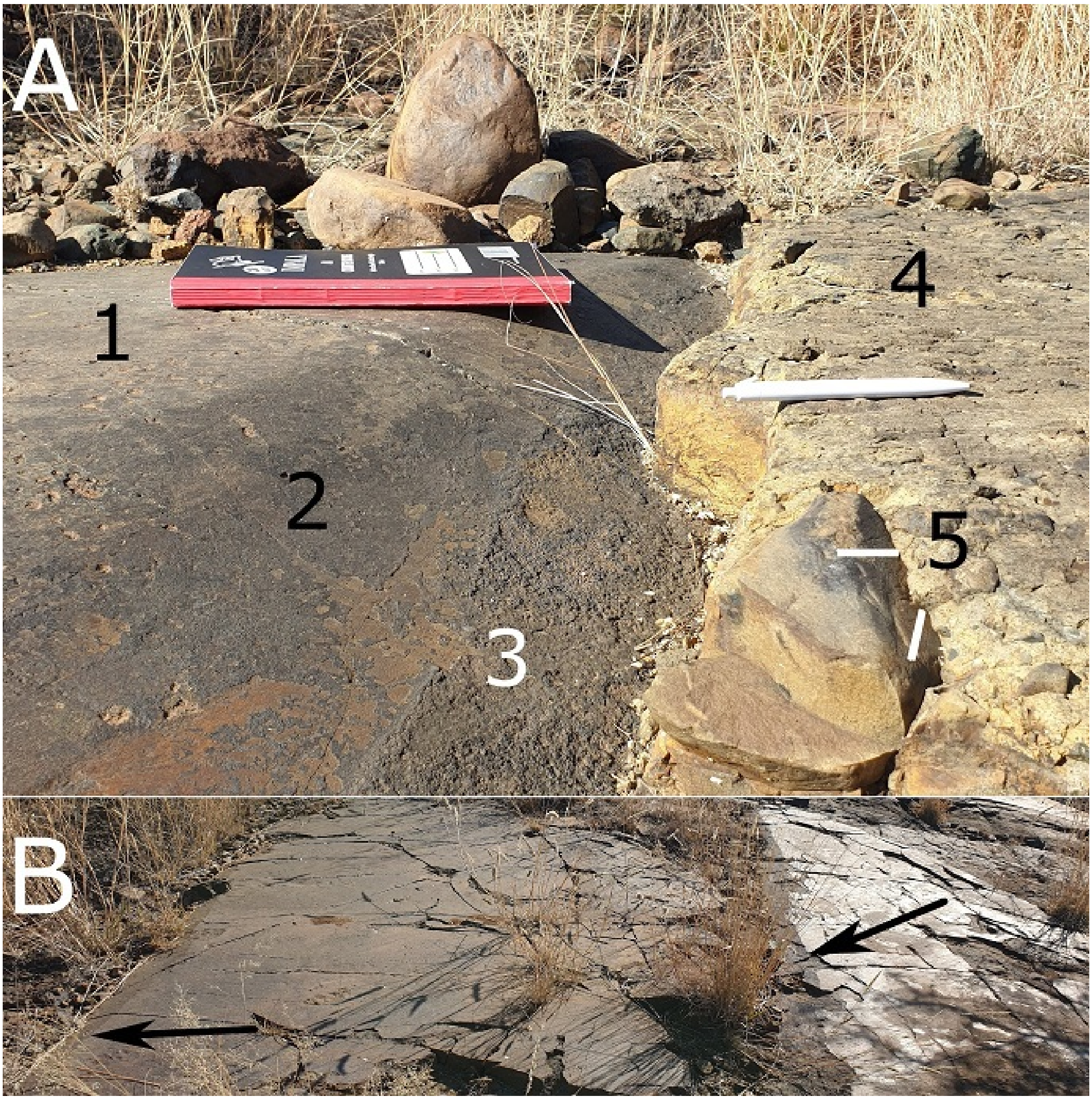

Fig. 11. A – A flat surface of Ventersdorp lava with striations (1), displaying a joint-like lee-side similar to many other lee-sides of the pavement area (2), a thin veneer-like layer of sediment below the diamictite (compare to Fig. 10C) (3), a diamictite with soft sediment striations at the same level as on the flat lava surface (4) and a boulder with striations in many different directions (striated clasts are common in gravity flow deposits; Molén, 2022a; two

more pronounced striations are marked with thin lines) (5). The striations on the bedrock and diamictite are in the direction of the pen. B – This small striated surface display two long but low straight-edged joint-like scarps (at the tips of the arrows). On the flat surface between the scarps there are few striations, except next to the left small scarp, and this flat surface therefore may be referred to as a small bypass zone. The general direction of the striations is marked with the long arrows, but both surfaces displays groups of striations with different bearings, slightly similar to those shown in Fig. 8B. On the surface to the right side there is a small exfoliated area with a rugged surface below (below right part of arrow).

4.2.2. Douglas

At Douglas there is a pavement displaying grooves and striations on Ventersdorp volcanic bedrock (Fig. 12). The striated surface is approximately 9000 m^2 in size (Stratten & Humphreys, 1974). Large grooves can be followed for tens of meters. These grooves are commonly a few centimeters deep and tens of centimeters wide. They display a pattern with the appearance of a washboard, and becomes deeper towards the green area of Fig. 12A which is marked with arrows and shown in Fig. 12B. Both striations and grooves are very long and parallel (variation is reported as approximately 1° by Stratten & Humphreys, 1974). They display no unequivocal evidence of the variety of glacial features that are prevailing on Pleistocene pavements, like deviations from a parallel path, and moving vertically and horizontally inside a glacier producing curvilinear paths (Figs. 12B-C).

There is no diamictite in the area, but there is shale nearby, with sparse outsized clasts up to 3 cm long. This shale is often interpreted to be postglacial or late glacial Ecca Group (but the interpretation is somewhat doubtful; Stratten & Humphreys, 1974).

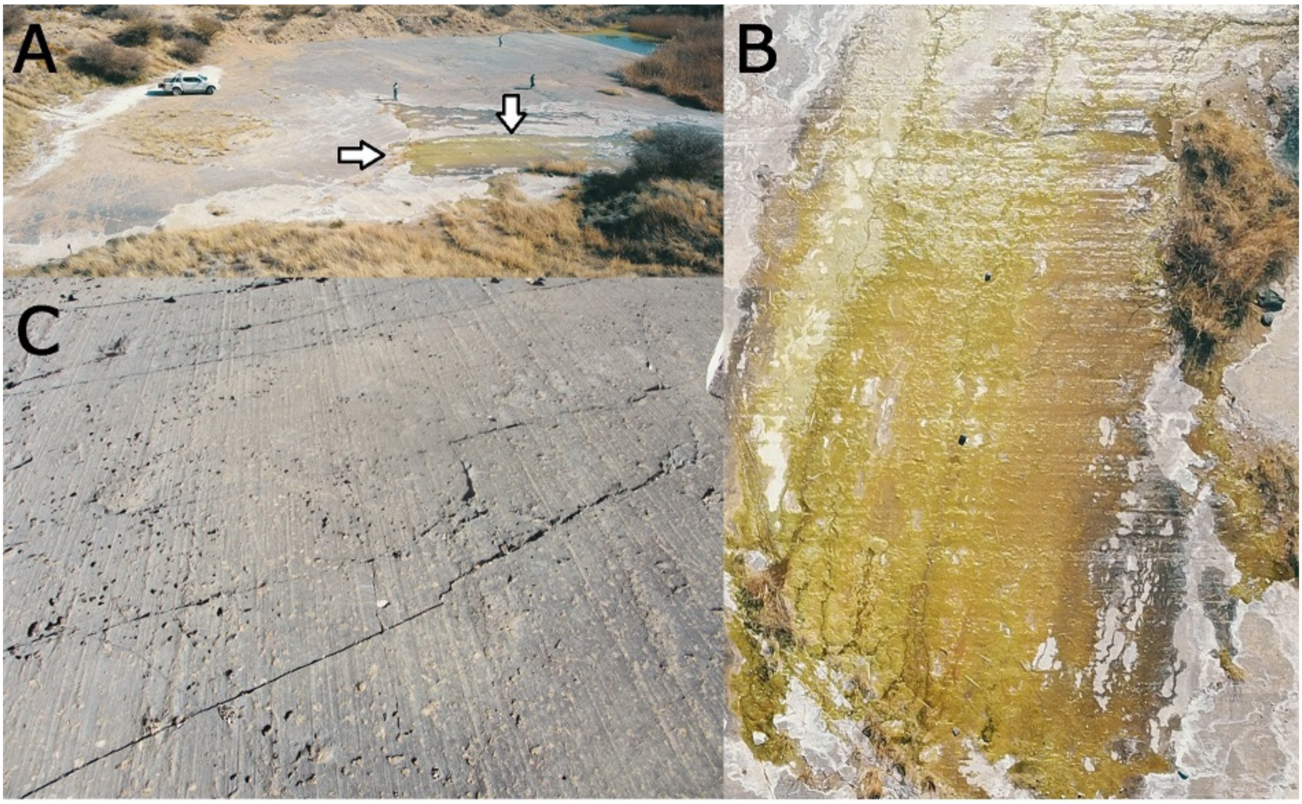

Fig. 12. Douglas pavement. A – Overview. The area marked with arrows is displayed in B. B – This area displays large parallel grooves forming a washboard pattern. Vegetation grow in the deeper parts of the grooves. Depth difference from top to bottom of grooves is less than 10 cm and commonly only a few cm. Scale is evident in Fig. 12A. C – Closeup of a section with only thin grooves and striations. The parallel direction of striations and grooves is clearly visible. The lower part of this photograph is about 1 m across.

4.2.3. Oorlogskloof

At Oorlogskloof there is a soft sediment sandstone pavement which is covered by sediments made up of sand containing little clay and a few outsized clasts. The pavement area is slightly higher compared to the surroundings, except for a quadrangle stretching from slightly north of the pavement and to the west. The covering sediments have been defined as sandstone or pebbly sandstone (Cape Geosites, 2014). The underlying striated sandstone surface contain similar outsized clasts as the sandstone covering the pavement. There is no diamictite in the near surroundings.

The pavement is striated, grooved and “fluted” parallel (Le Heron et al., 2019) in soft sand (Fig. 13). Four stacked levels of striated surfaces were recorded (Fig. 14B). The most outstanding structures in the pavement are parallel long stretched furrows and ridges which are V-shaped in appearance, with steeper north sides than south sides, the latter displaying grain flow lobes (Fig. 13B). The furrows and ridges have been interpreted as glaciogenic flutes by Le Heron et al. (2019). Three of these ridges are especially outstanding (Fig. 13C). The grain flow lobes on the south side are slightly deflected in the flow direction (Fig. 13B). The steeper north sides are more like a flat compressed wall, molded and planed off, and therefore are more compressed and cemented with an appearance of clay smear (Vrolijk et al.2016). In some areas, this steep surface is slightly vertically “ribbed”, i.e. with an appearance that are similar to vertical slip surfaces of many faults. Single or sometimes multiple tool marks in different directions, comparable to the size of pebbles in the overlying sandstone, have been imprinted onto the elongated forms (Fig. 13B).

There are a few fractures or joints which are perpendicular to the direction of the striations and grooves in the pavement, and in places next to where the pavement show slight vertical movement (Fig. 13A). The sandstone covering the pavement area has been deposited in an east-west path, like large sand lobes, in the same direction as the striations. The sand flowed upgradient while coming up from below of the pavement surface from the east, then covered, thrust and squeezed parts of the pavement (Fig. 13A, at number 4, and Fig. 14A). The sedimentary structures in the sandstone display upwards movement during deposition over the pavement area, at the north side (Fig. 13, number 3). These sand lobes are similar to sandy debris flow lobes. A large sand lobe at the east side of the striated surface deflected and warped the underlying pavement so that all “furrows” and striations have been remolded and have partly been obliterated (Fig. 14A). All data show that the pavement and the underlying sedimentary section were soft, probably in a semiplastic or apparent cohesion condition, during the whole depositional event.

Stratigraphically, above the pavement area are convex streamlined “sand bars”, the largest one more than 10 m long and 1 m high. The largest “sand bar” is described as a glaciogenic flute by Le Heron et al. (2019). This bedform consists of sand, partly conformable and following the surface of the “sand bar”, with the internal composition displaying bedding (Fig. 14C). Some smaller streamlined convex “sand bars” next to the largest one are partly descending below the base level of the pavement surface.

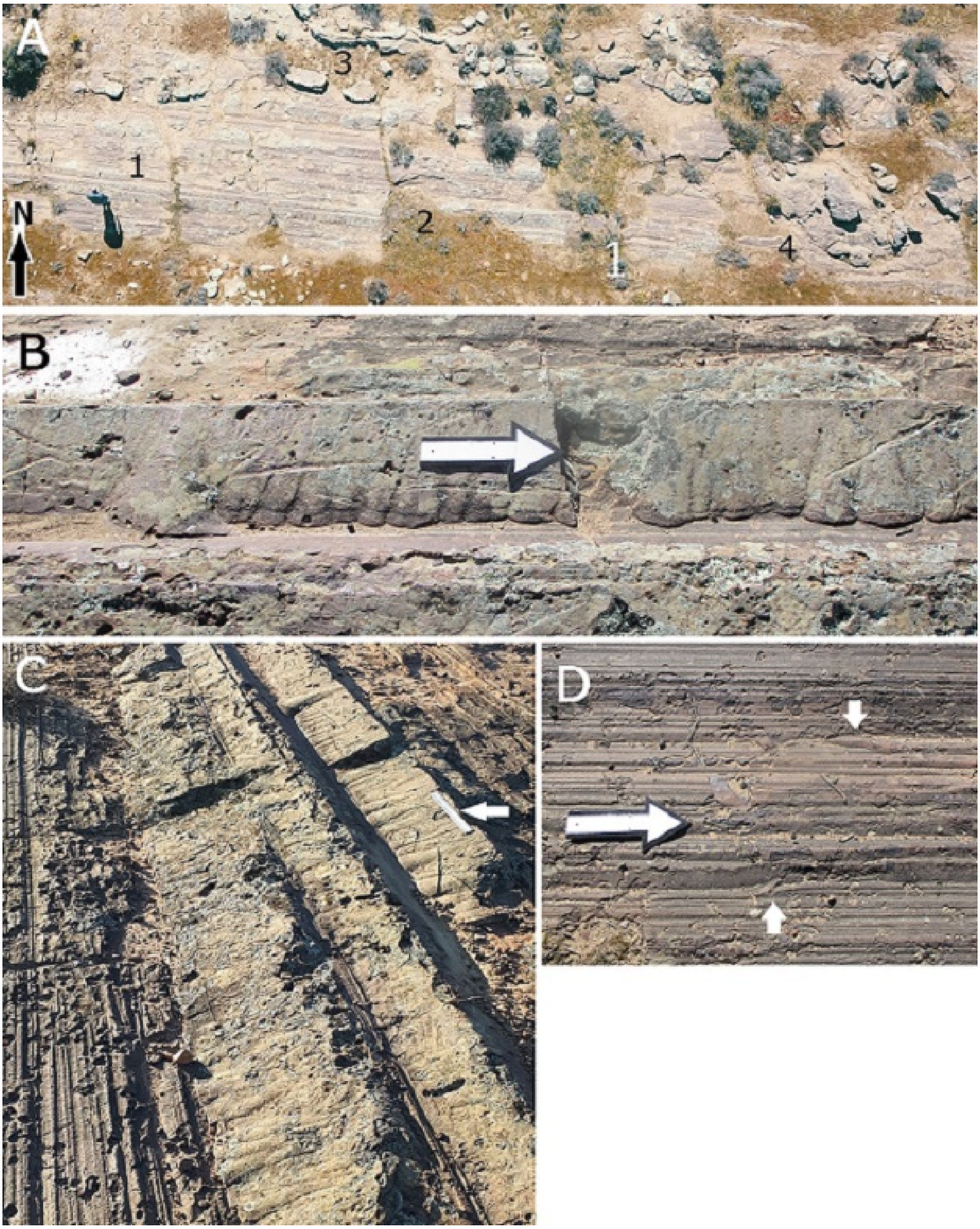

Fig. 13. Oorlogskloof. A – Vertical overview of part of the pavement. See person for scale. The surface of the striated surface is higher than the surroundings, except on the western and parts of the north side. Parallel furrows and ridges are visible over most part of the photograph, marked at two places with the number 1. At the white number 1, the “furrows”

are slightly soft tectonically bent and deflected towards the north. There are a few fractures in the pavement area which are perpendicular to the “furrows”. At number 2 it is easily observed that the pavement is lowered on the right side of one perpendicular fracture (pavement is partly covered with grass). Sediments are continuing in a path up from the lower areas (from the north and east) and are covering the pavement, and there are bedding planes in the sandstone in these overlying sediments (above numbers 3-4). B – Details of part of the area that is displaying small sand lobes, showing that these have flowed down onto and covered parts of the striated and grooved surface at the bottom of the V-shaped depressions. The grain flow lobes are slightly deflected in the flow direction, i.e. to the west (opposite to the direction of the arrow), which is more evident on the left side of the arrow. Straight or curved shorter single grooves pointing in different directions are superposed onto the grain flow lobes. These shorter grooves are also present on the far left of this photograph, where parts of the sand lobes have eroded away slightly after their deposition. C – The three most outstanding parallel elongated “furrows” or “flutes” which display sand grain flow lobes. Photograph is from in front of the person in Fig. 13A. Ruler in front of the arrow is 30 cm. D – Closeup of pavement. Notice that one groove is making a short bent “jump” (lower small arrow) and one groove is deflected and then molded together with the underlying one (upper small arrow), which indicate rotation of the tools making the marks (Peakall et al., 2020). Flow direction is opposite to the arrow. (Large white arrow is 25 cm.)

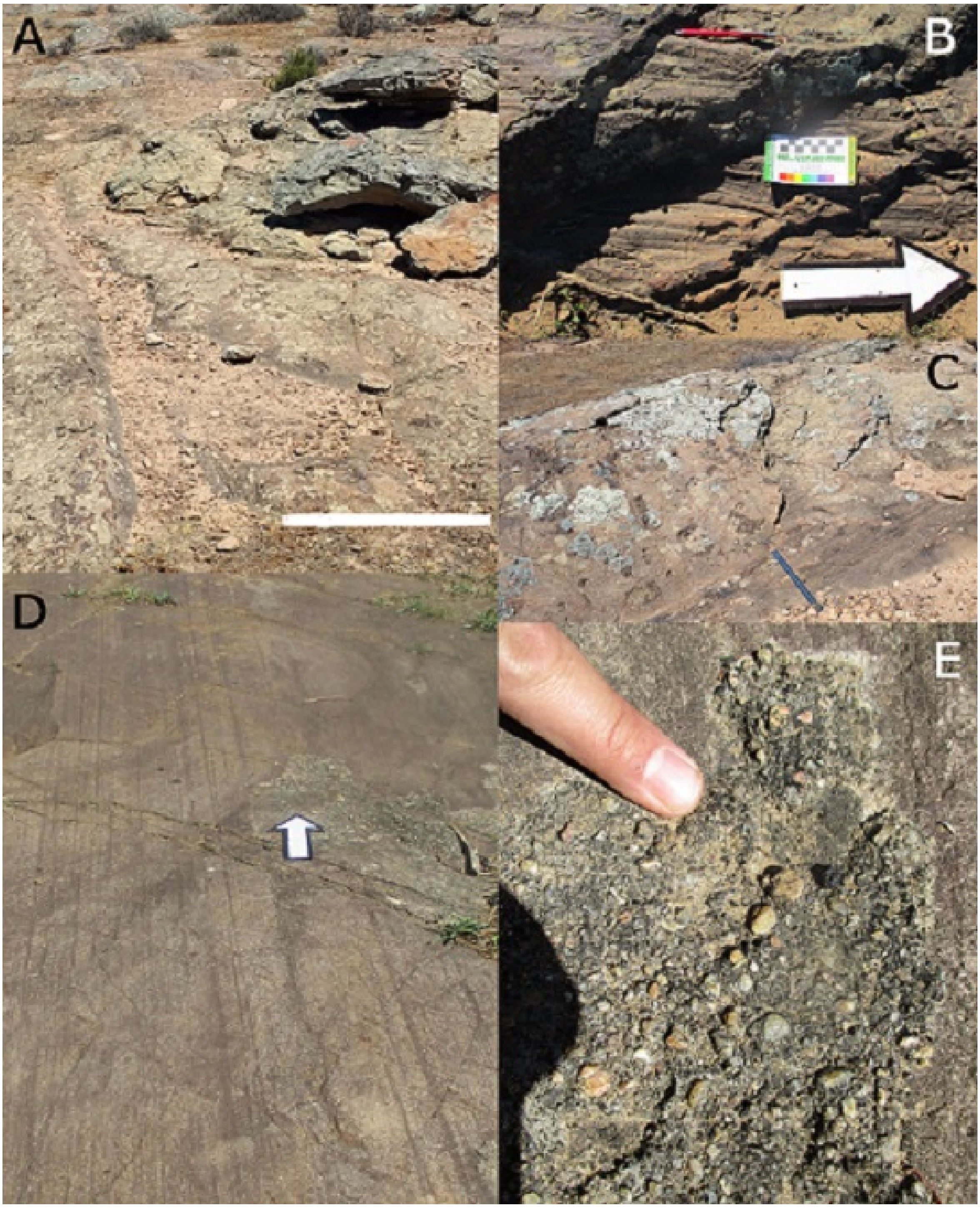

Fig. 14. A-C, Oorlogskloof. D-E, University of KwaZulu-Natal, Westville Campus, Durban. A – A large stratified sand lobe, with bedding planes, has deflected and remolded the sandstone of the striated surface a few meters, the latter which must have been in an apparent

cohesion or semiplastic condition. Sand lobe is visible in Fig. 13A, above and east of number 4. White marker is c. 1 m.) B – Four stacked soft sediment striated pavements, i.e. this is the internal structure of the sandstone in this area. C – Internal part of the large “flute”, displaying bedding planes similar to the sandstone which covers the pavement in Fig. 13A (numbers 3-4). This large “flute” is situated just north of Fig. 13A. Ruler is 30 cm. D – The striations on the sandstone surface are long and parallel. E – Small area on top of the striated surface in D, displaying a thin veneer of sand and gravel (sample L1c). (Arrow is 25 cm.)

4.2.4. Durban

At Durban´s University of KwaZulu-Natal Westville Campus there is a pavement of approximately 100 m^2 on sandstone, and similar soft sediment pavements are in a zone around Durban (Bangert & Von Brunn, 2001; Haldorsen et al., 2001). No confirmed diamictite is present. Striations and grooves on the pavement are long and parallel but not curvilinear (Fig. 14D). The longest striation is 6 m. On top of the pavement, there are small veneers of mainly sand and gravel (Fig. 14E). A sample of a sliver of sand and gravel on top of the pavement was studied by SEM (sample L1c; Supplemental material).

5. Discussion

5.1. General geology, Dwyka Group

The sediments of the Dwyka diamictites commonly are devoid of large sand grains. All diamictite matrix sediments appear to be mud where grains from different environments have mixed, mainly multicyclical grains but some that could have been incorporated more directly from bedrock.

Many diamictites are stratified on a large scale (Introduction), but some diamictite subsamples displayed stratification on a mm scale (Table 1). Most samples were small (usually <5x5x3 cm) so stratification was unexpected, and internal structures were not looked for.

At site H, Elandsvlei farm area (Blignault & Theron, 2015), an abundance of brown diamictite blocks within the gray diamictite were documented (Fig. 15). These have been transported and slid into position, as there are flow structures in the gray diamictite around the brown diamictite blocks. This also indicates that the lower gray diamictite was in a soft condition. Sediment gravity flows commonly pick up and transport intact weathered rocks, soft sediments, including aggregates of boulders and sediment gravity flow deposits, even with intact stratigraphy, without disintegrating them (Schneider & Fisher, 1998; Major et al., 2005).

Fig. 15. Many brown aggregates of diamictite boulders were inside the gray diamictite at site H, Elandsvlei farm area, with flow or load structures in the gray diamictite around these boulders. It was evident that the brown boulders have slid into place. The gray diamictite apparently was in a soft and wet condition during deposition of the brown aggregates. White line is c. 1 m long.

5.2. SEM Studies

5.2.1. Origin of surface microtextures and SEM study

There is nothing unusual about the appearance of the surface microtextures studied from South Africa, but similar surface microtextures are present in Quaternary samples from non-glaciogenic environments (Mahaney, 2002). There is no evidence of coatings detected during SEM-analysis, and the surface microtextures on the quartz grains is indisputable (compare to Somelar et al., 2018). The main difference between the South African samples and Quaternary glaciogenic samples is the combinations of surface microtextures. The typical glaciogenic combination of fractures that are irregularly abraded are not present on any quartz grain of the South African samples.

5.2.2. General, surface microtextures on quartz grains

Fig. 7 shows combinations of surface microtextures from Dwyka diamictites, which are different from, and actually in their details contrary in a<pperance to surface microtextures displayed by glaciogenic grains. No grain from any sample displays large fractures and irregular abrasion, i.e. the combination F1/A1 typical of glaciogenic grains. The samples display almost 100% occurence of A1/SP1 and small and/or older fractures (f1, F2, f2) (examples in Figs. 2-6). Furthermore, minute surface microtextures on grains from sandstone that has been interpreted as glacially reworked sediment by Le Heron et al. (2020), do not display any glaciogenic features.

When investigating for possible impact on the surface microtextures from post-depositional processes in the field and laboratory methods, there is no evidence for any modification of the results, except in some probably low degree for the origin of History-1 fractures/F1 (Supplemental material). No History-1 fractures (independent of their origin) in the samples show resemblance to glaciogenic surface microtextures, but all studied grains display original A1/SP1 followed by single unaltered F1-fractures. Hence, the F1 then reclassifies the older geologic history of A1/SP1 to A2/SP2. There was no evidence of almost simultaneous F1/A1 (irregular A1), as is the combination of surface microtextures which is generated by glaciers. A few grains displayed minute surface microtextures that often are present in glaciogenic material, like conchoidal fractures (Mahaney, 2002), but these minute surface microtextures do however originate in any high energy environment and not only by glaciation. In the South African samples these fractures show either no abrasion or only regular abrasion caused by long time exposure to fluid water (Molén, 2014). The samples contain a mix of grains which would be expected from non-glacial processes like e.g. tsunamis, mass wasting and sediment gravity flows (e.g. Mahaney 2002; Molén, 2017; Costa et al., 2019). Surface microtextures typical of glaciated areas, i.e. F1/A1, are absent from the Dwyka samples, and there is no evidence of obliterated F1/A1 surface microtextures in any sample.

It would be exceptional if all samples from all diamictites did not display any evidence of glaciation. Surface microtextures can be different or change, if transported with water, in periglacial areas, or if all samples are from supraglacial/englacial sediments, but there was no evidence of such environments from surface microtextures or macrotextures in the Dwyka Group diamcitites (Mahaney, 2014, Molén, 2014, 2017; Kalińska-Nartiša et al., 2017; Kalińska et al., 2022; Kut et al., 2021; Passchier et al., 2021; Górska et al., 2022). All diamictite samples are compressed and they do not show geological features of any other environments than those that would be interpreted as tills or debrites.

A further observation is that the southern samples (C-J) show 44-57% F2 compared to 48-70% for the northern samples (K-Q) (Table 1). This may indicate that grains from the south were transported over a longer distance, as they are more rounded and therefore display less F2. Samples from the northern sites display more protuberances which indicate sedimentary source rocks consisting of little rounded grains or magmatic/metamorphic source rocks (Molén, 2014). The rounding of the grains is not glaciogenic but only created from less energetic environments where a combination of regular mechanical abrasion and slight chemical surface weathering are the most common processes (Molén, 2014).

5.3. SEM. Detailed discussion of results

The diamictite at Nooitgedacht is of special interest because it is situated directly on top of a striated surface and displays mainly surface microtextures A1/SP1. The seldom reported thin sedimentary veneer-like layer between the pavement and the diamictite is present in many areas (Figs. 10, 11A). This thin sedimentary layer displays no large differences in surface microtextures compared to the diamictite except that there is more abrasion in a thicker brown bed (sample C3bm) and less in a thinner dark bed (sample C4m) (Figs. 3A, 10, 11A). Even if the thicker brown sediment (sample C3bm) was clearly deposited by a more fluid process than the overlying diamictite, it still is mostly in the clay, silt and fine sand sizes, and cannot have been transported a long distance apart from the overlying diamictite. The thinner dark sample C4m appears to be a mix of transported grains (i.e. surface mictrotextures A1/SP1), similar to all other diamictites from the Dwyka Group, and heavily weathered quartz grains displaying no surface microtextures indicating transport (e.g., no A1), but heavy weathering (SP1) indicating grains released from a possible saprolite. Sample C4m displays less A1, much less F2 and is much more weathered than other grains from Nooitgedacht (Fig.

3A and Supplemental material). The high degree of weathering explain the absence of F2 on many C4m-grains . The documentation of surface microtextures shows that there is commonly a single history of fracturing of sample C4m, either F1 or F2, which could also indicate that F1-grains from this sample may have been fractured during the preparation work because they were heavily weathered (one grain fractured during attachment of the sample to the SEM stub, but such grains were not recorded as F1). Slight weathering in some cases may create more rounded forms that can be mistaken for abrasion, and therefore the recorded abrasion surface microtextures (A1) may be slightly overestimated (Molén, 2014). The thin sedimentary beds in samples C3bm and C4m correspond to traction carpets, a common structure in the lowermost part of sediment gravity flows but not below till (Talling et al., 2012; Peakall et al., 2020).

Diamictites subsampled at sites F-Q display similar appearances as or have been interpreted to be glaciogenic by previous researchers (Table 1, examples in Figs. 2-6). Sample G diamictite has been interpreted by Visser (1996) to be deposited in front of a grounded marine ice sheet, but the surface microtextures are similar to all other diamictite samples, displaying the non-glaciogenic combination of A1/SP1 (Figs. 2D, 5). The difference in surface microtextures is clear when compared to grains from confirmed glacial deposits (Molén, 2014; Figs. 2E-F). None of the grains analyzed in any sample showed typical surface microtexture combinations associated with glaciation. Grains from sediments similar to the sandstone pavement at Durban (L-samples), inside of the conglomerate (F4-samples), and from weathered granite (small fragments of weathered granite, c. 2x1x0.5 cm, were present in samples P1a, P3b and P5b) have probably contributed to these diamictites (these grains display mainly the same basic appearance and surface microtextures; Supplementary material).

Even very small glaciers rapidly generate large numbers of glaciogenic surface microtextures (Molén, 2014), and there is no evidence of glaciogenic surface microtextures in any of the Dwyka diamictite samples (compare to tills from any Pleistocene and more recent glaciers, Figs. 2-7; Mahaney, 2002; Molén, 2014, 2017).

5.4. Pavements/striated surfaces

The pavements of the Dwyka Group display various features commonly associated with basal shear zones of submarine mass flows. The striations and grooves in the four striated surfaces studied do not display continual short distance variations, neither vertical nor horizontal deflections, similar to how these form by clasts which are frozen into ice (Iverson, 1991). Even if glaciers were cold-based, displaying none or almost no movement, a clast at the bottom is never frozen with no minute internal movement within the ice. This is as opposed to clasts in dense sediment gravity flows or slides where the process is so fast that clasts may move in a more straight manner, i.e. hundreds of meters in seconds or minutes (Piper et al., 1999; Peakall et al., 2020). But sediment gravity flow striations and grooves may also be short and curved (Introduction).

5.4.1. Nooitgedacht pavement

The striations at Nooitgedacht display many different bearings, but are mostly internally straight and ordered in generally parallel patterns. The striations are also grouped, deflected and differ in appearance between various confined areas. These appearances, including “conjoining” and crossing striations, are consistent with sediment gravity flow mechanisms (Draganits et al., 2008, e.g. see their Fig. 11), including flow diversion in an expanding current or flow (Potter & Pettijohn, 1963). The small area which displays perpendicular vertical striations could be interpreted to have formed by a boulder that suddenly settled under gravity after slowing to below the critical velocity of the flow (Fig. 9C). The areas with soft sediment-molded striations or grooves plastered onto the Ventersdorp lava, but with few striations below the sedimentary rock, indicate that it was not a thick glacier that was responsible for the striations. This evidence of striations and molds in soft sediments, which were not transferred onto the bedrock below, indicates a process by which sediment masses passed with only little downward pressure (Fig. 10C). Furthermore, this evidence is at odds with an interpretation that weathering of the underlying bedrock dissolved most of these tool marks after their formation, as an explanation of the decrease in both number and depth of striations and grooves. Areas with no striations on the Ventersdorp lava could then be classified as small bypass zones, since a large glacier would impact the overall bedrock more overall but with local variations in abrasion and plucking. And clasts within a glacier would always randomly change their vertical and horizontal directions, not commonly producing straight and invariable sub-parallel or parallel tool marks, but almost always constantly assymetrical tool marks. The full spectrum of striations and grooves at Nooitegedacht, i.e. the grouping, the parallelism and the minute appearance of the striations and grooves, are consistent with and indicate sediment gravity flow origins. Striations and grooves on hard basement rocks in the northeast of South Africa appear similar to those at Nooitgedacht, but these are covered by stratified diamictite which is interpreted as sediment gravity flow deposits (Dietrich & Hofmann, 2019).

Thin basal beds of sediments, i.e. traction carpets, are common below cohesive debris flows, and are similar to the thin sediment beds below the Nooitgedacht diamictites, but are not displayed by glaciogenic deposits. Soft sedimentary deposits are easily eroded away by glaciers except in more confined and shielded areas. The mm-thick dark layer (sample C4m), which we interpret as part of a traction carpet, contains a mix of a) highly weathered grains displaying no or little evidence of long transport, from a possible saprolite, and b) grains rounded from a long time of low energy impact which may be interpreted as from long distance transport (Mahaney, 2002; Molén 2014, 2017). The thicker brown layer of sediment below the diamicite, also resembles a traction carpet, and displays mostly far-transported grains (i.e. sample C3bm).

The smooth Ventersdorp lava surface below the diamictites is commonly exfoliated, displaying rugged surfaces beneath (Figs. 9B, 11B). There is evidence of slight erosion on top of the lava but no evidence of strong glacial abrasion, which would in at least the more outstanding/steep areas cut deeply into and bevel the bedrock surface straight through any former weakness planes. Furthermore, the pavement is in an area where the subjacent bedrock is mostly composed of Ventersdorp lava (Van der Westhuizen et al., 2006), but the clasts in the diamictite are composed of a mix of different lithologies and not mainly local lava clasts. The matrix of the diamictite is not composed of much dark material, except in the thin basal sediment layer which is probably blackened by weathering (sample C4m and partly in sample C-1-1; compare to Figs. 4 and 10B-C), but generally mostly light minerals. This observation enhances the indication that the bedrock was not heavily eroded by a thick glacier, but was only bypassed by sediment gravity flows.

The so-called drumlinoid complexes or roche moutonnées in the area do not display evidence of glacial sculpting, but mostly of weakness planes in the lava which have been only slightly abraded by the process which formed the striations and grooves. The small scarps and the regular and uniform bedrock areas next to these surfaces show no evidence of strong shifting, glacial plucking and irregular abrasion. These features simply display intermittent release of rocks along weakness zones of what appear to be sheet jointing in a more uniform, less erosive and brief process consistent with sediment gravity flows. All these observations are evidence that the general appearance of the bedrock (including possible residues of saprolites) was formed long before deposition of the diamictites, i.e. there is no evidence of strong glacial erosion. The major geomorphological bedrock features of the area may have been inherited from before the deposition of the diamictites.

5.4.2. Douglas pavement

The Douglas pavement is flat and very regular, which could be an argument for a glaciogenic origin. However, even if there had been a very slow moving cold-based glacier, one in which clasts would not move/rotate much inside the ice during transport and contact with the underlying surface, one would expect at least some movement in the basal part of the glacier with evidence of this displayed on the pavement. There is no obvious evidence for such movements. In a slide or cohesive debris flow, the material may be transported more or less as one large mass (Peakall et al., 2020), albeit with some internal movement inside the mass. The documented lack of diamictite close to the outcrop is more indicative of natural processes of a debris flow that simply passed through the area without depositing any sediments.

5.4.3. Oorlogskloof pavement

Le Heron et al. (2019) deduced three different episodes of deposition and erosion of sediments at Oorlogskloof as movements of a glacier that was grounded, partly uplifted by the sea, and grounded once more. However, there is no evidence for recurrent vertical movements of a marine glacier (or an iceberg) at Oorlogskloof, as the geological work has been generated mainly sequentially on the same surface. The erosional events and deposition of new sediments are localized, and there is no evidence of a large glacier.

If the parallel long ridge and furrows in the pavement were grooves or flutes made by glaciation, it would require the generation of very similar V-shaped elongated structures, either by a) a few almost identical boulders (or iceberg protuberances) moving straight next to each other, or b) squeezing by a glacier of many flutes next to each other made in the same V-shaped sharp-crested forms with similar inclinations. After the generation of these structures there would have to follow an uplift of the glacier and subsequent grain flows on the more gentle side of the "flutes".

Leaving the glaciogenic interpretation, the appearance of the V-shaped "flutes" displays similarities to joints followed by small faults in the sediment generated by tectonic movement, i.e. faulted joints (Wilkins et al., 2001). Joints in sandstone are commonly straight and may be parallel for long distances (Cruikshank & Aydin, 1995; Loope & Burberry, 2018), and the overall appearance of the V-shaped structures are similar to faulted joints (Wilkins et al., 2001). The subsidence of parts of the pavement area, and the perpendicular fractures, also may have originated during the vertical movement, as there commonly are perpendicular fractures where there are joints.

The exact origin of the streamlined convex "flutes" superposed on the pavement, the largest described by Le Heron et al. (2019), is unclear (Fig. 14C). The few less prominent but similar forms next to the larger bedform are partly below the base level of the pavement, indicating uplift of the pavement area. These forms partly display the appearance of linear sandbars, sand ridges or small flowbands (Dufresne & Davies, 2009). They are made up of mainly sand, and the "flute" of Le Heron et al. (2019) displays internal bedding planes. These "flutes" appear to be from sandstone that in some extent moved upwards, from the lower area next to the pavement, and covering part of the pavement, and are aligned in the same main general direction as the sand covering parts of the pavement (Fig. 13, numbers 3-4).

The striations and grooves at Oorlogskloof display similarities to striations and grooves in sediment gravity flows in many places (Enos, 1969; Peakall et al., 2020), and especially to Neoproterozoic/Lower Cambrian striations and grooves from submarine landslides at the base of superposed sandstone beds in India (Draganits et al., 2008). There are no similarities to any soft sediment glaciogenic striations and grooves. The appearance is fully consistent with pavements caused by debris flows which leave grooves, striations and shorter tool marks behind (compare to Ortiz-Karpf et al., 2017; Peakall et al., 2020).

The different episodes of deposition and erosion of sediments at Oorlogskloof may be interpreted as evidence of different sediment gravity flows. The sediments covering the pavement display sharp and irregular fronts, similar to sediment gravity flow debris tongues (Shanmugam, 2016). The paleoflow in the surrounding area is in one main direction and a few lesser “valley glacier” flow directions (Visser, 1981; Cape Geosites, 2014), similar to what has been observed from more recent large slides/sediment gravity flows (e.g. Haflidason et al., 2004).

5.4.4. Durban

The striated surface at Durban University is small, and the striations are more or less parallel. The small sliver of sediment on top of the striated pavement either was sediment between the pavement and any diamictite, or otherwise a part of a stacked pavement. Nothing on this striated surface makes it necessary to invoke glaciation, and the appearance is more consistent with a sediment gravity flow origin.

6. Conclusions

As briefly described in the Introduction, the evidence from paleochemistry, paleontology and paleomagnetism by themselves may be ambiguous and do not conclusively support continental glaciation in South Africa during the Late Carboniferous and Early Permian. The Dwyka Group deposits are present in downwarped basins controlled by tectonics, hence, the origin of the deposits is consistent with a subaqueous fan environment displaying debris flows. This is also supported by the great depth of the overlaying Ecca Group shales and sandstone, which show that the downwarping period persisted after the deposition of the diamictites until at least the southern parts of the area became a deep-water basin plain (Brooks et al., 2018; Hansen et al., 2019). This fact shows that the Dwyka Group deposits are different from Pleistocene tills, as the former are deposited in a downwarping area and the latter on a shield. Sediments deposited on top of shields are much more prone to erosion. But sediments deposited in synclines often persist and may later turn into positive topographic erosional remnants or mountains. This seems to be evident from the appearance of the local geology, especially in the south of South Africa, where the thickness of the sediments is greatest. In conclusion, if the sediments in the Dwyka Group were glaciogenic, then there are no deposits from former subaqueous fan environments from this period. This lack of fan deposits is problematic because subaqueous fan environments are very common in recent depositional settings, particularly in downwarping basins (Talling et al., 2015, Shanmugam, 2016), and the Dwyka Group diamictites are covered by sediments deposited in a fan environment (Hansen et al., 2019).

The four major cycles of glaciation, interpreted from the sedimentary succession of the southern parts of the Dwyka Group (Visser, 1997; Dietrich & Hofmann, 2019), can be equally well interpreted as four episodes of more or less extensive downwarping and sedimentation. There are no geological inconsistencies which follow from an interpretation of the Dwyka Group as formed mainly by recurrent flooding and sediment gravity flows of sometimes large magnitude.

The SEM study demonstrated that not one single quartz sand grain displays the typical glaciogenic combination of surface microtextures, fracturing and (irregular) abrasion (F1/A1), that would have been generated almost simultaneously below a glacier. Except for single F1- or f1-fractures, the grains display more or less surface microtextures that probable originated during release from weathered bedrock (mainly F2, f2, but a few EN2), but most grains display surface microtextures that need a long time to be generated, i.e. regular A1 and SP1 on more or less spherical multicyclical grains (compare to Molén, 2014, 2017). Quartz grains which had been transported a short distance display slightly more sharp fractures and protuberances compared to those that had been transported a long distance (comparing northern and southern samples from the Dwyka diamictites; Supplemental material). Finally, there is no evidence of artificial surface microtextures or chemical coatings on the grain surfaces that obscure the original surface microtextures.

The overall appearance of the pavements displays many structures that can be expected to be generated by sediment gravity flows but not by glaciers, even if some of the striations are not at odds with glaciers and marine ice sheets. This is evident from the appearance of the Nooitgedacht pavement but also from the Durban and Douglas pavements.

The history of formation of the more complex Oorlogskloof pavement area probably was some variation of the following episodes. Details are visible in Figs. 13-14, but the overview described below is in Fig. 16:

1) Tectonically generated sediment gravity flows passed across the area, forming surficial striations and internal hydroplastic slickenside striations in soft sediments.

2) Subsequently the small striated area was uplifted, or alternatively the area south, east and partly in the north was sinking. The long linear V-shaped "furrows" were formed, first by slight compression and then partly by jointing followed by slight faulting. Clay smearing took place in some areas of the steep sides.

3) During the minor vertical movement, sandy grain flow lobes were formed on the gentle sides of the “furrows”.

4) Almost simultaneously sandy debris flows pushed and deformed some of these V-shaped forms to smoother forms and also deposited the linear sand structures in the area. Because of apparent cohesion or semiplastic condition in the sediments, the V-shaped structures at this place were not flattened but only rounded, almost like a dough.

5) Subsequently faulting opened up perpendicular fractures, and parts of the pavement area were downwarped by 10-30 cm. The sediments were still not lithified and in at least one place were displaced northwards over a distance of some tens of centimeters.

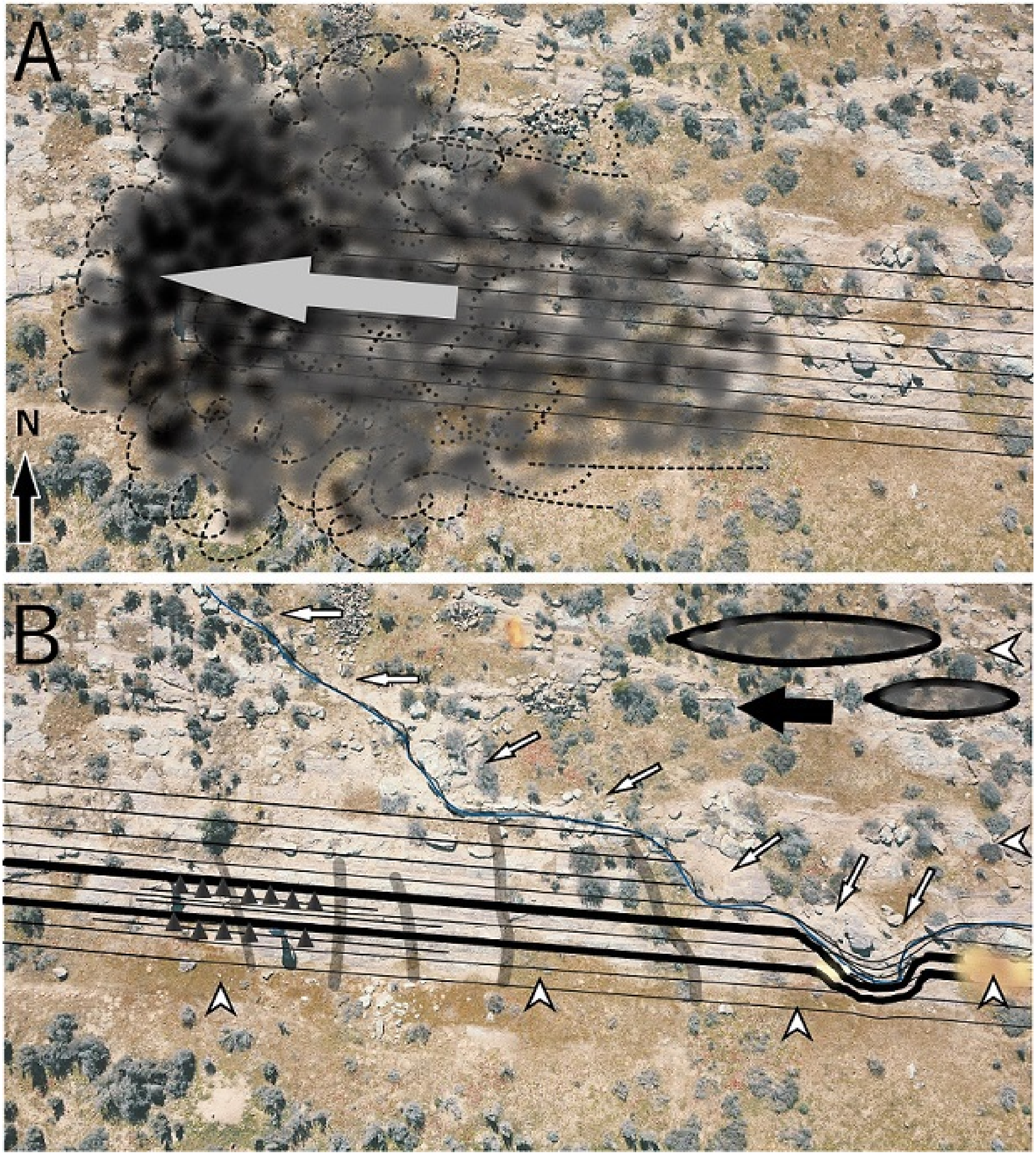

Fig. 16. Simplified drawings showing the possible sequence of events that led to the formation of the Oorlogskloof pavement area. A – Sediment gravity flow passed across the surface. B – V-shaped "furrows" marked as (two) thick parallel lines. The lower area is marked with white arrowheads. Small sandy grain flow lobes are marked as small black triangles. The direction of the sandy debris flows which pushed and deformed some of the V-shaped forms to smoother forms, marked with thin white arrows, and the outline of these

sandy debris flow lobe heads is marked with a thin irregular line in front of these arrows. Linear convex “sand bars” are depicted as two oblong structures in the upper right corner (direction marked with black arrow). The “sand bars” are outside of the photograph and not exactly next to each other, but have been drawn inside the photo. Perpendicular fractures are marked with thick, grey, almost vertical lines. Fractures are visible in Fig. 13A. See text for details.

Whatever the exact depositional history of the Dwyka Group is, there is no unequivocal evidence of glaciation. It appears possible to simply exchange the word glaciogenic with e.g. tectonics and sediment gravity flows. The diamictites and pavements in the area do not conform to the current paradigm of glaciation. This is especially evident by the absence of glacially formed surface microtextures (i.e. there are no F1/A1), but also by the overall appearance of the geologic features of the Dwyka Group.

Dietrich et al. (2019) wrote, after describing an area in Botswana that did not display any evidence of glaciation, that the deposits had been reinterpreted and there is an " ... emerging view that the (Late Paleozoic Ice Age) ice mass was in fact fragmented, covering only patches of southern Gondwana". From the evidence presented in the current paper, glaciers were not only patchy, but non-existent all over South Africa, or at least did not leave any imprint on the geology in the area. The implications of these data may help resolving some paradoxes concerning Late Paleozoic climates and inferred glaciations.

One can conclude with the words of Johan N. J. Visser, formerly of the University of the Orange Free State in South Africa and the probable foremost expert on the Dwyka Group, that: "... ancient deposits do not always correspond with Cenozoic glaciation models" (Visser, 1989a). If the Dwyka Group was not formed by glaciation, this statement is fully understandable. The present may be the key to the past, but past interpretations are not always the solution to past geologic processes.

The evidence of the geological features discussed in this paper, which are different when comparing glaciogenic and mass flow deposits, are summed up in a Diamict Origin Table, i.e. Table 4.

FEATURE	ORIGIN		
	Glacial.	Sediment gravity flow	Dwyka Group
Warm climate fossils	0-1	2	★
Streaks of different sediments/diamictites	1	2	★
Unconsolidated transported sediments	1	2	★
Pavement/striations/grooves	2	1	
Parallel striations	1	2	★★
Soft sediment pavements	1	2	★★
Stacked pavements	0-1	1-2	★★
Regular striations	0-1	1-2	★
Interlaminated sediments/traction carpet	-	1	★★
Iceberg keel scour marks and mimics	2	0-1	
Superposed/stacked in same direction	-	1	★
Parallel striations/grooves	1	2	★★
Roches moutonnés/plucking	2	(0-1)	★
Uneven surfaces	0-1	1	★
Fjords, overdeepened, regular, ridged outlet	2	(0-1)	★
Dropstones/outsized clasts	2	2	
Small size	1	2	★
Small size compared to other sediments	-	2	★
No/little penetration	1	2	★
Surface microtextures weathered and regularly abraded	-	2	★★

Table 4. Diamict Origin Table. Geologic features of Dwyka Group deposits for the outcrops which have been documented in the present study, comparing glaciogenic and mass flow features (more details of different features are documented by Molén, 2017, 2021, 2022a,

2022b). Not included are structures that form by non-glaciogenic processes in a glacial environment, e.g., debris flows. Tabulated features are only those that differ much between glaciogenic and non-glaciogenic deposits. Conjectural or insignificant (not fully) documented differences from the study area are not tabulated, but discussed in the text only. Last column summarizes what features are more indicative of sediment gravity flow. A single ★ indicate similarities to sediment gravity flow features, but not excluding a glaciogenic origin.. A double ★★ indicate a nonglaciogenic origin.

2 = more common, 1 = less common, 0 = very rare, - = no example known, parentheses = rare or commonly displaying a distinct appearance.

Acknowledgments

Thanks to many researchers who have given comments to earlier versions of this manuscript. The Hitachi SEM used was at the Department of Materials and Environmental Chemistry, University of Stockholm. This research did not receive any specific grant from funding agencies in the public, commercial, or not-for-profit sectors. The authors declare that they have no known competing financial interests or personal relationships that could have appeared to influence the work reported in this paper.

Supplemental material can be downloaded from https://doi.org/10.13140/RG.2.2.28657.35686 or ordered from the corresponding author.

References

Amblas, D., Gerber, T.P., Canals, M., Pratson, L.F., Urgeles, R., Lastras, G. & Calafat, A.M., 2011. Transient erosion in the Valencia Trough turbidite systems, NW Mediterranean Basin. *Geomorphology* 130, 173-184. https://doi.org/10.1016/j.geomorph.2011.03.013.

Anderson, A.M. & McLachlan, I.R., 1976. The plant record in the Dwyka and Ecca series (Permian) of the south-western half of the Great Karroo Basin, South Africa. *Palaeontologica Africana* 19, 31-42.

Baas, J.H., Tracey, N.D. & Peakall, J., 2021. Sole marks reveal deep-marine depositional process and environment: Implications for flow transformation and hybrid-event-bed models. *Journal of Sedimentary Research* 91, 986–1009. https://doi.org/10.2110/jsr.2020.104.

Baiyegunhi, C. & Gwavava, O., 2016. Variations in isochore thickness of the Ecca sediments in the eastern Cape Province of South Africa, as deduced from gravity models. *Acta Geologica Sinica* 90, 1699-1712. https://doi.org/10.1111/1755-6724.12811.

Bangert, B. & Von Brunn, V., 2001. Tuffaceous beds in glaciogenic argillites of the Late Palaeozoic Dwyka Group of KwaZulu-Natal, South Africa. *Journal of African Earth Sciences* 32, 133-140.

Barbolini, N., Rubidge, B. & Bamford, M.K., 2018. A new approach to biostratigraphy in the Karoo retroarc foreland system: utilising restricted-range palynomorphs and their first appearance datums for correlation. *Journal of African Earth Sciences* 140, 114-133.

https://doi.org/10.1016/j.jafrearsci.2017.11.031.

Bechstädt, T., Jäger, H., Rittersbacher, A., Schweisfurth, B., Spence, G., Werner, G. & Boni, M.. 2018. The Cryogenian Ghaub Formation of Namibia – New insights into Neoproterozoic glaciations. *Earth-Science Reviews* 177, 678–714. https://doi.org/10.1016/j.earscirev.2017.11.028.

Bell, D., Hodgson, D.M., Pontén, A.S.M., Hansen, L.A.S., Flint, S.S. & Kane, I.A., 2020. Stratigraphic hierarchy and three-dimensional evolution of an exhumed submarine slope channel system. *Sedimentology* 67, 3259-3289. https://doi.org/10.1111/sed.12746.

Bennett, M.R., Doyle, P. & Mather, A.E., 1996. Dropstones: their origin and significance. *Palaeogeography, Palaeoclimatology, Palaeoecology* 121, 331-339.

Blignault, H.J. & Theron, J.N., 2015. The facies association tillite, boulder beds, boulder pavements, liquefaction structures and deformed drainage channels in the Permo-Carboniferous Dwyka Group, Elandsvlei area, South Africa. *South African Journal of Geology* 118, 157-172. https://doi.org/10.2113/gssajg.118.2.157.

Blomenkemper, P., Kerp, H. & Bomfleur, B., 2020. A treasure trove of peculiar Permian plant fossils. *PalZ* 94, 409–412. https://doi.org/10.1007/s12542-019-00489-4.

Bouma, A.H., 1964. Turbidites. [In:] A.H. Bouma & A.Brouwer (Eds): *Turbidites*. Elsevier, Amsterdam, pp. 251-256.

Brooks, H.L., Hodgson, D.M., Brunt, R.L., Peakall, J., Hofstra, M. & Flint, S.S., 2018. Deep-water channel-lobe transition zone dynamics: Processes and depositional architecture, an example from the Karoo Basin, South Africa. *Bulletin of the Geological Society of America* 130, 1723–1746. https:// doi .org /10 .1130 /B31714.

Cape Geosites, 2014. Oorlogskloof glacial floor, Council for Geoscience, Western Cape Branch of the Geological Society of South Africa. https://c38e147f-b0d8-493b-a025-63dcdcddec22.filesusr.com/ugd/0de4bd_0c9446dc737e43b1acfa0f0f205464ad.pdf. (Accessed February 3, 2021).

Caputo, M.V. & Santos, R.O.B. dos, 2020. Stratigraphy and ages of four Early Silurian through Late Devonian, Early and Middle Mississippian glaciation events in the Parnaíba Basin and adjacent areas, NE Brazil. *Earth-Science Reviews* 207, 103002. https://doi.org/10.1016/j.earscirev.2019.103002.

Cardona, S., Wood, L.J., Dugan, B., Jobe, Z. & Strachan, L.J., 2020. Characterization of the Rapanui mass-transport deposit and the basal shear zone: Mount Messenger Formation, Taranaki Basin, New Zealand. *Sedimentology* 67, 2111-2148. https://doi.org.10.1111/sed.12697.

Catuneanu, O., Wopfner, H., Eriksson, P.G., Cairncross B., Rubidge, B.S., Smith, R.M.H. & Hancox, P.J., 2005. The Karoo basins of south-central Africa. *Journal of African Earth Sciences* 43, 211-253.

Cesta, J.M., 2015. *Soft-sediment slickensides in the Stockton Formation, Stockton, New*

Jersey. Geological Society of America, Paper No. 45-1. https://gsa.confex.com/gsa/2015NE/finalprogram/abstract_253490.htm.

Chumakov, N.M. & Zharkov, M.A., 2002. Climate during Permian-Triassic biosphere reorganizations. Article 1: Climate of the Early Permian. *Stratigraphy and Geological Correlation* 10, 586–602.

Coles, R.J., 2014. *The Cross-Sectional Characteristics of Glacial Valleys and their Spatial Variability* (Ph.D. thesis). Geography Department, University of Sheffield, 335 pp.

Costa, P.J.M., Rasteiro da Silva, D., Figueirinhas, L. & Lario, J., 2019. The importance of coastal geomorphological setting as a controlling factor on microtextural signatures of the 2010 Maule (Chile) tsunami deposit. *Geologica Acta* 17, 1-10. https://doi.org/10.1344/GeologicaActa2019.17.4.

Craddock, J.P., Ojakangas, R.W., Malone, D.V., Konstantinou, A., Mory, A., Bauer, W., Thomas, R.J., Affinati, S.C., Pauls, K., Zimmerman, U., Botha, G., Rochas-Campos, A., dos Santos, P.R., Tohver, E., Riccomini, C., Martin, J., Redfern, J., Horstwood, M. & Gehrels, G., 2019. Detrital zircon provenance of Permo-Carboniferous glacial diamictites across Gondwana. *Earth-Science Reviews* 192, 285-316. https://doi.org/10.1016/j.earscirev.2019.01.014.

Crowell, J.C., 1957. Origin of pebbly mudstones. *Bulletin of the Geological Society of America* 68, 993-1010.

Cruikshank, K.M. & Aydin, A., 1995. Unweaving the joints in Entrada Sandstone, Arches National Park, Utah, U.S.A. *Journal of Structural Geology* 17, 409-421.

Dahl, T.W. & Arens, S.K.M., 2020. The impacts of land plant evolution on Earth´s climate and oxygenation state – An interdisciplinary review. *Chemical Geology* 547, 119665. https://doi.org/10.1016/j.chemgeo.2020.119665.

Dakin, N., Pickering, K.T., Mohrig, D. & Bayliss, N.J., 2013. Channel-like features created by erosive submarine debris flows: field evidence from the Middle Eocene Ainsa Basin, Spanish Pyrenees. *Marine and Petroleum Geology* 41, 62-71.

Deynoux, M. & Ghienne, J.-F., 2004. Late Ordovician glacial pavements revisited: a reappraisal of the origin of striated surfaces. *Terra Nova* 16, 95-101. https://doi.org/10.1111/j.1365-3121.2004.00536.x.

Deynoux, M. & Trompette, R., 1976. Discussion: Late Precambrian mixtites: glacial and/or nonglacial? Dealing especially with the mixtites of West Africa. *American Journal of Science* 276, 1302-1315.

Dietrich, P. & Hofmann, A., 2019. Ice-margin fluctuation sequences and grounding zone wedges: The record of the Late Palaeozoic ice age in the eastern Karoo Basin (Dwyka Group, South Africa). *Depositional Record* 5, 247–271. https ://doi.org/10.1002/dep2.74.

Dietrich, P., Franchi, F., Setlhabi, L., Prevec, R. & Bamford, M., 2019. The nonglacial diamictite of Toutswemogala Hill (Lower Karoo Supergroup, Central Botswana):

Implications on the extent of the Late Paleozoic ice age in the Kalahari–Karoo Basin. *Journal of Sedimentary Research* 89, 875–889. http://dx.doi.org/10.2110/jsr.2019.48.

Dietrich, P., Griffis, N.P., Le Heron, D.P., Montañez, I.P., Kettler, C., Robin, C. & Guillocheau, F., 2021. Fjord network in Namibia: A snapshot into the dynamics of the late Paleozoic glaciation. *Geology* 49. https://doi.org/10.1130/G49067.1.

Dill, R.F., 1964. Sedimentation and erosion in Scripps Submarine Canyon head. [In:] R.L. Miller (Ed.): *Papers in Marine Geology*. Macmillan, New York, pp. 23-41.

Draganits, E., Schlaf, J., Grasemann, B. & Argles, T., 2008. Giant submarine landslide grooves in the Neoproterozoic/Lower Cambrian Phe Formation, northwest Himalaya: Mechanisms of formation and palaeogeographic implications. *Sedimentary Geology* 205, 126–141. https://doi.org/10.1016/j.sedgeo.2008.02.004.

du Toit, A.L., 1926. *The Geology of South Africa.* Oliver & Boyd, Edinburgh, pp. 205-215.

Dufresne, A.& Davies, T.R., 2009. Longitudinal ridges in mass movement deposits. *Geomorphology* 105, 171-181.

Dufresne, A., Zernack, A., Bernard, K., Thouret, J.-C., Roverato, M., 2021. Sedimentology of volcanic debris avalanche deposits. [In:] M. Roverato, A. Dufresne & J. Procter (Eds.): *Volcanic Debris Avalanches. Advances in Volcanology*. Springer, Cham, pp. 175-210. https://doi.org/10.1007/978-3-030-57411-6_8.

Dunlevey, J.N. & Smith, A.M., 2011. Sedimentological evidence for an interglacial in the Permo-Carboniferous Dwyka Group, Coedmore Quarry, Durban, South Africa. *South African Journal of Geology* 114, 159-166. https://doi.org/10.2113/gssajg.114.2.159.

Embley, R.W., 1982. Anatomy of some Atlantic margin sediment slides and some comments on ages and mechanisms. [In:] S. Saxov & J.K. Nieuwenhuis (Eds): *Marine Slides and Other Mass Movements*. Plenum Press, New York, pp. 189-213.

Enos, P., 1969. Anatomy of flysch. *Journal of Sedimentary Research* 39, 680-723.

Evenson, E.B., Dreimanis, A. & Newsome, J.W., 1977. Subaquatic flow tills: a new interpretation for the genesis of some laminated deposits. *Boreas* 6, 115-133.

Eyles, N., 1993. Earth´s glacial record and its tectonic setting. *Earth-Science Reviews* 35, 1-248.

Eyles, N. & Januszczak, N., 2007. Syntectonic subaqueous mass flows of the Neoproterozoic Otavi Group, Namibia: where is the evidence of global glaciation? *Basin Research* 19, 179-198.

Fagereng, Å., 2014. Significant shortening by pressure solution creep in the Dwyka diamictite, Cape Fold Belt, *South Africa. Journal of African Earth Sciences* 97, 9-18. http://dx.doi.org/10.1016/j.jafrearsci.2014.04.022.

Fedorchuk, N.D., Isbell, J.L., Griffis, N.P., Montañez, I.P., Vesely, F.F., Iannuzzi, R., Mundil, R., Yin, Q-Z., Pauls, K.N. & Rosa, E.L.M., 2019. Origin of paleovalleys on the Rio Grande do Sul Shield (Brazil): implications for the extent of late Paleozoic glaciation in west-central Gondwana. *Palaeogeography, Palaeoclimatology, Palaeoecology* 531, Part B, 108738. https://doi.org/10.1016/j.palaeo.2018.04.013.

Festa, A., Ogata, K., Pini, G.A., Dilek, Y. & Alonso, J.L., 2016. Origin and significance of olistostromes in the evolution of orogenic belts: a global synthesis. *Gondwana Research* 39, 180–203. https://doi.org/10.1016/j.gr.2016.08.002.

Fleisher, P.J., Lachniet, M.S., Muller, E.H. & Bailey, P.K., 2006. Subglacial deformation of trees within overridden foreland strata, Bering Glacier, Alaska. *Geomorphology* 75, 201-211. https://doi.org/10.1016/j.geomorph.2005.01.013.

Flint, R.F., 1961. Geological evidence of cold climate. [In:] A.E.M. Nairn (Ed.): *Descriptive Palaeoclimatology*. Interscience Publishing, New York, pp. 140-155.

Geophysical Discussion of the Royal Astronomical Society, 1960. *Geophysical journal of the Royal Astronomical Society (incorporating the Geophysical Supplement to the Monthly Notices of the R.A.S.)* 3, 127-132.

Glicken, H., 1996. *Rockslide-debris avalanche of May 18, 1980, Mount St. Helens Volcano, Washington.* U.S. Geological Survey, Open-File Report 96-677, 98 pp,

Górska, M.E., Woronko, B., Kossowski, T.M. & Pisarska-Jamroży, M., 2022. Micro-scale frost-weathering simulation – Changes in grain-size composition and influencing factors.

Catena 212, 106106. https://doi.org/10.1016/j.catena.2022.106106.

Götz, A.E., Ruckwied, K. & Wheeler, A., 2018. Marine flooding surfaces recorded in Permian black shales and coal deposits of the Main Karoo Basin (South Africa): implications for basin dynamics and cross-basin correlation. *International Journal of Coal Geology* 190, 178–190. http://dx.doi.org/10.1016/j.coal.2017.10.014.

Griffis, N., Montañez, I., Mundil, R., Le Heron, D., Dietrich, P., Kettler, C., Linol, B., Mottin, T., Vesely, F., Iannuzzi, R., Huyskens, M. & Yin, Q.-Z., 2021. High-latitude ice and climate control on sediment supply across SW Gondwana during the late Carboniferous and early Permian. *Bulletin of the Geological Society of America* 133, 2113–2124. https://doi.org/10.1130/B35852.1.

Haflidason, H., Sejrup, H.P., Nygård, A., Mienert, J., Bryn, P., Lien, R., Forsberg, C.F., Berg, K. & Masson, D., 2004. The Storegga Slide: architecture, geometry and slide development. *Marine Geology* 213, 201-234. https://doi.org/10.1016/j.margeo.2004.10.007

Haldorsen, S., Von Brunn, V., Maud, R. & Truter, E.D., 2001. A Weichselian deglaciation model applied to the early Permian glaciation in the northeast Karoo Basin, South Africa. *Journal of Quaternary Science* 16, 583-593. https://doi.org/10.1002/jqs.637.

Hancox, P.J. & Götz, A.E., 2014. South Africa's coalfields – A 2014 perspective. *International Journal of Coal Geology* 132, 170–254. http://dx.doi.org/10.1016/j.coal.2014.06.019.

Hansen, L.A.S., Hodgson, D.M., Pontén, A., Bell, D. & Flint, S., 2019. Quantification of basin-floor fan pinchouts: examples from the Karoo Basin, South Africa. *Frontiers in Earth Science* 7, article 12. https://doi.org/10.3389/feart.2019.00012.

Hawkes, L., 1943. The erratics of the Cambridge Greensand – their nature provenance and mode of transport. *Quaterly Journal of the Geological Society of London* 99, 93-104.

Horan, K., 2015. *Falkland Islands (Islas Malvinas) in the Permo-Carboniferous.* Springer Earth System Sciences, Cham, pp. 45-70. https://doi.org/10.1007/978-3-319-08708-5_4.

Huber, H., Koeberl, C., Mcdonald, I. & Reimold, W.U., 2001. Geochemistry and petrology of Witwatersrand and Dwyka diamictites from South Africa: search for an extraterrestrial component. *Geochimica et Cosmochimica Acta* 65, 2007-2016.

Isbell, J.L., Cole, D.I. & Catuneanu, O., 2008. Carboniferous-Permian glaciation in the main Karoo Basin, South Africa: Stratigraphy, depositional controls, and glacial dynamics. [In:] C.R. Fielding, T.D. Frank, & J.L. Isbell (Eds): *Resolving the Late Paleozoic Ice Age in Time and Space*. Geological Society of America Special Paper 441, pp. 71–82. https://doi.org/10.1130/2008.2441(05).

Isbell, J.L., Henry, L.C., Gulbranson, E., Limarino, C.O., Fraiser, M.L., Koch, Z.J., Ciccioli, P.L. & Dineen, A.A., 2012. Glacial paradoxes during the late Paleozoic ice age: evaluating the equilibrium line altitude as a control on glaciation. *Gondwana Research* 22, 1–19.

Isbell, J.L., Henry, L.C., Reid, C.M & Fraiser, M.L., 2013. Sedimentology and palaeoecology of lonestone-bearing mixed clastic rocks and cold-water carbonates of the Lower Permian basal beds at Fossil Cliffs, Maria Island, Tasmania (Australia): Insight into the initial decline of the late Palaeozoic ice age. [In:] A. Gasiewicz & M. Słowakiewicz (Eds): *Palaeozoic Climate Cycles: Their Evolutionary and Sedimentological Impact*. Geological Society, London, Special Publications 376, pp. 307–341. https://doi.org/10.1144/SP376.2.

Iverson, N.R., 1991. Morphology of glacial striae: Implications for abrasion of glacier beds and fault surfaces. *Bulletin of the Geological Society of America* 103, 1308-1316.

John, B.S., 1979. The great ice age: Permo-Carboniferous. [In:] B.S. John (Ed.): *The Winters of the World*. Davies & Charles, Newton Abbot, pp.154-172.

Johnson, M.R., Van Vuuren, C.J., Visser, J.N.J., Cole, D.I., Wickens, H.D.V., Christie, A.D.M. & Roberts, D.L., 1997. The foreland Karoo Basin, South Africa [In:] R.C. Selley (Ed.): *African Basins, Sedimentary Basins of the World 3.* Elsevier, Amsterdam, pp. 269-317.

Kalińska-Nartiša, E., Woronko, B. & Ning, W., 2017. Microtextural inheritance on quartz sand grains from Pleistocene periglacial environments of the Mazovian Lowland, Central Poland. *Permafrost and Periglacial Processes* 28, 741-756. https://doi.org/10.1002/ppp.1943.

Kalińska, E., Lamsters, K., Karušs, J., Krievāns, M., Rečs, A. & Ješkins, J., 2022. Does glacial environment produce glacial mineral grains? Pro- and supra-glacial Icelandic sediments in microtextural study. *Quaternary International* 617, 101-111. https://doi.org/10.1016/j.quaint.2021.03.029.

Kennedy, K. & Eyles, N., 2021. Syn-rift mass flow generated ‘tectonofacies’ and ‘tectonosequences’ of the Kingston Peak Formation, Death Valley, California, and their bearing on supposed Neoproterozoic panglacial climates. *Sedimentology* 68, 352-381. https://doi.org/10.1111/sed.12781.

Kent, D.V. & Muttoni, G., 2020. Pangea B and the Late Paleozoic ice age. *Palaeogeography, Palaeoclimatology, Palaeoecology* 553, 109753. https://doi.org/10.1016/j.palaeo.2020.109753.

Kneller, B.C., Edwards, D., McCaffrey, W.D. & Moore, R., 1991. Oblique reflection of turbidity currents. *Geology* 14, 250-252.

Kut, A.A.,Woronko, B., Spektor, V.V. & Klimova, I.V., 2021. Grain-surface microtextures in deposits affected by periglacial conditions (Abalakh High-Accumulation Plain, Central Yakutia, Russia). *Micron* 146, 103067. https://doi.org/10.1016/j.micron.2021.103067.

Lamb, M.P., 2008. *Formation of Amphitheater-Headed Canyons* (Ph.D. thesis). University of California, Berkeley, 311 pp.

Le Heron, D.P, Sutcliffe, O.E., Whittington, R.J. & Craig, J., 2005. The origins of glacially related soft-sediment deformation structures in Upper Ordovician glaciogenic rocks: implication for ice-sheet dynamics. *Palaeogeography, Palaeoclimatology, Palaeoecology* 218, 75-103.

Le Heron, D.P., Busfield, M.E. & Collins, A.S., 2014. Bolla Bollana boulder beds: a

Neoproterozoic trough mouth fan in South Australia? *Sedimentology* 61, 978–995. https://doi.org/10.1111/sed.12082.

Le Heron, D.P., Dietrich, P., Busfield, M.E., Kettler, C., Bermanschläger, S. & Grasemann, B., 2019. Scratching the surface: footprint of a late Carboniferous ice sheet. *Geology* 47, 1034-1038. https://doi.org/10.1130/G46590.1.

Le Heron, D.P., Heninger, M., Baal, C. & Bestmann, M., 2020. Sediment deformation and production beneath soft-bedded Palaeozoic ice sheets. *Sedimentary Geology* 408, 105761. https://doi.org/10.1016/j.sedgeo.2020.105761.

Le Heron, D.P., Kettler, C., Griffis, N.P., Dietrich, P., Montañez, I.P., Osleger, D.A., Hofmann, A, Douillet, G. & Mundil, R., 2021. The Late Palaeozoic Ice Age unconformity in southern Namibia viewed as a patchwork mosaic. *Depositional Record* 00:1-17. https://doi.org/10.1002/dep2.163.

Lindsay, J.F., 1970. Depositional environment of Paleozoic glacial rocks in the Central Transantarctic Mountains. *Bulletin of the Geological Society of America* 81, 1149-1171.

Liu, Y. & Gastaldo, R.A., 1992. Characteristics and provenance of log-transported gravels in a Carboniferous channel deposit. *Journal of Sedimentary Petrology* 62, 1072-1083.

Loope, D.B. & Burberry, C.M., 2018. Sheeting joints and polygonal patterns in the Navajo Sandstone, southern Utah: Controlled by rock fabric, tectonic joints, buckling, and gullying. *Geosphere* 14, 1818–1836. https://doi.org/10.1130/GES01614.1.

Mahaney, W.C., 2002. *Atlas of Sand Grain Surface Textures and Applications*. Oxford University Press, New York, 237 pp.

Major, J.J., Pierson, T.C. & Scott, K.M., 2005. Debris flows at Mount St. Helens, Washington, USA. [In:] M. Jakob, & O. Hungr (Eds): *Debris-Flow Hazards and Related Phenomena.* Praxis/Springer, Berlin, pp. 685-731.

Mangerud, J., Hughes, A.L.C., Sæle, T.H. & Svendsen, J.I., 2019. Ice-flow patterns and precise timing of ice sheet retreat across a dissected fjord landscape in western Norway. *Quaternary Science Reviews* 214, 139-163. https://doi.org/10.1016/j.quascirev.2019.04.032.

Martin, H., 1981. The late Palaeozoic Gondwana glaciation. *Geologische Rundschau* 70, 480-496.

Master, S., 2012. Hertzian fractures in the sub-Dwyka Nooitgedacht striated pavement, and implications for the former thickness of Karoo strata near Kimberley, South Africa. *South African Journal of Geology* 115, 561-576. https://doi.org/10.2113/gssajg.115.4.561.

McLoughlin, S., 2011. Glossopteris – insights into the architecture and relationships of an iconic Permian Gondwanan plant. *Journal of the Botanical Society of Bengal* 65, 1-14.

Mitchell, N.C., 2006. Morphologies of knickpoints in submarine canyons. *Bulletin of the Geological Society of America* 18, 589–605. https://doi.org/10.1130/B25772.1.

Molén, M.O., 2014. A simple method to classify diamicts by scanning electron microscope from surface microtextures. *Sedimentology* 61, 2020-2041. https://doi.org/10.1111/sed.12127.

Molén, M.O., 2017. The origin of Upper Precambrian diamictites; Northern Norway: A case study applicable to diamictites in general, *Geologos* 23, 163-181. https://doi.org/10.1515/logos-2017-0019.

Molén, M.O., 2021. Field evidence suggests that the Palaeoproterozoic Gowganda Formation in Canada is non-glacial in origin. *Geologos* 27, 73-91. https://doi.org/10.2478/logos-2021-0009.

Molén, M.O., 2022a. Glaciation or not? An analytic review of features of glaciation and sediment gravity flows: introducing a methodology for field research. Submitted. Under review. Submitted 2021. Preprint DOI: 10.1002/essoar.10510880.1.

Molén, M.O., 2022b. Glaciation and mass flows: patterns, processes and models – a short analytic review. In progress. ***

Montañez, I.P. & Poulsen, C.J., 2013. The Late Paleozoic Ice Age: An evolving paradigm. *Annual Review of Earth and Planetary Sciences* 41, 629-656. https://doi.org/10.1146/annurev.earth.031208.100118.

Montañez, I.P., McElwain, J.C., Poulsen, C.J., White, J.D., DiMichele, W.A., Wilson, J.P., Griggs, G. & Hren, M.T., 2016. Climate, pCO_2 and terrestrial carbon cycle linkages during late Palaeozoic glacial-interglacial cycles. *Nature Geoscience* 9, 824-828. https://doi.org/10.1038/ngeo2822.

Myers, T.S., 2016. CO_2 and late Palaeozoic glaciation. *Nature Geoscience* 9, 803-804.

Norman, N., 2013. *Geology of the Beaten Track*. Struik Nature, Cape Town, 256 pp.

Normandeau, A., Lajeunesse, P. & St-Onge, G., 2015. Submarine canyons and channels in the Lower St. Lawrence Estuary (Eastern Canada): Morphology, classification and recent sediment dynamics. *Geomorphology* 241, 1-18. http://dx.doi.org/10.1016/j.geomorph.2015.03.023.

Ortiz-Karpf, A., Hodgson, D.M., Jackson, C.A.-L. & McCaffrey, W.D., 2017. Influence of seabed morphology and substrate composition on mass-transport flow processes and pathways: insights from the Magdalena Fan, offshore Colombia. *Journal of Sedimentary Research* 87, 189-209, http://dx.doi.org/10.2110/jsr.2017.10.

Passchier, S., Hansen, M.A. & Rosenberg, J., 2021. Quartz grain microtextures illuminate Pliocene periglacial sand fluxes on the Antarctic continental margin. *Depositional Record* 7, 564-581. https://doi.org/10.1002/dep2.157.

Peakall, J., Best, J., Baas, J.H., Hodgson, D.M., Clare, M.A., Talling, P.T., Dorrell, R.M. & Lee, D.R., 2020. An integrated process-based model of flutes and tool marks in deep-water environments: Implications for palaeohydraulics, the Bouma sequence and hybrid event beds. *Sedimentology* 67, 1601–1666. https://doi.org/10.1111/sed.12727.

Petit, J.P. & Laville, E., 1987. Morphology and microstructures of hydroplastic slickensides in sandstone. [In:] M.E. Jones & R.M. Preston (Eds): *Deformation of Sediments and*

Sedimentary Rocks. Geological Society, London, Special Publications 29, pp. 107-121.

Pickering, K.T, Underwood, M.B. & Taira, A., 1992. Open-ocean to trench turbidity-current flow in the Nankai Trough: flow collapse and reflection. *Geology* 20, 1099-1102.

Piper, D.J.W., Cochonat, P. & Morrison, M.L., 1999. The sequence of events around the epicentre of the 1929 Grand Banks earthquake: initiation of debris flows and turbidity current inferred from sidescan sonar. *Sedimentology* 46, 79–97.

Potter, P.E. & Pettijohn, F.J., 1963. *Paleocurrents and basin analysis.* Springer, Berlin, 296 pp.

Price, P.H., 1932. Erratic boulders in Sewell Coal of West Virginia. *Journal of Geology* 40, 62-73.

Puga Bernabéu, Á., Webster, J.M., Beaman, R.J., Thran, A., López Cabrera, J., Hinestrosa, G. & Daniell, J., 2020. Submarine landslides along the mixed siliciclastic carbonate margin of the great barrier reef (offshore Australia). [In:] K. Ogata, A. Festa, & G.A. Pini (Eds): *Submarine Landslides: Subaqueous Mass Transport Deposits from Outcrops to Seismic Profiles.* Geophysical Monograph 246, Wiley & Sons, pp. 313-337. https://doi.org/10.1002/9781119500513.ch19.

Rampino, M.R., 2017. Are some tillites impact-related debris-flow deposits? *Journal of Geology* 125, 155-164. https://doi.org/10.1086/690212.

Ruban, D.A., Al-Husseini, M.I. & Iwasaki, Y., 2007. Review of Middle East Paleozoic plate tectonics. *GeoArabia* 12, 35-56.

Ryder, J. M. & Thomson, B., 2011. Neoglaciation in the southern Coast Mountains of British Columbia: Chronology prior to the late Neoglacial maximum. *Canadian Journal of Earth Science* 23, 273-287. https://doi.org/10.1139/e86-031.

Sandberg, C.G.S., 1928. The origin of the Dwyka Conglomerate of South Africa and other "glacial" deposits. *Geological Magazine* 65, 117-138.

Savage, N.M., 1972. Soft-dediment glacial grooving of Dwyka Age in South Africa. *Journal of Sedimentary Petrology* 42, 307-308.

Scheffler, K., Hoernes, S. & Schwark, L., 2003. Global changes during Carboniferous–Permian glaciation of Gondwana: Linking polar and equatorial climate evolution by geochemical proxies. *Geology* 31, 605-608. https://doi.org/10.1130/0091-7613(2003)031<0605:GCDCGO>2.0.CO;2

Scheiber-Enslin, S.E., Ebbing, J. & Webb, S.J., 2015. New depth maps of the main Karoo Basin, used to explore the Cape isostatic anomaly, South Africa. *South African Journal of Geology* 118, 225-248. https://doi.org/10.2113/gssajg.118.3.225.

Schermerhorn, L.J.G., 1970. Saharan ice. *Geotimes* 15, 7-8.

Schermerhorn, L.J.G., 1971. Upper Ordovician glaciation in Northwest Africa? Discussion.

Bulletin of the Geological Society of America 82, 265-268.

Schermerhorn, L.J.G., 1974. Late Precambrian mixtites: glacial and/or nonglacial? *American Journal of Science* 274, 673-824.

Schermerhorn, L.J.G., 1976a. Reply. *American Journal of Science* 276, 375-384.

Schermerhorn, L.J.G., 1976b. Reply. *American Journal of Science* 276, 1315-1324.

Schermerhorn, L.J.G., 1977. Late Precambrian glacial climate and the Earth´s obliquity – a discussion. *Geological Magazine* 114, 57-64.

Schneider, J.L. & Fisher, R.V., 1998. Transport and emplacement mechanisms of large volcanic debris avalanches: evidence from the northwest sector of Cantal Volcano (France). *Journal of Volcanology and Geothermal Research* 83, 141–165.

Scotese, C.R., Song, H., Mills, B.J.W. & van der Meer, D.G., 2021. Phanerozoic paleotemperatures: The earth´s changing climate during the last 540 million years. *Earth-Science Reviews* 215, 103503. https://doi.org/10.1016/j.earscirev.2021.103503.

Scott, K.M., 1988. *Origin, Behavior and Sedimentology of Lahars and Lahar-runout Flows in the Toutle-cowlitz River System*. U.S. Geological Survey Professional Paper 1447A, 76 pp.

Shanmugam, G., 2016. Submarine fans: a critical retrospective (1950-2015). *Journal of Palaeogeography* 5, 110-184.

Shanmugam, G., 2019. Reply to discussions by Zavala (2019) and by Van Loon, Hüeneke, and Mulder (2019) on Shanmugam, G. (2018), Journal of Palaeogeography, 7 (3): 197–238): ‘the hyperpycnite problem’. *Journal of Palaeogeography* 8, 31. https://doi.org/10.1186/s42501-019-0047-1.

Shanmugam, G., 2021. *Mass Transport, Gravity Flows, and Bottom Currents*. Elsevier, 571 pp. https://doi.org/10.1016/C2019-0-03665-5.

Shanmugam, G., Lehtonen, L.R., Straume, T., Syvertsen, S.E., Hodgkinson, R.J. & Skibej, M., 1994. Slump and debris-flow dominated upper slope facies in the Cretaceous of the Norwegian and Northern North Seas (61-67°N): implications for sand distribution. *AAPG Bulletin* 78, 910-937.

Shepard, F.P. & Dill, R.F., 1966. *Submarine Canyons and Other Sea Valleys.* Rand McNally, Chicago, 381 pp.

Simms, M.J., 2007. Uniquely extensive soft-sediment deformation in the Rhaetian of the UK: evidence for earthquake or impact? *Palaeogeography, Palaeoclimatology, Palaeoecology* 244, 407–423.

Slater, G., du Toit, A.L. & Haughton, S.H., 1932. The glaciated surfaces of Nooitgedacht, near Kimberley, and the Upper Dwyka boulder shales of the eastern part of Griqualand West (Cape Province), 1929. *Transactions of the Royal Society of South Africa* 20, 301-325. https://doi.org/10.1080/00359193209518862.

Somelar, P., Vahur, S., Hamilton, T.S., Mahaney, W.C., Barendregt, R.W. & Costa, P. 2018. Sand coatings in paleosols: evidence of weathering across the Plio-Pleistocene boundary to modern times on Mt. Kenya. *Geomorphology* 317, 91–106.

Stavrakis, N., 1986. Sedimentary environments and facies of the Orange Free State coalfield. [In:] C.R. Anhaeusser & S. Maske (Eds): *Mineral Deposits of Southern Africa vols. I and II.* Geological Society of South Africa, Johannesburg, pp. 1939–1952.

Stavrakis, N. & Smyth, M., 1991. Clastic sedimentary environments and organic petrology of coals in the Orange Free State, South Africa. *International Journal of Coal Geology* 18, 1-16.

Stratten, T. & Humphreys, A.J.B., 1974. Extensive glacial pavement of Dwyka age near Douglas, Cape Province. *South African Journal of Science* 70, 44-45.

Talling, P.J., Wynn, R.B., Masson, D.G., Frenz, M., Cronin, B.T., Schiebel, R, Akhmetzhanov, A.M., Dallmeier-Tiessen, S., Benetti, S., Weaver, P.P.E., Georgiopoulou, A., Zühlsdorff, C. & Amy, L.A., 2007. Onset of submarine debris flow deposition far from original giant landslide. *Nature* 450, 541-544.

Talling, P.J., Masson, D.G., Sumner, E.J. & Malgesini, G., 2012. Subaqueous sediment density flows: depositional processes and deposit types. *Sedimentology* 59, 1937-2003.

Talling, P.J., Allin, J., Armitage, D.A., Arnott, R.W.C., Cartigny, M.J.B., Clare, M.A., Felletti, F., Covault, J.A., Girardclos, S., Hansen, E., Hill, P.H., Hiscott, R.N., Hogg, A.J., Clarke, J.H., Jobe, Z.R., Malgesini, G., Mozzato, A., Naruse, H., Parkinson, S., Peel, F.J., Piper, D.J., Pope, E., Postma, G., Rowley, P., Sguazzini, A., Stevenson, C.J., Sumner, E.J., Sylvester, Z., Watts, C. & Xu, J., 2015. Key future directions for research on turbidity currents and their deposits. *Journal of Sedimentary Research* 85, 153-169.

Tavener-Smith, T. & Mason, T.R., 1983. A late Dwyka (Early Permian) varvite sequence near Isandlwana, Zululand, South Africa. *Palaeogeography, Palaeoclimatology, Palaeoecology* 41, 233-249.

Van der Westhuizen, W.A., de Bruiyn, H. & Meintjes, P.G., 2006. The Ventersdorp Supergroup. [In:] M.R. Johnson, C.R. Anhaeusser & R.J. Thomas (Eds): *The Geology of South Africa*. Geological Society of South Africa, Johannesburg, pp. 187–208.

Vesely, F.F., Rodrigues, M.C.N.L., da Rosa, E.L.M., Amato, J.A., Trzaskos, B., Isbell, J.L. & Fedorchuk, N.D., 2018. Recurrent emplacement of non-glacial diamictite during the late Paleozoic ice age. Geology 46, 615-618. https://doi.org/10.1130/G45011.1.

Visser, J.N.J., 1981. Carboniferous topography and glaciation in the North-Western part of the Karoo Basin, South Africa. *Annals of the Geological Survey of South Africa* 15, 13-24.

Visser, J.N.J., 1982. Upper Carboniferous glacial sedimentation in the Karoo Basin near Prieska, South Africa. *Palaeogeography, Palaeoclimatology, Palaeoecology* 38, 63-92.

Visser, J.N.J., 1983a. Glacial marine sedimentation in the Late Paleozoic Karoo Basin, Southern Africa. [In:] B.F. Molnia (Ed.): *Glacial-Marine Sedimentation.* Plenum Press, New York, pp. 667-701.

Visser, J.N. J., 1983b. The problems of recognizing ancient subaqueous debris flow deposits in glacial sequences. *Transactions of the Geological Society of South Africa* 86, 127-135.

Visser, J.N.J., 1986. Lateral lithofacies relationships in the glacigene Dwyka Formation in the western and central parts of the Karoo Basin. *Transactions of the Geological Society of South Africa* 89, 373-383.

Visser, J.N.J., 1987. The palaeogeography of part of southwestern Gondwana during the Permo-Carboniferous glaciation. *Palaeogeography, Palaeoclimatology, Palaeoecology* 61, 205-219.

Visser, J.N.J., 1988. A Permo-Carboniferous tunnel valley system east of Barklay West, Northern Cape Province. *South African Journal of Geology* 91, 350-357.

Visser, J.N.J., 1989a. The Permo-Carboniferous Dwyka Formation of Southern Africa: deposition by a predominantly subpolar marine ice sheet. *Palaeogeography, Palaeoclimatology, Palaeoecology* 70, 377-391.

Visser, J.N.J., 1989b. Stone orientation in basal glaciogenic diamictite: four examples from the Permo-Carboniferous Dwyka Formation, South Africa. *Journal of Sedimentary Petrology* 59, 935-943.

Visser, J.N.J., 1990. Glacial bedforms at the base of the Permo-Carboniferous Dwyka Formation along the western margin of the Karoo Basin, South Africa. *Sedimentology* 37, 231-245.

Visser, J.N.J., 1994. The interpretation of massive rain-out and debris-flow diamictites from the glacial marine environment. [In:] M. Deynoux, J.M.G. Miller, E.W. Domack, N. Eyles, I.J. Fairchild & G.M. Young (Eds): *Earth´s Glacial Record.* Cambridge University Press, Cambridge, pp. 83-94.

Visser, J.N.J., 1996. A Late Carboniferous subaqueous glacial valley fill complex: Fluctuations in meltwater output and sediment flux. *South African Journal of Geology* 99, 285-291.

Visser, J.N.J., 1997. Deglaciation sequences in the Permo-Carboniferous Karoo and Kalahari basins of southern Africa: a tool in the analysis of cyclic glaciomarine basin fills. *Sedimentology* 44, 507-521.

Visser, J.N.J. & Kingsley, C.S., 1982. Upper Carboniferous glacial valley sedimentation in the Karoo Basin, Orange Free State. *Transactions of the Geological Society of South Africa* 85, 71-79.

Visser, J.N.J. & Loock, J.C. 1982. An investigation of the basal Dwyka tillite in the southern part of the Karoo Basin, South Africa. *Transactions of the Geological Society of South Africa* 85, 179-187.

Visser, J.N.J. & Loock, J.C., 1988. Sedimentary facies of the Dwyka Formation associated with the Nooitgedacht Glacial Pavements, Barkly West District. *South African Journal of Geology*, 91, 38-48.

Visser, J.N.J., Loock, J.C. & Colliston, W.P., 1987. Subaqueous outwash fan and esker sandstones in the Permo-Carboniferous Dwyka Formation of South Africa. *Journal of Sedimentary Petrology* 57, 467-478.

Visser, J.N.J., van Niekerk, B.N. & van der Merwe, S.W., 1997a. Sediment transport of the late Palaeozoic glacial Dwyka Group in the southwestern Karoo Basin. *South African Journal of Geology* 100, 223-236.

Visser, J.N.J., Colliston, W.P. & Terreblanche, J.C., 1997b. The origin of soft-sediment deformation structures in Permo-Carboniferous glacial and proglacial beds, South Africa. *Journal of Sedimentary Petrology* 54, 1183-1196.

Von Brunn, V., 1994. Glaciogenic deposits of the Permo-Carboniferous Dwyka Group in the eastern region of the Karoo Basin, South Africa. [In:] M. Deynoux, J.M.G. Miller, E.W. Domack, N. Eyles, I.J. Fairchild & G.M. Young (Eds.): *Earth´s Glacial Record*. Cambridge University Press, Cambridge, pp. 60-69.

Von Brunn, V. 1996. The Dwyka Group in the northern part of Kwazulu/Natal, South Africa: sedimentation during late Palaeozoic deglaciation. *Palaeogeography, Palaeoclimatology, Palaeoecology* 125, 141-163.

Vrolijk, P.J., Urai, J.L. & Kettermann, M., 2016. Clay smear: Review of mechanisms and applications. *Journal of Structural Geology* 86, 95-152. http://dx.doi.org/10.1016/j.jsg.2015.09.006.

Whipple, K.X., Hancock, G.S. & Anderson, R.S., 2000. River incision into bedrock: Mechanics and relative efficacy of plucking, abrasion and cavitation. *Bulletin of the Geological Society of America* 112, 490-503. https://doi.org/10.1130/0016-7606(2000)112<490:RIIBMA>2.0.CO;2.

Wilkins, S.J., Gross, M.R., Wacker, M., Eyal, Y. & Engelder, T., 2001. Faulted joints: kinematics, displacement – length scaling relations and criteria for their identification. *Journal of Structural Geology* 23, 315-327.

Woronko, B., 2016. Frost weathering versus glacial grinding in the micromorphology of quartz sand grains: Processes and geological implications. *Sedimentary Geology* 335, 103-119. http://dx.doi.org/10.1016/j.sedgeo.2016.01.021.

Yincan., Y. et al., 2017. Marine Geo-Hazards in China. China Ocean Press, Elsevier, pp. 193-194. https://doi.org/10.1016/B978-0-12-812726-1.00006-1.

Zavala, C., 2019. The new knowledge is written on sedimentary rocks – a comment on Shanmugam's paper "The hyperpycnite problem". *Journal of Palaeogeography* 8, 23. https://doi.org/10.1186/s42501-019-0037-3.

Zavala, C., 2020. Hyperpycnal (over density) flows and deposits. *Journal of Palaeogeography* 9, 17. https://doi.org/10.1186/s42501-020-00065-x.

Zavala, C. & Arcuri, M., 2016. Intrabasinal and extrabasinal turbidites: origin and distinctive characteristics. *Sedimentary Geology* 337, 36–54.

http://dx.doi.org/10.1016/j.sedgeo.2016.03.008.

Reconsidering the glaciogenic origin of Gondwana diamictites, Dwyka Group, South Africa

Supplemental material

Headings refer to the similar parts in the published article.

S1. Introduction

S2. Research area, detailed site and sample description

S3. Methods, details of the laboratory preparation of samples

S4. Results

S5. Detailed discussion of sampling and laboratory work

S1. Introduction

There is a large literature describing diamictites and paleoclimates. This is documented by Molén (2022a). The Supplemental information is mainly detailed descriptions of the laboratory work (S2-S5).

SA = South Africa

SM = surface microtextures

ss = sandstone

S2. Research area, detailed site and sample description

.

C. Nooitgedacht, diamictite on Ventersdorp lava pavement, -28.5995, 24.6124 (Slater et al., 1932). Brown color in all samples is recent weathering.

C-1-1	Pavement 1. Sampled material is thin hard crust exactly on top of pavement. Brown, but black surface.
C1b	Pavement 1. Brown
C2a	Pavement 1. Brown, gray.
C2b, C2bb, C2c	Pavement 1. Brown
C3a, C3b	Pavement 2, c. 100 m southwest. This diamictite sample is from exactly on top of ca 1 mm of sediment, that is between pavement and diamictite. Brown
C3bm	Pavement 2, c. 100 m southwest. Sample is a part of a ca 5-6 mm string of sediment between pavement and diamictite (Fig. S1). Light brown.
C3c	Pavement 2, c. 100 m southwest. Diamictite sample from on top of the ca 1 mm of sediment between pavement and diamictite. Brown.
C4	Pavement 2. Diamictite sampled on top of 2-3 mm sediment layer on top of sample C4m, on top of pavement. Brown.
C4m	Pavement 2. Sample is c. 2-3 mm of sediment between pavement and diamictite, below sample C4. Dark/black and brown. Sediment.

D	Douglas Ventersdorp lava pavement, -29.14621, 23.6985 (Stratten & Humphreys, 1974). Pavement, no samples.

E	Oorlogsklof, soft sediment sandstone pavement, -31.4375, 19.1449 (Visser, 1990). Pavement, no samples.

1641 F. Roadcut c. 5 km north of Nieuwoudtville, close to waterfall, -31.3055, 19.1229 (Visser,
1642 1990). Stratigraphy: diamictite, sandstone and conglomerate, diamictite.

1643	F1a	East side of road, middle. Gray.
1644	F1aa	East side of road, low. Gray.
1645	F1b	East side of road, upper. Gray.
1646	F2, F2b	Below large heavily weathered granite boulder in sandstone. Gray.
1647	F3a, F3b. F3c	In upper diamictite, with sandstone containing large heavily weathered granite boulder between. Samples in diamictite above weathered granite. Gray.
1648	F4	West side of road. Sample is conglomerate part in sandstone ca 1 m above diamictite. (All parts from sample F4c was separated away, including loose material of F4 that was mixed with F4c). Brown to gray.
1649	F4b	West side. Sample is conglomerate part ca 1 m above diamictite. Brown.
1650	F4c	West side. Sample is weathered sandstone pebble in sample F4 conglomerate that disintegrates easily, i.e. source rock. Sample also contains matrix from F4. Red sandstone rock.
1651	F5	West, Dwyka diamictite, 1 m below conglomerate i.e. below sample F4 and F4b. Gray.

1652 G. Kransgat River, next to Koringhuis homestead/farm, about 20 km NE of
1653 Nieuwoudtville, -31.1629, 19.3157 (Visser, 1996).

1654	G1a, G1b, G1c	Samples in 1 m exposed diamictite. Lowermost sample. Gray.
1655	G2a, G2b, G2c	About 5 m above samples G1, in exposed diamcitite and c. 0.5 m below clay with outsized clasts. Gray.

H. Elandsvlei farm area. -32.3292, 19.6406 (H1-samples) -32.3291, 19.6358 (H2-samples) (Visser et al., 1997a; Blignault & Theron, 2015).

H1, H1a	Gray.
H2b	Sample from brown diamictite boulder that was within gray diamictite. Brown on the outside but gray on the inside. (Fig. 15 in article.)
H2c	Next to brown diamictite boulder within diamictite. Gray.

J. South of Matjiesfontein, road N1, -33.2390, 20.4793 (Visser et al., 1997a).

J1a	Weathered sample. Gray.
J1b, J1c, J1d	Fresh samples. Gray.

K. Umkomaas River Valley, roadcut next to railway line,.-301909, 30.7765. (Closest described site at Durban, and descriptions of Dwyka in the area, in Dunlevey & Smith, 2011.) Brown material is recently weathered.

K1a	Upper. Probably some blasting impacts to the rocks (no borings observed at exactly this spot). Weathered. Brown.
K1b, K1bb	Top area. Blasted, fresh. Gray.
K1c	Top area, weathered. Brown.
K2, K2b	Middle. Small fault plane that originated by an internal slide is within sample. Fault plane is not analyzed, but grains from fault plane may be inside sample. Weathered. Brown.
K3b	Lower, fresh. Gray.
K3c	Sample c. 50 m west and less weathered. Gray.

L. Durban, University of KwaZulu-Natal Westville Campus, -29.8187, 30.944. Sandstone pavement. (Bangert & Von Brunn, 2001; Haldorsen et al., 2001.)

L1	Sand in joint of pavement, no/little fine sand, silt and clay. Light brown. Mainly sand and silt.
L1b	Sample from sandstone pavement. Light brown. Mainly sand and silt.
L1br	Harder sandstone piece or rock from within sample L1b, that was separated after sample L1b had disintegrated. Light brown. Mainly sand and silt.
L1c	Sample exactly at pavement. Appears diamictic. Light brown to gray. Mainly sand and silt.

M. Durban, Coedmore Quarry, -29.8980, 30.94852 (Dunlevey & Smith, 2011). All samples, but mostly samples M1 and M4, appear a little metamorphosed and contain more clay than other SA samples.

M1, M2, M3, M4	Extra hard, from rocks. Black.
M6	Extra hard, from wall. Black.

N. West of Denny Dalton, dirt road, -28.2843, 31.2251 (N1a, N2a), -28.2840, 31.2211 (N2b) (Norman, 2013; Hancox & Götz, 2014).

N1a, N2a	Samples above pavement. Samples are covered by chemical precipitation.
N2b	Isolated diamictite rock c. 400 m west. Black.

O. Southwest of Denny Dalton, roadcut at R34, -28.2994, 31.2215 (Norman, 2013; Hancox & Götz, 2014).

O1a	Gray.
O2	Ca. 1 m above and 10 m from O1a. Gray.

P. Dwyka, roadcut, turn east from R66 at Ulundi, road eastwards, next to Langakazi. -28.3161, 31.5163. (Map by Von Brunn, 1996.) Brown color is recently weathered.

P1, P1a	Upper. Gray.
P3a, P3b	Middle. Brown.
P5b	Lower. Brown, gray.
P5c	Lower. Black/gray.
P5e	Part of P5 normal, but extra freeze and thaw. Lower. Brown, gray.
P5 normal	Lower. Brown, gray.
P5s	Lower. Sample is thin sandy string integrated in and separated from diamictite sample P5 normal. Gray. Sandy

Q. Dwyka, roadcut, R34, south of Surreyvale. -28.0883, 31.0444. (Map by Von Brunn, 1996.)

Q1	Gray.
Q3	Black, gray.

Table S1. Detailed site and sample descriptions. All samples consist of > 90% clay, silt and fine sand, except if otherwise mentioned.

S3. Methods, details of the laboratory preparation of samples

In the current research, a small variation was made to the original classification of SM published by Molén (2014). The preparation processes for releasing the quartz grains from the sediment included some slight mechanical work which could induce simple fracturing, especially small fractures, f1. Therefore, SP1 was not reclassified to SP2 by f1-fractures (as done in earlier publications), but only by F1-fractures. This variation resulted in more grains in the A1/SP1 group, which would be the correct classification if the mechanical work conducted on the sample induced artificial fractures. If grains display close to 50% f1, as a sum of many small 5-20% f1, then the 50% limit which would reclassify f1 to F1 could be reached. However, usually there were just one or a few small f1-fractures (or otherwise F1-fractures) on the grains in this study and therefore there were no extensive number of SM to reclassify. (Fracturing during processing of the samples was verified by the SEM studies, which showed a few grains that had fractured during application with soft hand pressure when the quartz grains were attached to the SEM-stub. These fractures were not used for the classificcation work of surface microtextures.)

The Dwyka samples were not strongly lithified, often covered with iron oxides, and there was no or extremely little calcite/limestone in the diamictites. The samples commonly consisted of at least 90% inorganic clay, silt and fine sand, with only few sand grains >0.25 mm in each sample. Most samples were collected with a rock hammer and chisel, and the samples were then mechanically and chemically treated in the laboratory to release and prepare quartz grains for SEM studies.

To some extent sample-specific treatment procedures had to be designed, to release the quartz grains needed for the SEM study from the surrounding clay (Fig. 2A, in article, Fig. S2). These procedures are outlined in a general way below, and the number of treatment steps, but not all details, are shown in Table S2. One example of treatment procedures of a sample is described in minute detail, below, section S3.1.

In short, the laboratory methods started with soaking the samples in water and drying at 90°C. The samples were then studied with a polarizing microscope to identify quartz sand grains. The process was repeated, and almost all samples were softly wet rubbed commonly 30 to 90 s by hand before they were restudied. When a sufficient number of complete quartz grains had been totally cleaned from clay, quartz sand was subsampled by hand with a small brush, under a fixed magnifying glass. Only crystal clear quartz grains were subsampled. The quartz grains were fixed to a copper plate covered with adhesive before positioning the sample on a SEM stub. Following the first two verification steps, the grains were verified a third time to be quartz by EDS whenever there was reason for doubt.

In more detail, samples were treated by the following methods, and these were repeated as needed.

1. Soak in water.

2. Rub the wet sample with soft hand pressure on a sieve (mesh 0.125 or 0.25 mm) wearing rubber dishwashing gloves, for about 30-90 s.

3, Dry at 90°C.

4. Study sample in a polarizing microscope to determine if an adequate number of complete quartz grains were visibile.

5. Treat with different concentrations of HCl, commonly for 30-90 minutes. Start with a water solution at room temperature, put the sample in a heating cabinet, and allow the sample to reach 90°C after 10-20 minutes.

6. Treat with different concentrations of H_2O_2, commonly for 30-90 minutes. Heating in some cases.

7. Soak samples in water in a plastic bag or in a small plastic bottle and expose to freeze and thaw cycles in a common refrigerator. Samples in plastic bottles were commonly shaken by hand for 30 s to a few minutes during each freeze and thaw cycle.

8. Pressure sample slowly in a vice until sample just slightly yields and is broken up. After

this treatment the sample disintegrates easily. (This step was only needed for a few samples.) 9. Separate clay particles from the quartz grains. Samples were processed with low energy sonification in water together with a “knife edge” of sodium pyrophosphate ($Na_4P_2O_7$) added. This was commonly done for 10 minutes, usually one time but sometimes repeated.

The HCl used was fuming, 37%/12M, which almost always was diluted to 15% or less. The H_2O_2 was 30%/13M, and it was often diluted to lower concentrations.

After each treatment, the sample was a) rinsed with water (if it had been treated with acids), b) soft wet rubbed in a sieve, c) dried at 90°C, and 4) studied with a polarizing microscope. Samples that were treated with freeze and thaw cycles were commonly restudied after every 10-20 cycles, after which they were processed by soft wet rubbing, dried at 90°C, and studied under a polarizing microscope.

S3.1. Full description of details of treatments of one sample

The full details of the preparatory treatments of one sample, C-1-1, from the diamictite blanketing the Dwyka pavement at Nooitgedacht, is documented below. Comments on the treatments are inside parentheses. The preparation of all other samples is fully documented (ca. 30 pages, not published) and was similar to sample C-1-1, i.e. processes were repeated, with different methods, until an adequate amount of quartz sand grains was displayed under polarized light. The summary of all treatments is reported in Table S2.

Sample C-1-1 only needed a few freeze and thaw cycles, and most of these cycles were completed before the sample disintegrated to smaller pieces when <2 mm particles could be separated. Other samples had also to be treated with many freeze and thaw cycles after the <2 mm particles had been separated in order to remove clay which was stuck to the surface of the quartz sand grains. Between each new chemical treatment, sample C-1-1was washed with water, softly wet rubbed (commonly 30 to 90 s but sometimes more) by hand while wearing rubber dishwashing gloves, and dried at 90°, before it was restudied with polarizing microscope and put for a new treatment. Other samples, where the rock quickly disintegrated but much clay was still stuck to the surfaces of the quartz grains were softly wet rubbed after every c.10-20 freeze and thaw cycles.

* 38 freeze and thaw cycles, 2x10 min sonification. Rock was intact until the last treatment.
* Rock had disintegrated. From now on only work with < 2 mm. Rock pieces >2 mm were separated away with a sieve.

a) Treatment with 15% H_2O_2 produced effervescence of gas. After 3 minutes, the liquid containing the sample had started to boil by self heating. Dilute to c. 2.5% H_2O_2 and still bubbling for 20 minutes, but not as hot.*

b) 15% H_2O_2 for 40 min, bubbles observed.

c) 10 freeze and thaw cycles.

d) 30% H_2O_2, gave off white smoke and sample started to boil by self heating after one minute. Dilute solution to 10%, and leave for 1h at room temperature.

e) 15% HCl, 40 min at 90°C. Yellow-red water, and the surface of every particle (pieces of clay and sand grains) turned red.

f) 30% H_2O_2. Bubbles, water solution turned red, solution gave off white smoke and self heated to boiling after 5 minutes. Diluted solution with the sample to 10%. After 40 minutes, bubbling had stopped.

g) 15% HCl, 1 h at 90°C. Water turned first yellow and then red. Many flat “grains” had turned white and disappeared with very little force (almost only by rinsing with water), and most of the brown-red clay also disappeared.

h) 30% H_2O_2, bubbles, red-brown supernatant, and after 10 min sample started to boil by self heating. Diluted to 20% for 45 min.

i and j) 15% HCl for 1h at 90°C., yellow-red. Many flat "grains" had turned white and disappeared with very little force (almost only by rinsing with water), and most of the brown-red clay also disappeared.

k) 30% H_2O_2 for 30 min. Few bubbles.

l) 15% HCl for 40 min at 90°C. Water-acid solution was yellow-red, but much less color than before.

m) 10 min sonification + sodium pyrophosphate ($Na_4P_2O_7$).

n) Subsampling of quartz sand grains for SEM.

* All samples from C except C3c, and samples N1a and N2a, heated up spontaneously when treated with H_2O_2. They commonly started to boil within a minute, while releasing O_2. These samples were close to soils and the surface and, similar to all other SA samples, were collected from inside hard rock. The self-heating process often was accelerated after a few treatments with HCl, H_2O_2, and/or freezing. There was no visible evidence of organic material in these samples. As iron ions are catalysts to H_2O_2 reactivity, and the heating process accelerated after more disintegration of the rocks, this indicate a stronger reaction from precense of more iron ions, i.e. the well known exothermic Fenton reaction (Pędziwiatr et al., 2018), and not any organic substances. There was no difference in the appearance of the SM in these samples compared to other samples.

Reference:

Pędziwiatr, P., Mikołajczyk, F., Zawadzki, D., Mikołajczyk, K. & Bedka, A., 2018. Decomposition of hydrogen peroxide – kinetics and review of chosen catalysts. *Acta Innovations* 26, 45-52. https://doi.org/10.32933/ActaInnovations.26.5.

S3.2. Artificial SM

To address the problem of artificial emerging fractures, F1-fractures were dismissed in a separate classification of SM, and the last geological history before this fracturing was re-labelled as History-1. The result of this reclassification of the data was similar to grains that do not display F1, i.e. there was no "hidden" history behind the F1-grains, but commonly only a single unaltered fracture on grains with mainly former A1/SP1 SM and therefore are normally classified as A2/SP2 after fracturing (F1) (Table S3 below, and Molén, 2017).

To further assure that the laboratory processes have not induced any important number of artificial SM, except possibly some F1 and f1, the samples which were processed most times by freeze and thaw cycles have been compared to those that were processed the least times. As documented in Table S4 (below), there is very little difference, and no systematic trend, in the number of SM displayed by this comparison. Likewise, other laboratory processes, like the number of treatments by acids, display no pattern and no trend for different SM (documented in Tables S2 and S5).

The last test to find out if a large quantity of SM may have originated during the laboratory processes, is a comparison of the percentage of large fractures, F1, from all Dwyka sites (Table S5). The number of A1/A2 and SP1/SP2 are directly connected to the number of F1, because F1 is reclassifying all weathered surfaces to History-2 (see Table 3). There is no trend at all in the number of F1, when comparing geographical location, more or less laboratory processing, nor if the samples were collected at road cuts or a mine where blasting or other heavy mechanical work could be detected or indicated. As an example, M4 display no F1, and this sample is from an open mine where dynamite was used (apart from other heavy equipment), and the sample was processed by 202 freeze and thaw cycles, often with mechanical shaking in a plastic bottle, followed by abrasion with soft hand pressure about 20 times. Similarly, samples from site K, where there was indication of dynamite blasting, display very few F1. Samples from sites C, G and H are from completely natural environments where the only post-depositional processes probably were wind and water, and there were no heavy mechanical work conducted on the bedrock. The only trend seen is that there are more F1 on samples from sites in diamictites close to a pavement (C, N1a and N2a), from a pavement (L), and from a conglomerate (F4 and F4b).

The different methods of laboratory treatments were further compared and analyzed in sections Results and Discussion, in the main text.

S4. Results

Table S2. Description of the different columns is at the end of the table.

C. Nooitgedacht, diamictite on pavement, -28.5995, 24.6124.

Sample	Grains	F1	f1	A1	SP1	EN1	C1	F2	f2	A2	SP2	EN2	C2	WD	FT	H	H2	P
C-1-1	42	0	11	38	42	0	0	17	2	1	0	0	0	0	48	6	5	0
C1b	46	0	18	41	46	0	0	17	1	3	0	1	0	0	55	3	3	0
C2a	44	0	8	43	44	0	0	20	10	0	0	2	0	0	46	6	6	0
C2b	31	0	9	29	31	0	0	17	6	0	0	1	0	0	127	2	1	0
C2bb	48	0	8	48	48	0	0	22	1	0	0	0	0	0	176	5	3	0

C2c	42	0	8	42	42	0	0	12	0	0	0	0	0	0	57	5	3	0
C3a	40	0	5	40	40	0	0	22	3	0	0	0	0	0	94	6	5	0
C3b	30	0	8	30	30	0	0	16	1	0	0	0	0	0	192	7	7	0
C3c	41	0	9	37	41	0	0	20	13	0	0	0	0	0	183	5	2	0
C4	31	0	8	30	31	0	0	14	6	0	0	0	0	0	84	2	5	0
	395	0	92	378	395	0	0	177	43	4	0	4	0					Sum
	395	0	23	96	100	0	0	45	11	1	0	1	0					%AS
	119	100	0	0	0	0	0	44	21	72	61	0	0					%FF

The diamictite samples at Nooitgedacht were slightly weathered and stained by iron oxides all through. Many grains are still partly covered with Fe-oxides, even after the chemical processing. There was much effervescence of gas from treatment by H_2O_2 in all samples except C3c. A few grains fractured when attached with light pressure to a SEM-stub, especially from sample C1b. Sample C1b is the most weathered of all samples in this study (example in Fig. S3). Sample C-1-1 is a thin hard diamictite crust directly on top of the pavement (Fig. 4 in article). Sample C3a is from the diamictite just above a 1 mm sedimentary material between the pavement and diamictite. Samples C3b and C3c are just above 1-6 mm of light sedimentary material that is between diamictite and pavement. Sample C4 is just above sample C4m. During laboratory processing it became evident that samples C1b, C2b, C2c, C3b and C3c are stratified, displaying 2-5 mm thick laminae.

C. Nooitgedacht, sediment between pavement and diamictite, -28.5995, 24.6124.

Sample	Grains	F1	f1	A1	SP1	EN1	C1	F2	f2	A2	SP2	EN2	C2	WD	FT	H	H2	P
C3bm (AS)	62	0	6	62	62	0	0	25	12	0	0	0	0	0	55	3	8	1
C4m (AS)	98	0	19	81	98	0	0	46	19	1	0	0	0	0	55	3	8	1
	160	0	25	143	160	0	0	71	31	1	0	0	0					Sum
C3bm (AS)	62	0	10	100	100	0	0	40	19	0	0	0	0					%A1
C4m (AS)	98	0	19	83	100	0	0	47	19	1	0	0	0					%A1
C3bm (FF)	11	100	0	0	0	0	0	55	18	100	100	0	0					%FF
C4m (FF)	16	100	0	0	0	0	0	6,3	19	69	75	0	0					%FF
All C (AS)	395	0	23	96	100	0	0	45	11	1	0	1	0					%AS
All C (FF)	119	100	0	0	0	0	0	44	21	72	61	0	0					%FF

This table displays the documentation from the sediment between the pavement and the diamictites compared to all C-samples. Sample C3bm is a light-colored stratified sediment between pavement and diamictite, c. 6 mm thick (Fig. S1). Sample C4m is c. 2-3 mm of black and brown material between the pavement and the diamictite.

The grains from sample C3bm are very similar to other samples from site C, except for displaying less f1 for the AS-group, and more A2 and SP2 for the FF-group (i.e., 100%).

Grains from sample C4m are often deeply weathered (Fig. 3A in article). This is shown by the lower percentage of A compared to SP in the AS-group. The grains also commonly have not been through two histories of fracturing, which is shown from the very low F2 displayed in the group of F1-samples of C4m (only one of 16 grains). The heavily weathered grains in sample C4m are mixed with grains with the same appearance as grains from all other Nooitgedacht samples, i.e. grains displaying SM A1/SP1 or F1/A2/SP2, but these have not been separated in the table.

F. Road cut ca 5 km north of Nieuwoudtville, close to waterfall, -31.3055, 19.1229.

Sample	Grains	F1	f1	A1	SP1	EN1	C1	F2	f2	A2	SP2	EN2	C2	WD	FT	H	H2	P
F1a	30	0	8	29	30	0	0	16	8	0	0	0	0	0	43	0	0	0
F1aa	53	0	7	53	53	0	0	20	9	0	0	0	0	0	131	4	1	0
F1b	26	0	4	25	26	0	0	15	7	0	0	0	0	0	14	1	1	0
F2	97	0	4	94	97	0	0	39	5	0	0	1	0	0	32	2	2	0
F2b	58	0	5	53	58	0	0	30	1	0	0	0	0	50	0	1	0	0
F3a	34	0	14	32	34	0	0	22	2	0	0	0	0	0	46	4	1	0
F3b	31	0	5	31	31	0	0	18	1	0	0	0	0	0	19	1	1	0
F3c	44	0	6	44	44	0	0	24	4	1	0	0	0	0	26	1	0	0
F5	53	0	13	53	53	0	0	29	13	0	0	0	0	0	296	2	0	0
	426	0	66	414	426	0	0	213	50	1	0	1	0					Sum
	426	0	16	97	100	0	0	50	12	0,2	0	0,2	0					%AS
	82	100	0	0	0	0	0	44	13	70	78	0	0					%FF

F4	29	0	2	26	29	0	0	15	0	0	0	0	0	0	309	2	0	1
F4b	20	0	2	19	20	0	0	4	3	0	0	0	0	0	314	2	0	1
F4c	31	0	3	31	31	0	0	12	5	0	0	0	0	0	296	2	1	1
	80	0	7	76	80	0	0	31	8	0	0	0	0					Sum
	80	0	9	95	100	0	0	39	10	0	0	0	0	0				%AS

F4 (FF)	14	14	0	0	0	0	0	3	1	10	9	0	0	0	309	2	0	1
F4b (FF)	15	15	0	0	0	0	0	0	0	10	11	0	0	0	314	2	0	1
F4c (FF)	4	4	0	0	0	0	0	1	1	3	3	0	0	0	296	2	1	1
	33	33	0	0	0	0	0	4	2	23	23	0	0					Sum
	33	100	0	0	0	0	0	12	6,1	70	70	0	0					%FF

Two diamictites separated by sandstone. F1-F2 is from lower diamictite. F3 is from upper diamictite Fig. S2, showing clay in F3c, but this appearance is simlar in all Dwyka diamictite samples. F5 is from lower diamictite on west side of road, and during laboratory processing it became evident that it is stratified on a mm scale.

F4 is conglomerate within sandstone (west side of road) above lower diamictite, i.e. this may be a source rock for the upper diamicite. F4c is a small red sandstone rock from inside conglomerate, mixed with loose grains from the conglomerate (Fig. S4). It was not possible to separate the mix of grains in sample F4c, because the red sandstone rock immediately disintegrated into the rest of the sample. Except for much fewer fractures (F1) and more weathering (SP1), the overall appearance in F4c was similar compared to the other F4-samples. This is also what would be expected from sample F4c, as the grains have not been moved separately in the conglomerate.

G. Kransgat River, next to Koringhuis homestead/farm, about 20 km NE of Nieuwoudtville, -31.1629, 19.3157.

Sample	Grains	F1	f1	A1	SP1	EN1	C1	F2	f2	A2	SP2	EN2	C2	WD	FT	H	H2	P
G1a	96	0	7	96	96	0	0	57	5	0	0	0	0	0	283	2	0	1

G1b	59	0	15	59	59	0	0	19	7	0	0	0	0	0	205	5	0	0
G1c	57	0	5	56	57	0	0	31	8	0	0	0	0	0	263	1	0	1
G2a	83	0	4	82	83	0	0	27	14	0	0	0	0	0	206	1	0	1
G2b	86	0	3	86	86	0	0	44	6	0	0	0	0	0	138	5	2	0
G2c	33	0	3	33	33	0	0	14	1	0	0	0	0	0	337	3	0	0
	414	0	37	412	414	0	0	192	41	0	0	0	0					Sum
	414	0	9	100	100	0	0	46	9,9	0	0	0	0					%AS
	55	100	0	0	0	0	0	40	9,1	85	80	0	0					%FF

These sediments have formerly been interpreted to have been deposited in front of a grounded marine ice sheet (Visser, 1996). (Examples in Figs. 2D, 5, in article.)

H. Elandsvlei farm area. -32.3292, 19.6406 (H1-samples) -32.3291, 19.6358 (H2-samples).

Sample	Grains	F1	f1	A1	SP1	EN1	C1	F2	f2	A2	SP2	EN2	C2	WD	FT	H	H2	P
H1	69	0	12	68	69	0	0	33	8	0	0	1	0	0	191	4	3	0
H1a	68	0	9	68	68	0	0	44	3	0	0	1	0	0	309	1	0	0
H2b	50	0	9	50	50	0	0	26	2	0	0	0	0	0	108	6	2	0
H2c	43	0	4	43	43	0	0	28	0	0	0	0	0	0	91	5	0	0
	230	0	34	229	230	0	0	131	13	0	0	2	0					Sum
	230	0	15	100	100	0	0	57	5,7	0	0	87	0					%AS
	13	100	0	0	0	0	0	46	15	69	77	0	0					%FF

Samples H1, H1a and H2c are from the main diamictite. Sample H2b is from a brown diamictite boulder within the main diamictite (Fig. 15 in article). Sample H2b easily disintegrated to smaller pieces, but there was much iron oxide on the grains. Acid reaction for sample H2b indicated calcite. Sample H2c displayed a few bubbles during treatment with HCl. (There was chemically precipitated calcite in the surrounding area.) There were very few F1-fractured grains (i.e. 13) from all samples from this site.

J. South of Matjiesfontein, road N1, -33.2390, 20.4793.

Sample	Grains	F1	f1	A1	SP1	EN1	C1	F2	f2	A2	SP2	EN2	C2	WD	FT	H	H2	P

J1a	52	0	3	52	52	0	0	31	4	0	0	0	0	0	112	4	2	0
J1b	47	0	11	46	47	0	0	28	2	0	0	0	0	0	236	1	0	1
J1c	71	0	5	70	71	0	0	26	7	0	0	0	0	0	345	1	0	1
J1d	60	0	6	60	60	0	0	33	0	0	0	0	0	0	93	1	0	0
	230	0	25	228	230	0	0	118	13	0	0	0	0					Sum
	230	0	11	99	100	0	0	51	5,7	0	0	0	0					%AS
	36	100	0	0	0	0	0	33	11	72	64	0	0					%FF

Sample J1a is from recently weathered rock. J1b-d are from fresh rocks. There is not much difference between the samples, except the less important f1, for J1b. There was a slight reaction for calcite, from samples J1a, J1b and J1c.

K. Umkomaas River Valley, road cut next to railway line, -30.1909, 30.7765.

Sample	Grains	F1	f1	A1	SP1	EN1	C1	F2	f2	A2	SP2	EN2	C2	WD	FT	H	H2	P
K1a (9)	53	0	7	53	53	0	0	35	5	0	0	0	0	0	118	2	0	0
K1b (17)	63	0	5	63	63	0	0	45	3	0	0	0	0	0	319	1	0	1
K1bb (4)	55	0	13	53	55	0	0	42	2	0	0	0	0	0	315	3	0	0
K1c (6)	44	0	2	44	44	0	0	39	2	0	0	0	0	0	76	4	0	0
K2 (4)	57	0	2	57	57	0	0	35	12	0	0	0	0	0	146	4	0	0
K2b (4)	50	0	2	48	50	0	0	35	6	0	0	0	0	0	94	5	0	0
K3b (17)	45	0	9	44	45	0	0	30	7	0	0	0	0	0	294	1	0	1
K3c (6)	76	0	4	70	75	0	0	49	3	0	0	0	0	0	274	2	0	1
	443	0	44	432	442	0	0	310	40	0	0	0	0					Sum
	443	0	10	98	100	0	0	70	9	0	0	0	0					%AS
	67	100	0	0	0	0	0	72	3	70	81	0	0					%FF

In the first column in the table the numbers of F1-grains are reported within parentheses.

Area around K1-K2 was blasted with dynamite. Samples K1b and K1bb were nearest to boreholes. K3c was sampled c. 50 m west from the area of former blasting. There is no trend of more fractured grains (F1) in samples closer to the blasting area, as is displayed within parentheses in the first column.

L. Durban, University of KwaZulu-Natal Westville Campus, sandstone pavement, -29.8187, 30.9441.

Sample	Grains	F1	f1	A1	SP1	EN1	C1	F2	f2	A2	SP2	EN2	C2	WD	FT	H	H2	P
L1 (16)	53	0	11	52	53	0	0	30	10	0	0	1	0	0	29	6	2	0
L1b (11)	57	0	10	55	57	0	0	37	2	0	0	0	0	0	52	1	1	0
L1br (23)	66	0	19	66	66	0	0	18	6	0	0	4	0	0	314	2	1	1
L1c (24)	81	0	15	78	81	0	0	62	3	0	0	0	0	0	23	2	0	0
	257	0	55	251	257	0	0	147	21	0	0	5	0					Sum
	257	0	21	98	100	0	0	57	8,2	0	0	2	0					%AS
	74	100	0	0	0	0	0	64	12	70	72	5,4	0					%FF

In the first column the number of F1-grains is reported within parentheses. Sample L1br differs most from the others in having little F2 (27%). Sample L1c has the highest percentage of F2 (77%), but is not very different from samples L1 (57%) and L1b (65%). Sample L1br does not display much more F1 than the other samples, even though it was processed with 6-10 times more treatments with freeze and thaw cycles (26% F1, compared to 23% for L1, 16% for L1b and 23% for L1c).

L1 is (lithified) sand in joint of pavement (Fig. S5). L1b is a piece of the pavement. L1br is a harder lithified part of sample L1b, i.e. a small rock piece of sandstone inside the sandstone pavement. L1c is a small part of what could be interpreted as diamictite on top of the pavement. But most of this sample is sand and there is only little clay, silt and fine sand (except for some gravel), and therefore it is not considered to be a diamictite.

Grains in sample L1br are more weathered than the other samples from this site. This can be understood from the table, because there are few F2 on these grains, i.e. in this case the grains are so much weathered and abraded that it is difficult or impossible to interpret any SM as F2. This sample also displays the most EN of all samples except sample A.

L1 displayed a small calcite reaction after a few laboratory treatments, and L1c displayed large calcite reactions during two treatments with HCl.

M. Durban, Coedmore Quarry, -29.8980, 30.94852.

Sample	Grains	F1	f1	A1	SP1	EN1	C1	F2	f2	A2	SP2	EN2	C2	WD	FT	H	H2	P
M1	64	0	2	64	64	0	0	18	16	0	0	0	0	0	421	3	1	0
M2	63	0	6	63	63	0	0	30	6	0	0	1	0	0	126	7	1	0
M3	40	0	2	40	40	0	0	23	1	0	0	0	0	0	95	4	1	0
M4	15	0	7	15	15	0	0	8	0	0	0	0	0	100	202	1	1	0
M6	42	0	3	42	42	0	0	29	1	0	0	0	0	0	351	2	0	1
	224	0	20	224	224	0	0	108	24	0	0	1	0					
	224	0	9	100	100	0	0	48	11	0	0	0,45	0					%AS
	26	100	0	0	0	0	0	73	0	73	73	0	0					%FF

All samples from this quarry appear to be slightly metamorphosed, or contained more clay (i.e. samples are slightly “thin sectioned” and “glossy”), especially samples M1 and M4. All M samples are more strongly lithified than most other samples from SA. But, there are no large differences in SM when these samples are compared to other SA diamictites (examples in Fig. 6 in article).

During the laboratory processing it first was unclear if sample M1 was a diamictite, even if the sample was collected from the diamictite and appeared similar to the other samples from this site. The sample was very poor in large grains, so that every quartz grain >0.25 mm was subsampled. However, the result from SM-analysis is similar to the other samples from this site. It appears that this diamictite sample was a part of the deposit that was extra muddy.

In sample M4 there were almost no quartz grains, and all >0.25 mm quartz grains were subsampled. This was similar to sample M1.

(Note: The %FF of History-2 SM happened to be similar just by chance, as there were different numbers of SM in all F1-samples.)

N. West of Denny Dalton, small road, -28.2843, 31.2251 (N1a, N2a), -28.2840, 31.2211 (N2b).

Sample	Grains	F1	f1	A1	SP1	EN1	C1	F2	f2	A2	SP2	EN2	C2	WD	FT	H	H2	P
N1a	28	0	6	28	28	0	0	24	3	0	0	1	0	0	54	6	6	0
N2a	38	0	16	36	38	0	0	22	8	0	0	0	0	0	23	3	2	0
N2b	64	0	9	64	64	0	0	40	5	0	0	0	0	0	315	1	0	0
	130	0	31	128	130	0	0	86	16	0	0	1	0					Sum
	130	0	24	99	100	0	0	66	12	0	0	0,77	0					%AS
	36	100	0	0	0	0	0	39	8,3	75	89	0	0					%FF

N1a and N2a were sampled exactly at a small pavement, and they were covered or appeared to be a part of a chemical precipitate on the pavement. The matrix of the sample was similar to all other diamictite samples, i.e. it consisted of mostly clay, silt and fine sand. N2b is from a loose rock c. 400 m west of the pavement. The grains from these three samples display a very similar general appearance compared to each other and to those at site O, which is c. 2 km south.

O. Southwest of Denny Dalton, road cut at R34, -28.2994, 31.2215.

Sample	Grains	F1	f1	A1	SP1	EN1	C1	F2	f2	A2	SP2	EN2	C2	WD	FT	H	H2	P
O1a	48	0	7	48	48	0	0	24	5	0	0	0	0	0	64	1	0	0
O2	43	0	3	43	43	0	0	22	8	0	0	1	0	0	40	0	0	0
	91	0	10	91	91	0	0	46	13	0	0	1	0					Sum
	91	0	11	100	100	0	0	51	14	0	0	1,1	0					%AS
	6	100	0	0	0	0	0	50	0	100	100	0	0					%FF

This site is about 2 km south of site N, and is Dwyka Group diamictite along a road cut at road R34. The sample conforms well to all other sites and display no special features (Fig. 2C in article).

P. Dwyka, roadcut, turn east from R66 at Ulundi, road eastwards, next to Langakazi. -28.3161, 31.5163.

Sample	Grains	F1	f1	A1	SP1	EN1	C1	F2	f2	A2	SP2	EN2	C2	WD	FT	H	H2	P
P1	41	0	9	40	41	0	0	27	3	0	0	0	0	0	59	1	0	0
P1a	24	0	5	24	24	0	0	17	1	0	0	0	0	0	39	1	0	0
P3a	34	0	8	33	34	0	0	16	10	0	0	0	0	0	75	1	0	0
P3b	36	0	6	36	36	0	0	27	5	0	0	0	0	0	58	3	1	0
P5b	51	0	3	51	51	0	0	34	4	0	0	0	0	0	107	4	0	0
P5c	50	0	10	50	50	0	0	29	16	0	0	0	0	0	225	1	0	1
P5e	70	0	3	69	70	0	0	45	9	0	0	0	0	0	146	3	0	0
P5 norm	48	0	9	47	48	0	0	34	5	0	0	0	0	0	98	1	0	0
P5s	30	0	5	30	30	0	0	16	10	0	0	0	0	0	15	3	0	0
	384	0	58	380	384	0	0	245	63	0	0	0	0					Sum
	384	0	15	99	100	0	0	64	16	0	0	0	0					%AS
	73	100	0	0	0	0	0	44	9,6	82	81	0	0					%FF

P1a, P3b and P5b include small granite rock pieces that disintegrated by simply pouring water on them. There were numerous quartz grains in sample P1a compared to all other samples from the Dwyka diamictites.

P5s is a few millimeters thick sandy “parting” from inside sample P5 norm. P5e is sample P5 norm that has been processed through 48 extra freeze and thaw cycles and more HCl treatment in order to see if the percentages of SM was changed. As seen from the table above there is almost no differences, except for f1 – and there actually were fewer f1 in the sample that was processed more times (which is interpreted to be only by chance).

All samples from this site display similar SM. Only in f1/F2/f2 there are large differences (if recalculated to percentages). But the differences in f1 and especially f2 are of less significance as small fractures are easily opened up. The slightly higher occurence of F2, compared to most other samples from this site, in samples P1a (71%), P3b (75%) and P5b (67%), may actually in part be portions of flat weathered EN that have an appearance of flat F2 (compare to Molén, 2014).

There are more protuberances on these grains from northern outcrops, compared to those from southern outcrops (e.g. Fig. S6, and Discussion and Results.)

Q. Dwyka, roadcut, R34 south of Surreyvale. -28.0883, 31.0444.

Sample	Grains	F1	f1	A1	SP1	EN1	C1	F2	f2	A2	SP2	EN2	C2	WD	FT	H	H2	P
Q1	78	0	7	75	78	0	0	51	18	0	1	0	0	0	170	4	3	0
Q3	65	0	13	65	65	0	0	46	10	0	0	0	0	0	236	2	2	0
	143	0	20	140	143	0	0	97	28	0	1	0	0					Sum
	143	0	14	98	100	0	0	68	20	0	0,7	0	0					%AS
	17	100	0	0	0	0	0	53	0	71	88	0	0					%FF

There is nothing to comment on for these samples, but they are similar to all other samples and especially those close by, i.e. samples N, O and P.

Table S2. All samples, including laboratory treatments and comments.

Quartz sand grains were separated into two groups, which are 1) A1/SP1 (which are labelled AS in the tables), which are all grains that do not display only F1 as the most recent surface microtexture and nothing else, and 2) those that display only F1 as the single most recent surface microtexture (labelled FF in tables). (There is an exception for sample A. See description in the table.) The values of the A1/SP1 group are reported in detail, but for F1-grains commonly only the sum is reported. First column – “Grains” – in all tables, are the number of grains that do NOT display F1, if nothing else is mentioned. Then follows the sum of all different SM from all these (12 columns). The value %AS is the percentage of grains displaying one of the different SM compared to the total number of A1/SP1 grains. The value %FF is all grains that have acquired F1 as the last geological history, and the percentage is number of SM compared to the numbers of F1-grains. F1-grains are not used in the final analysis of the SM from the Dwyka sediments as it is not possible to know how many of these are recent or are from the time of deposition. But for comparison, these grains are reported from all sites.

Last five columns display the number of treatments with different processes. These are

WD = Number of cycles of only wetting in tap water and drying at 90°C, followed by slight rubbing.

FT = Freeze and thaw cycles in a common refrigerator.

H = Commonly a water solution of c. 15% HCl. Start at c. 20°C (room temperature), and warm up to to 90°C for 30-90 min, soak in water, rub gently and dry at 90°C.

H2 = Commonly a water solution of c. 15% H_2O_2. Start at c. 20°C (room temperaure) warm to 90°C if possible (30-90 min). The treatment was followed by water soaking, soft rubbing and drying at 90°C.

P = Slowly increasing pressure in a vice.

*** table ends here ***

No. of samples		Grains	F1	A1	SP1	F2	A2	SP2	
1	12 C:s	555	0	94	100	45	0,9	0	%AS
2	9 F:s -F4	426	0	97	100	50	0,2	0	%AS
3	5 M:s	224	0	100	100	48	0	0	%AS

4	12 C:s	146	100	0	0	40	74	65	%FF
5	9 F:s -F4	82	100	0	0	44	70	78	%FF
6	5 M:s	26	100	0	0	73	73	73	%FF
7	**12 C:s**	**146**		**74**	**65**	**40**			**Rem. %FF**
8	**9 F:s -F4**	**82**		**70**	**78**	**44**			**Rem. %FF**
9	**5 M:s**	**26**		**73**	**73**	**73**			**Rem. %FF**
10	C3bm	62	0	100	100	40,3	0	0	%AS
11	C4m	98	0	83	100	47	1	0	%AS
12	C3bm	11	100	0	0	55	100	100	%FF
13	C4m	16	100	0	0	6,3	69	75	%FF
14	**C3bm**	**11**		**100**	**100**	**55**			**Rem. %FF**
15	**C4m**	**16**		**69**	**75**	**6,3**			**Rem. %FF**

Table S3. Removal of F1-fractures. Normal text rows in table are raw data, and bold rows are after removal of F1 and reinterpretation of History-2 SM, i.e. rows 4-6 are reinterpreted in rows 7-9, and rows 12-13 are reinterpreted in rows 14-15. Rows 1-3 are only for comparison to grains that display no F1. The A1/SP1 group is labelled AS in table

**** End of table ***

Three sites with many samples (12, 9 and 5 samples, as shown in the Table S3) have been chosen as relevant examples for reclassification, to uncover if there are any “hidden” glaciogenic grains (i.e. F1/A1; Molén, 2014) in the samples. Samples from these sites include little weathered (F and M samples) and the most weathered (C samples) diamictites. In order to detect similar appearances of SM in the sediment between the diamictite and the pavement at Nooitgedacht, samples C3bm and C4m also are in the table.

The more weathered diamictite samples do not display 100% A1 but sometimes only SP1 (e.g. only 94% A1 for C-samples). Samples from site C are the most recently weathered of all samples in this study. F-samples are from a roadcut far south and may be slightly weathered, and M-samples are from Coedmore Quarry (a mine) in the north and are recently released during mining operations. (F4-samples are from a conglomerate, and these were not included in this comparison of diamictites).

The reclassifying and theoretical removal of F1 fractures is conducted as a change of A2/SP2 to A1/SP1, when F1 are dismissed. This is done in order to reveal whether recent F1 may hide an original history of F1/A1, i.e. glaciogenic grains. In the procedure of reclassifying F2 have been left as is, as these fractures are older than the A2/SP2 and have been altered by both of these processes, and there is no evidence of simultaneous abrasion and fracturing (F/A) of F2-surfaces, in contrast to glaciogenic grains which commonly display F1/A1. The reclassifying reveals a) if there have been any recent environmental or mechanical processes (i.e. mechanical fracturing or even recent abrasion from sampling, laboratory processing, road work or mining) which have changed the SM in the samples so that earlier histories have been masked, and b) if there are any differences between these differently weathered samples after the reclassification.

Any F1 that may have originated as the last process during final deposition, i.e. fractures which have not been weathered, are also excluded in the process of reclassifying of the SM. The f1-f2 SM and those which are very rare (EN and C), are of less importance, and cannot be compared with any certainity, so these have been excluded from this comparison.

No “hidden” F1/A1 history is revealed in the data in the table after dismissing all F1, but only older A1/SP1 (i.e. classified normally as A2/SP2) that were subsequent to an even older history of fracturing, i.e. older F2-fractures (which could be defined as F3 or maybe EN3, if such a classification would be developed).

The only large differences, when comparing grains where F1 has been removed (bold five rows in table, which are reclassified from rows 4-6 and 12-13) to grains that do not display F1 (i.e. %AS), between the SM is in A1/SP1. So where F1 has been removed, the A1/SP1 is close to 70% instead of close to 100%. This is because the surface of grains which have been heavily fractured often has changed so much that most or all A2 and SP2 SM have disappeared, and almost exclusively the most recent F1-fractures are visible.

.

Sample, no.	Grains	F1	f1	A1	SP1	EN1	C1	F2	f2	A2	SP2	EN2	C2	
G 138-337	414	0	8,9	100	100	0	0	46	9,9	0	0	0	0	%AS
F1b-F3c: 0-46	290	0	13	96	100	0	0	51	6,9	0,345	0	0,34	0	%AS
G 138-337	55	100	0	0	0	0	0	40	9,1	86	80	0	0	%FF
F1b-F3c: 0-46	49	100	0	0	0	0	0	47	12	65	80	0	0	%FF

Table S4. Comparison of samples that have been processed by many cycles of freeze and thaw cycles, compared to those that have not.

There is very little difference in the occurence of SM when comparing samples with many and few freeze and thaw cycles (138-337 cycles for six samples from site G, and 0-46 for six samples from site F).

In the comparison above, it is only A2 on F1-grains that display a large difference (86% and 65%). Samples from site G have the largest percentage of A2 on F1-grains of all samples independent of number of freeze-thaw cycles. Because A2 is an older SM, it cannot have been generated from the laboratory processing. Other samples display between 69-82% A2, except sample O which displayed only six F1-grains, and all six display A2. (Compare to Table S2.)

The A1/SP1 group is labelled AS in table.

*** End of table ***

Sample	Grains	F1	%	WD	FT	H	H2	P
M4	**15**	**0**	**0**	**100**	**202**	**1**	**1**	**0**
G2c	33	0	0	0	337	3	0	0
H1a	68	0	0	0	309	1	0	0
G1c	58	1	2	0	263	1	0	1
O2	**45**	**2**	**4**	**0**	**40**	**0**	**0**	**0**
H2c	45	2	4	0	91	5	0	0
M1	**67**	**3**	**4**	**0**	**421**	**3**	**1**	**0**
J1d	64	4	6	0	93	1	0	0
K2	**61**	**4**	**7**	**0**	**146**	**4**	**0**	**0**
K1bb	**59**	**4**	**7**	**0**	**315**	**3**	**0**	**0**
Q1	**84**	**6**	**7**	**0**	**170**	**4**	**3**	**0**
K3c	**82**	**6**	**7**	**0**	**274**	**2**	**0**	**1**
K2b	**54**	**4**	**7**	**0**	**94**	**5**	**0**	**0**
G2b	93	7	8	0	138	5	2	0
O1a	**52**	**4**	**8**	**0**	**64**	**1**	**0**	**0**
H1	75	6	8	0	191	4	3	0
H2b	55	5	9	0	108	6	2	0
F2b	64	6	9	50	0	1	0	0
N2b	**71**	**7**	**10**	**0**	**315**	**1**	**0**	**0**
J1c	79	8	10	0	345	1	0	1
P5c	**56**	**6**	**11**	**0**	**225**	**1**	**0**	**1**
F4c	35	4	11	0	296	2	1	1
J1a	59	7	12	0	112	4	2	0
K1c	**50**	**6**	**12**	**0**	**76**	**4**	**0**	**0**
M6	**48**	**6**	**13**	**0**	**351**	**2**	**0**	**1**
C2c	*48*	*6*	*13*	*0*	*57*	*5*	*3*	*0*
F2	111	14	13	0	32	2	2	0
P5 norm	**55**	**7**	**13**	**0**	**98**	**1**	**0**	**0**
M3	**46**	**6**	**13**	**0**	**95**	**4**	**1**	**0**
C4m	*114*	*16*	*14*	*0*	*55*	*3*	*8*	*1*
G1a	112	16	14	0	283	2	0	1
P5s	**35**	**5**	**14**	**0**	**15**	**3**	**0**	**0**
P3b	**42**	**6**	**14**	**0**	**58**	**3**	**1**	**0**
Q3	**76**	**11**	**14**	**0**	**236**	**2**	**2**	**0**
K1a	**62**	**9**	**15**	**0**	**118**	**2**	**0**	**0**
C3c	*48*	*7*	*15*	*0*	*183*	*5*	*2*	*0*

C1b	*54*	*8*	*15*	*0*	*55*	*3*	*3*	*0*
M2	**74**	**11**	**15**	**0**	**126**	**7**	**1**	**0**
C3a	*47*	*7*	*15*	*0*	*94*	*6*	*5*	*0*
P3a	**40**	**6**	**15**	**0**	**75**	**1**	**0**	**0**
C3bm	*73*	*11*	*15*	*0*	*55*	*3*	*8*	*1*
F3c	52	8	15	0	26	1	0	0
All samp	4271	664	16					
F5	63	10	16	0	296	2	0	0
F1b	31	5	16	0	14	1	1	0
G2a	99	16	16	0	206	1	0	1
L1b	***68***	***11***	***16***	***0***	***52***	***1***	***1***	***0***
F3b	37	6	16	0	19	1	1	0
P5e	**85**	**15**	**18**	**0**	**146**	**3**	**0**	**0**
P1	**50**	**9**	**18**	**0**	**59**	**1**	**0**	**0**
P5b	**63**	**12**	**19**	**0**	**107**	**4**	**0**	**0**
F1aa	66	13	20	0	131	4	1	0
C2bb	*60*	*12*	*20*	*0*	*176*	*5*	*3*	*0*
G1b	74	15	20	0	205	5	0	0
K1b	**80**	**17**	**21**	**0**	**319**	**1**	**0**	**1**
C-1-1	*54*	*12*	*22*	*0*	*48*	*6*	*5*	*0*
C2b	*40*	*9*	*23*	*0*	*127*	*2*	*1*	*0*
P1a	**31**	**7**	**23**	**0**	**39**	**1**	**0**	**0**
F3a	44	10	23	0	46	4	1	0
L1c	***105***	***24***	***23***	***0***	***23***	***2***	***0***	***0***
L1	***69***	***16***	***23***	***0***	***29***	***6***	***2***	***0***
N1a	***37***	***9***	***24***	***0***	***54***	***6***	***6***	***0***
F1a	40	10	25	0	43	0	0	0
L1br	***89***	***23***	***26***	***0***	***314***	***2***	***1***	***1***
C4	*42*	*11*	*26*	*0*	*84*	*2*	*5*	*0*
J1b	64	17	27	0	236	1	0	1
K3b	**62**	**17**	**27**	**0**	**294**	**1**	**0**	**1**
C2a	*64*	*20*	*31*	*0*	*46*	*6*	*6*	*0*
F4	*43*	*14*	*33*	*0*	*309*	*2*	*0*	*1*
N2a	***58***	***20***	***34***	***0***	***23***	***3***	***2***	***0***
F4b	*35*	*15*	*43*	*0*	*314*	*2*	*0*	*1*
C3b	*57*	*27*	*47*	*0*	*192*	*7*	*7*	*0*

Table S5. Data enhancing transport distance from north to south, laboratory processing, and number of large fresh fractures, F1.

Column “Grains” shows all grains from the samples, both with and without F1. Column F1 is number of grains that display F1. The column % is percentage of F1-grains, compared to all grains. Other columns are similar to and described in Table S2.

Samples that are from the north, samples K-Q, are bolded. Samples from sites in diamictites next to a pavement (C, N1a and N2a), from a pavement (L), and from a conglomerate (F4 and F4b) are marked with italics. (F4c is a separate weathered red sandstone rock from within the conglomerate and not grains from the matrix that have been directly mechanically impacted by the surrounding rocks and sand.)

The only trend seen in the table is that there are more F1 on samples from sites in diamictites next to a pavement (C, N1a and N2a), from a pavement (L), and from a conglomerate (F4 and F4b).

Length (cm)	Quantity.
1 - 5	46
6 - 10	36
11 - 20	10
21 - 50	6
51 - 101	2
Sum	100

Table S6. Measurement of 100 striations in an area of approximately four square meters, displaying almost solely short striations (Fig. 9A, in article).

Fig. S1. Sediment from between the pavement and the diamictite at Nooitgedacht, sample C3bm. The piece in the picture is 8 mm thick, but most of the sample was 5-6 mm thick.

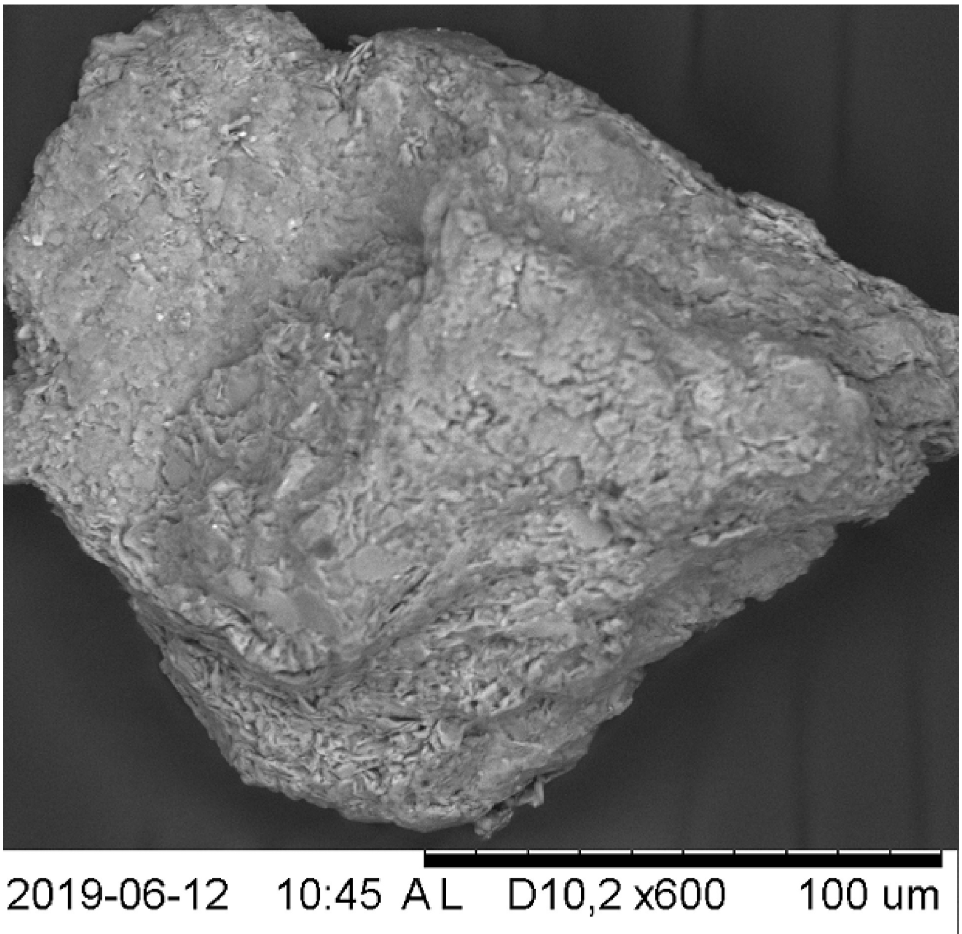

Fig. S2. Piece of clay (sample F3c). These aggregations of allochtonous clay form the matrix in all diamictite samples. The clay disintegrated to smaller pieces and became rounded during the rubbing procedure. At the same time, during the rubbing procedure, the clay protected the quartz grains from too much mechanical forces as the aggregations were still often larger than the quartz grains. The samples still often consisted of 90-95% of clay aggregates even during the final subsampling.

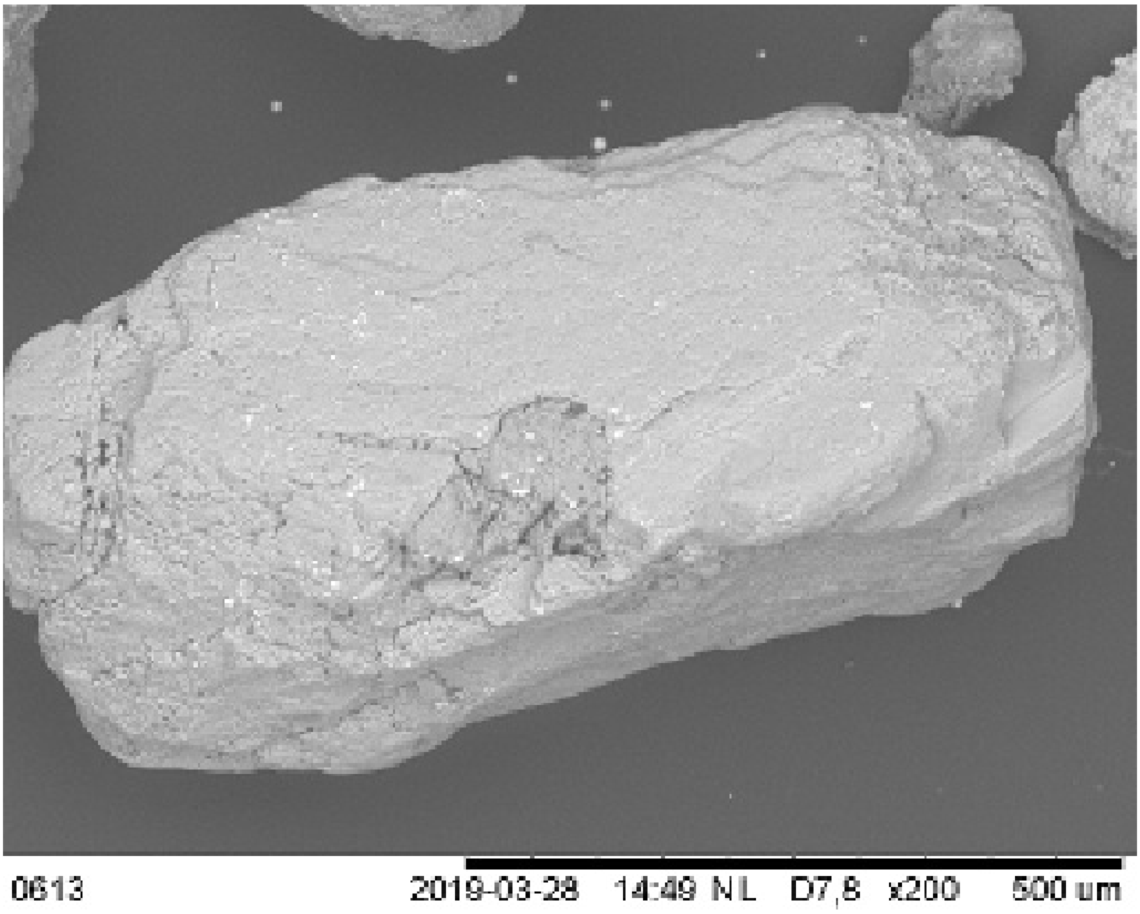

Fig. S3. A heavily weathered grain, from the sample that is the most recently weathered (C1b). A1, SP1, F2 (and a very small probably recent fracture, which is too small to be considered even a f1). This grain displays similarities in appearance to some grains in the sample from the thin dark layer of sediment between the pavement and the diamictite, sample C4m (Fig. 3A in article).

.

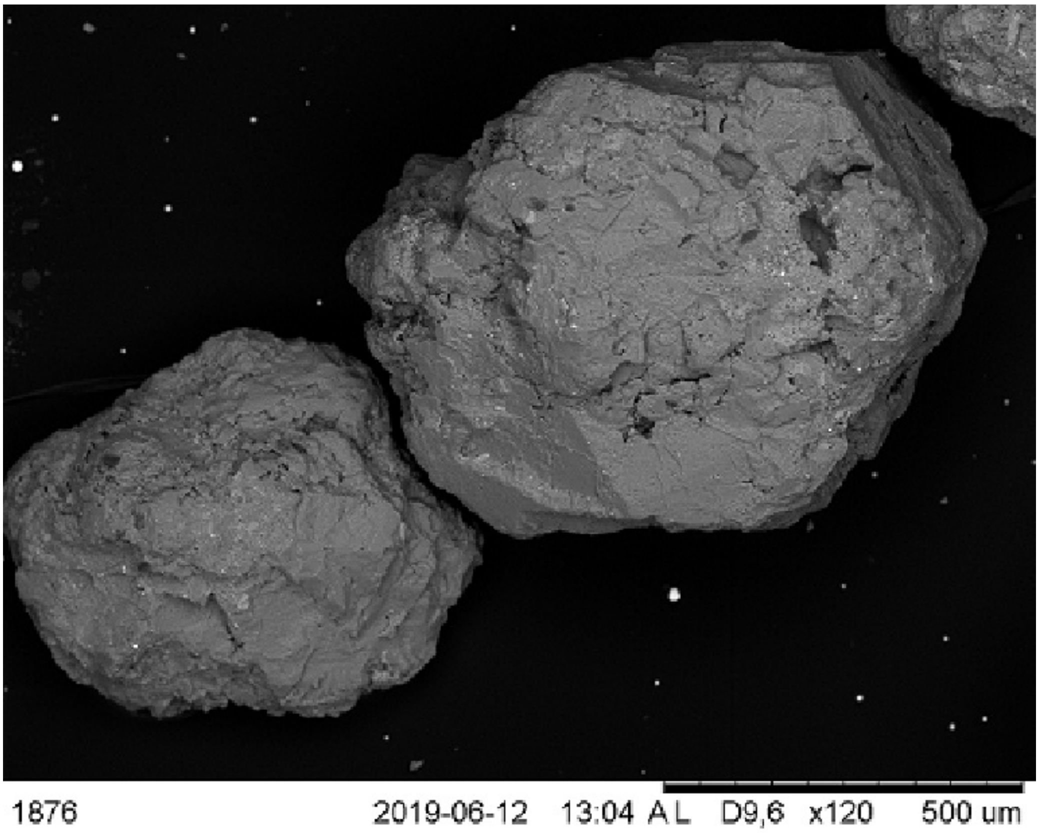

Fig. S4. Grains from a small piece of weathered red sandstone from inside of the conglomerate at Nieuwoudtville, sample F4c. The grains display SP1, but some rounding which is interpreted as A1, and some small fractures (f2).

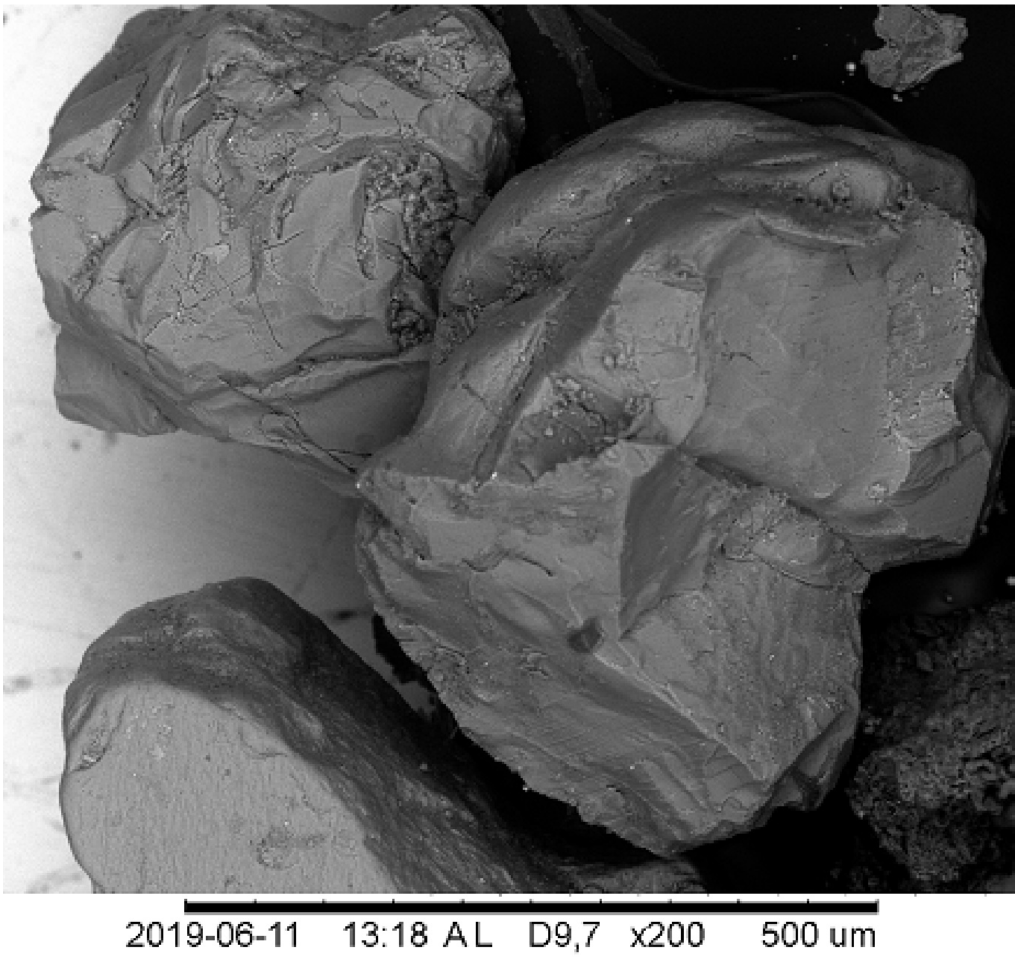

Fig. S5. Typical grains from the sandstone pavement at Durban University. The two upper grains display F1, F2, A2, SP2. The third, lower left grain (only partly visible in this picture), is classified as A1/SP1/F2. (Sample L1.)

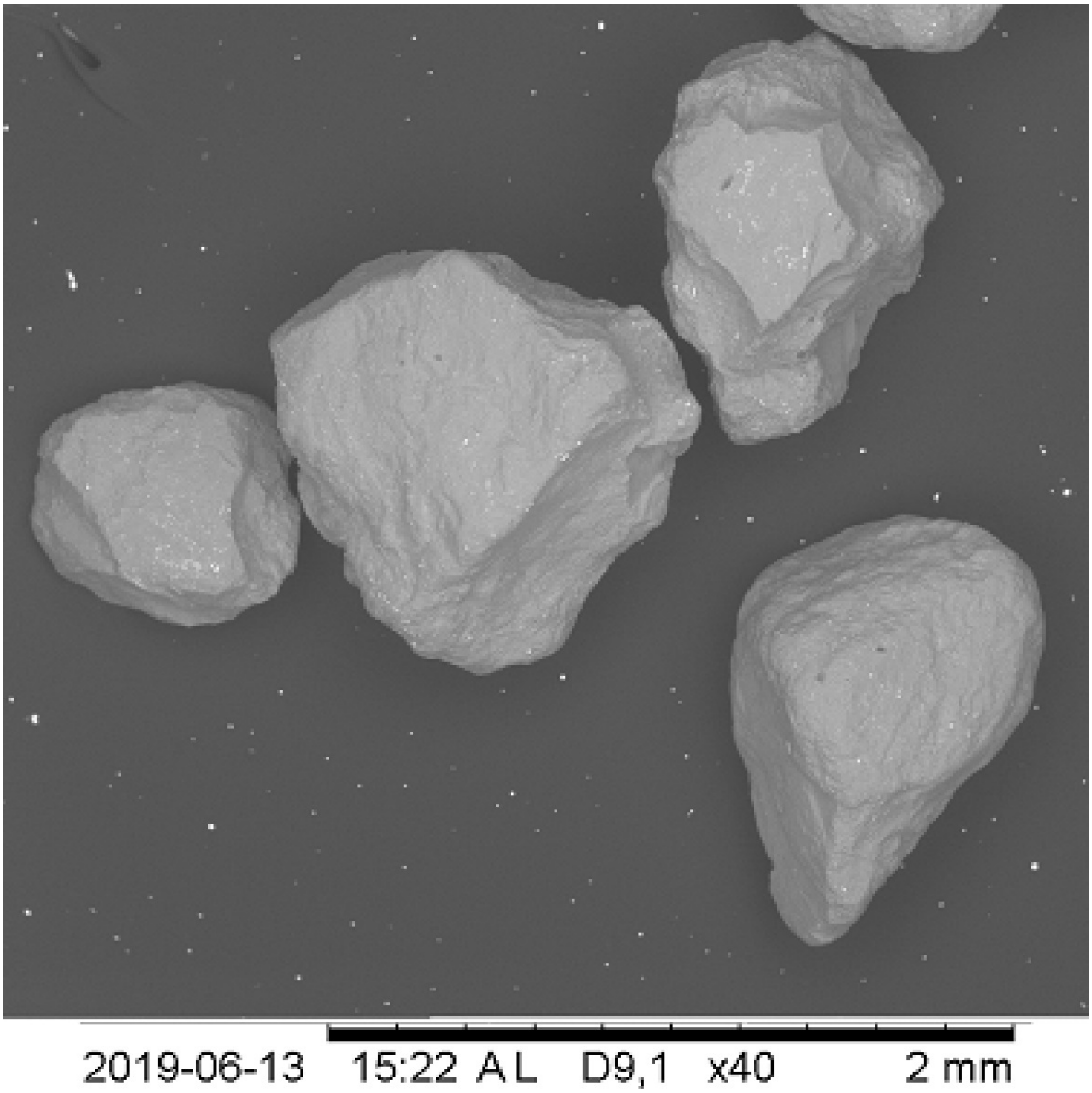

Fig. S6. Four grains from the northeastern part of the Dwyka Group, sample P5c, in which most grains are less rounded than those in the south. Only the right upper grain is classified as displaying F1, but it is close to f1. The upper flat surface of this grain could be an EN2, but it is classified as F2 (Molén, 2014). (Final classification is F1, F2, A2, SP2). The other grains display f1 (except grain in lower right), A1, SP1 and F2.

Grains especially from the northeastern part of the Dwyka Group display more outstanding edges and/or protuberances, similar to the upper right grain, compared to those in the southern parts of SA. It appears that this grain could have been released from weathered bedrock, e.g. granite, and transported in low energy environments for only a short period. The three other grains, and especially the lower right grain, were transported for a longer time so that the sharp edges have more or less been rounded off.

S5. Detailed discussion of sampling and laboratory work

Sampling in the field was carefully done with as little and as indirect force as possible so that fracturing of quartz grains should be avoided. Loose material was taken away from the samples before the laboratory processing started if it could be suspected that loose grains a) could have aquired more fractures during sampling than those inside the sample, b) were heavily weathered and therefore were loose and had been released before the sampling process, or c) could be contamination. The chemical processing was continued until there was no more evidence of coatings, especially not iron oxides.

As >90% of all diamictite samples consisted of clay, silt or fine sand, fine-grained material had to be removed during processing. Almost no grains of any kind were >2 mm, and the very few quartz grains present were commonly <1 mm. The lithified sediments commonly showed up as large aggregations of clay during disintegration of the samples, from which smaller quartz grains slowly emerged (Figs. 2A in article and Fig. S3). The removal of the quartz sand particles mainly took place during the soft mechanical rubbing of the samples. Therefore, because there always was a surplus of large clay aggregates in the samples, quartz grains were not rubbed (by soft pressure) much against the metal in the sieves (stainless steel) or against each other during the release process. Thus, this process avoided acquiring much changed SM, except possibly some fracturing of grains. Even during the final subsampling of quartz sand grains, commonly more than 90% of all grains still were aggregations of clay that were larger than the quartz grains. Some samples were almost devoid of the >0.25 mm quartz grains needed for the SEM-study.

After the laboratory work was finished there was no evidence of any coatings on the grain surfaces originating from the slight lithification process of the sediments. This observation was independent of possible different burial depth or strength of the sediment. Neither was there any evidence of systematic or even single SM from any laboratory or other post-lithification processes which could possible corrupt the result (compare to Mahaney, 2002; Molén, 2014). There were still minute strokes of ironoxide in a very few parts on a few grains, but these areas were easily identified by the SEM and did not cover any original quartz SM so that any SM could be misidentified. Whatever the chemical or other process that was used during the preparation of the samples, whether almost no process at all or hundreds of processing steps, the SM displayed the same appearance (Tables S2-S5). Also, the sedimentary deposits which were studied were not lithified by silica or calcite, but it was single quartz grains that were embedded in a soft clay matrix. Any clay coatings were removed during the laboratory process so that the SM of the quartz surfaces were fully visible, except a few grains on which clay was preserved in order to study the appearance of these by SEM (e.g. Fig. 2A in article and Fig.

S3). This was illustrated both on grains which showed their cross section within the clay matrix (Fig. 2A), fractured grains and abraded grains. There was no evidence of any grain coatings, other than possible less than about a micrometer. Such minute coatings were not observed and so thin coatings – if they are present – do not change the appearance of any SM that were studied in the current research (Molén, 2014).

The various comparisons of the processing of quartz grains for the SEM studies showed that in general neither did the physical environment at the sampling sites, the sampling methods nor the laboratory processes, create numerous SM. Samples from areas that had been close to blasting and those that were completely natural, samples that had been processed many times and those that had been processed few times, displayed about the same numbers of SM. No trend was visible in any case (Tables S2-S5).

The main complication from the SEM studies was that large fractures (F1/F2) came in all states of weathering. Some were fresh and some much weathered. Therefore it was sometimes difficult to classify fractures as F1 or F2.

Because of the different states of weathering, it was not known how many grains were fractured during transport and deposition, and how many were fractured after deposition, i.e. during road work, blasting, sampling and laboratory processing. But, as there were no F1- or F2-fractures that displayed simultaneous or subsequent irregular abrasion, this is no obstacle to the aim of the current research, i.e. to find out if the Dwyka Group is glaciogenic or not. If fractures were abraded at all, it was slight regular abrasion all over the grain including all over the fractures.

The only trend displayed in the number of fractures which is apparent from the SM is that there is a greater abundance of F1-fractures on grains close to pavements (C, N1a, N2a), within a pavement (L), and within the matrix-supported conglomerate that was studied (F4 and F4b) (Table S5). This may indicate that grains from these samples were more or less internally fractured but maybe not broken during transport and deposition, because they are from environments displaying stronger mechanical forces (i.e. more magmatic/metamorphic clasts or next to such bedrock), in contrast to the soft material which was present in all diamictite samples. Some of the F1-fractures may therefore be original, from the deposition of the sediments, and some may have been opened up by the laboratory or other processes subsequent to deposition. The exact origin of all F1-fractures is impossible to determine, but the F1-grains exhibit no History-1 SM except fractures. There is no irregular abrasion on the fractures, as in glaciogenic grains.

It was observed that some F1 were created during mounting of the grains on the SEM stub, with slight finger pressure, as seen from a few SEM-pictures. Such fractures were not recorded as F1, but only other SM were recorded.